Synthesis and Characterization of Glycopolymer Brushes

by

Reda Ali Fleet

Dissertation is presented in partial fulfillment of the requirements for the degree of PhD in chemistry and Polymer Science at the University of Stellenbosch

Promoter: Prof. B. Klumperman

December 2010

DECLARATION

By submitting this dissertation electronically, I declare that the entirety of the work contained therein is my own, original work, that I am the owner of the copyright thereof (unless to the extent explicitly otherwise stated) and that I have not previously in its entirety or in part submitted it for obtaining any qualification.

Signature: .....Reda..... Date: .....22/10/2010.....

Abstract

In recent years, the synthesis of polymer brushes has received significant attention, partly due to their unique properties and applications. Polymer brushes usually refer to an assembly of polymer chains in the brush regime, which are densely tethered by one end to an interface. The immobilized ends prevent polymer chains from escaping from their neighbours, which leads to a stretched conformation to avoid overlapping. Considerable advances have been made in the understanding of the way in which the mechanical properties of polymers can be related to their chemical structure. The primary aim, of this study is the synthesis and structural characterization of novel glycopolymer brushes.

A successful "grafting from" approach via the atom transfer radical polymerization (ATRP) technique was used for the synthesis of novel glycopolymer brushes, namely P(2-(2-bromoisobutyryloxy) ethyl methacrylate))-g-P(methyl 6-O-methacryloyl-α-D-glucoside) (P(BIEM)-g-P(6-O-MMAGIc)), P(2-(2-bromoisobutyryloxy) ethyl methacrylate-co-methyl methacrylate)-g-P(methyl 6-O-methacryloyl-α-D-glucoside) (P(BIEM-co-MMA)-g-P(6-O-MMAGIc)), P(2-(2-bromoisobutyryloxy) ethyl methacrylate-b-methyl methacrylate)-g-P(methyl 6-O-methacryloyl-α-D-glucoside) (P(BIEM-b-MMA)-g-P(6-O-MMAGIc)) and P(4-vinylbenzyl chloride-alt-maleic anhydride)-g-P(methyl 6-O-methacryloyl-α-D-glucoside) (P(S_d-alt-MA)-g-P(6-O-MMAGIc)). The formation of well-defined glycocylindrical brushes with narrow molar mass distribution was confirmed by ^{1}H-NMR spectroscopy and size exclusion chromatography (SEC) with a multi-angle laser light scattering detector (SEC-MALLS).

The P(6-O-MMAGIc) side chains were cleaved from the backbones and the cleaved side chains were analyzed by ^{1}H-NMR and SEC-MALLS. The grafting efficiency of P(6-O-MMAGIc) from the macroinitiators P(BIEM), P(BIEM-co-MMA), P(BIEM-b-MMA) and P(S_d-alt-MA) were determined to be in the range $0.37 < f < 0.55$.

Thermal analysis showed little difference between the glass transition temperatures of the different glycopolymer brushes. The thermal degradation of these glycopolymer brushes was almost identical, and found to be independent of the number of glycopolymer side chains incorporated in the glycopolymer brushes. All glycopolymer brushes showed viscoelastic responses that are characteristic for

brushes. The elastic features of each polymer predominate (G'>G") at low angular frequency, while at higher frequency the G" curve overtakes the G' curve, indicating the predominance of the viscous response. Atomic force microscopy (AFM) revealed that the molecular brushes adsorbed on a mica surface, and only islands of polymer molecules were visible as opposed to individual brushes showed in earlier studies.

Opsomming

Polimerieseborsels (Eng. polymer brushes) het onlangs baie aandag getrek, veral as gevolg van hulle unieke eienskappe en toepassings. Die term ‘polimerieseborsels’ verwys gewoonlik na ‘n samestelling van polimeerkettings in ‘n borselstyl (Eng ‘brush regime’), waar hulle dig geheg is aan die polimeerrugraat (of tussenvlak). Die geimmobiliseerde punte verhoed dat die polimeersykettings andersins ontsnap van hulle bure, as gevolg van opeenhoping, wat dan lei tot ‘n uitgerektekonformasie, om oorvleueling te verhoed.

Baie vordering is al gemaak met die begrip van die manier waarop die meganiese eienskappe van polimere afhang van die chemiesesamestelling van die polimere. Die hoofdoel van hierdie studie was die sintese en karakterisering van nuwe glikopolimerieseborsels.

‘n Suksesvolle ‘ent vanaf’ metode, via atoomoordrag-radikaalpolimerisasie (ATRP), is gebruik vir die sintese van die nuwe glikopolimerieseborsels: P(2-(2-bromoisobutirieloksi)etiel-metakrilaat))-g-P(metiel-6-O-metakriloïel-α-D-glukosied) (P(BIEM)-g-P(6-O-MMAGIc)), P(2-(2-bromoisobutirieloksi)etiel-metakrilaat-ko-metiel metakrilaat)-g-P(metiel-6-O-metakriloïel-α-D-glukosied) (P(BIEM-co-MMA)-g-P(6-O-MMAGIc)), P(2-(2-bromoisobutirieloksi)etiel metakrilaat-b-metiel metakrilaat)-g-P(metiel 6-O-metakriloïel-α-D-glukosied) (P(BIEM-b-MMA)-g-P(6-O-MMAGIc)) en P(4-vinielbensiel chloried-alt-maleïensuuranhidried)-g-P(metiel-6-O-metakriloïel-α-D-glukosied) (P(Sd-alt-MA)-g-P(6-O-MMAGIc)). Goedgedefinieerde glikosilindriese borsels met noue molekulêremassaverspreiding is berei. Dit is bevestig m.b.v. 1H-KMR-spektroskopie en grootte-uitsluitingschromatografie (SEC) met ‘n multi-hoek laser ligverstrooiingdetektor (SEC-MALLS).

Die P(6-O-MMAGIc) sykettings is gesplit vanaf die ruggraat en die sykettings wat afgesplit is is geanaliseer m.b.v. 1H-KMR en SEC-MALLS. Die entdoeltreffendheid van P(6-O-MMAGIc) vanaf die makroafsetters P(BIEM), P(BIEM-co-MMA), P(BIEM-b-MMA) en P(Sd-alt-MA) was $0.37 < f < 0.55$.

Thermieseanaliese het getoon dat daar min verskil was tussen die glasoorgangstemperatuurvan die verskillende glikopolimerieseborsels. Die termieseafbreek van die glikopolimerieseborsels was amper eenders, en daar is gevind dat dit onafhanklik is van die aantal glikopolimeriese syketting wat in die glikopolimerieseborsels geinkorporeer is. Alle glikopolimerieseborsels het viskoelastiese terugvoer gehad wat tipies is van borsels. Die elastieseeienskappe van alle polimere predomineer (G'>G") by laehoekfrekwensies, terwyl by hoër frekwensies die G" kurwe die G' kurwe verbystek, wat daarop dui dat die viskeuse terugvoer oorheers. Atoomkragmikroskopie het getoon dat die molelulêreborsels op die oppervlak van die mika geabsorbeer het, en net eilande van polimeriesemolekules te sien is, in teenstelling met alleenstaande borsels wat in vroeër studies bevind is.

Dedication

This work is dedicated to the people who have always believed in me and supported me and brought joy to my life: my family, Mother, Father, Sisters, brothers and the light of the family, little Ali and my darling Kate.

Table of contents

List of figures

List of schemes

List of tables

List of symbols

C_m	Chain transfer constant
C	Transfer constant
CuBr	Cupper bromide
DP_n	Average degree of polymerization
$DP_{n,sc}$	Degree of polymerization of the side chains
dn/dc	Refractive index increment
f	Radical efficiency
f	Grafting efficiency
G’	Storage modulus
G”	Loss modulus
h*ν*	Energy
I	Initiator
[*I*]	Initiator concentration
$[I]_o$	Initial concentration of initiator
k_d	Dissociation constant
k_i	Initiation constant
K_{-add}	Fragmentation rate coefficient
K_{add}	Addition rate coefficient
K_{act}	Rate constant of activation
K_{deact}	Rate constant of deactivation
k_{tr}	Transfer rate coefficient
k_p	Propagation rate coefficient
k_{tc}	Termination rate constant
k_{td}	Termination by disproportionation rate coefficient
k_{tm}	Transfer to monomer rate coefficient
k_{ts}	Transfer to solvent rate coefficient
k_{tt}	Transfer to agent rate coefficient
k_{tp}	Transfer to polymer rate coefficient
[M]	Concentration of monomer
M	Monomer
$[M]_o$	Initial concentration of monomer

$Mw_{monomer}$	Molecular weight of monomer
Mw_{RAFT}	Molecular weight of RAFT agent
[Monomer]	Monomer concentration
M^n_t/L	Transition metal complex for atom transfer reaction
M_n	Number average molar mass
$M_{n,theory}$	Calculated number average molar mass
R	RAFT agent leaving group
$R^{\bullet}$	Primary radical
[RAFT]	RAFT agent concentration
$[RAFT]_o$	Initial concentration of RAFT agent
R_i	Rate of initiation
R_p	Rate of propagation
R_t	Rate of termination
S	Solvent
[S]	Concentration of the chain transfer agent in form of solvent
T	Chain transfer agent
t	Time
T_g	Glass transition temperature
Tanδ	Loss factor
$t_{1/2}$	Initiator half-life
x	Fractional conversion
Z	RAFT agent stabilizing group
λ	Fraction of termination by disproportionation
λ	Absorbance

List of acronyms

AIBN	2,2-Azobis (isobutyronitrile)
AFM	Atomic force microscopy
ATRP	Atom transfer radical polymerization
BIEM	2-(2-Bromoisobutyryloxy) ethyl methacrylate
bpy	2,2'-Bipyridine
$CDCl_3$	Deuterated chloroform
CIPDB	2-Cyanoprop-2-yl dithiobenzoate
^{13}C-NMR	Carbon nuclear magnetic resonance spectroscopy
DBN	Di-tert-butylnitroxide
DCM	Dichloromethane
DMA	Dynamic mechanical analysis
DMSO-d6	Deuterated dimethyl sulfoxide
DEPN	N-tert-butyl-N-(1-diethylphosphono-2,2-dimethylpropyl)
DMF	N,N-Dimethylformamide
DMAc	N,N-dimethylacetamide
dNbpy	4,4'-Di(5-nonyl)-2,2'-bipyridine
DP	Degree of polymerization
DSC	Differential scanning calorimetry
EGDMA	Ethylene glycol dimethacrylate
ESR	Electron spin resonance
GAMA	2-Gluconamidoethyl methacrylate
HEMA	2-Hydroxyethyl methacrylate
HEMA-TMS	2-(Trimethylsilyloxy)ethyl methacrylate
HMTETA	1,1,4,7,10,10-Hexamethyltriethylenetetramine
^{1}H-NMR	Proton nuclear magnetic resonance spectroscopy
LAMA	2-Lactobionamidoethyl methacrylate
LRP	Living radical polymerization
MA	Maleic anhydride
MAIGlc	3-O-Methacryloyl-1,2:5,6-di-O-isopropylidene-D-glucofuranose
MALLS	Multi-Angle Laser Light Scattering

MEK	Methyl ethyl ketone
Me_6TREN	Tris(2-(dimethylamino)ethyl)amine
MMA	Methyl methacrylate
6-O-MMAGlc	Methyl 6-O-methacryloyl-α-D-glucoside
MMD	Molar mass distribution
NMP	Nitroxide mediated polymerization
NMR	Nuclear magnetic resonance spectroscopy
n-Pr-1	N-(n-propyl)-2-pyridylmethanimine
PDI	Polydispersity index
PMDETA	N,N,N',N',N"Pentamethyldiethylenetriamine
RAFT	Reversible addition-fragmentation chain transfer
RI	Refractive index
S_d	4-Vinylbenzyl chloride
SEC	Size exclusion chromatography
TBAF	Tetrabutylammonium fluoride solution
TEA	Triethylamine
TEMPO	2,2,6,6-Tetramethyl-1-piperidinyloxy free radical
TGA	Thermogravimetric analysis
TMS-Cl	P-toluenesulfonyl chloride
UV	Ultraviolet
WAXD	Wide angle X-ray diffraction

Acknowledgements

Firstly, I would like to thank God for blessing me with the gift of life during my study. I know that God gave me guidance, courage, strength and joy in times of despair.

Secondly I would like to thank and acknowledge the institutions that have made this project possible. The Libyan International Centre for Macromolecules Chemistry and Technology and the department of chemistry and polymer science, without whose generous sponsorship this would not have been possible.

From a personal financial aspect, it is important to thank Stellenbosch University as well as the Harry Crossley foundation.

To my supervisor and friend Bert Klumperman, your knowledge, input, motivation and encouragement during this time of study were invaluable. Your belief in me gave me strength and confidence in my work; it has been a great privilege and honor to work with you. You were not only a wonderful supervisor but also a great friend and I will treasure our friendship long into the future.

To my friend, Eric T. A van den Dungen. You are not only a brilliant scientist but a truly amazing friend. Your help and the endless hours you spent reading my work will never be forgotten.

I would like to take this opportunity to thank the following people for their contributions to this project:

Prof Sanderson, for giving me the opportunity to study at this world class institution.

I owe a lot of gratitude to Dr JB McLeary, who made me feel at home in the free radical lab. His constructive criticism and endless assistance are gratefully acknowledged and much appreciated.

Dr Margie Hurndall is thanked for assisting with preparing this manuscript. Dr, thank you for your time and energy.

My friends and colleagues in the polymer science department for their support and encouragement. Also, members of the free radical lab are acknowledged for making work in the lab enjoyable.

To my friends from Libya, who came for the world and brought with them endless hours of laughter. You inspired me to reach my goal and set bigger goals for the future.

To Kate McGill, my beautiful dearest darling, thank you for your love and support when things seemed impossible.

Finally, I would like to thank my mother and father for their patience, understanding and support as well as their unequivocal belief in me. You are my anchor.

Chapter 1: Introduction and objectives

1.1 Introduction

Numerous synthetic polymeric products have been produced over the past few decades in order to improve the quality of life of the all people who use them.[1,2] One needs only think of life without them to realize that they have become an integral part of our society.[3] This is not a coincidence, since they are based on nature which is full of polymeric structures. DNA, for example, is one of the better known natural polymers and one of the fundamental building blocks of life.

Human beings have long realized the importance of surfaces and interfaces, because they are so closely related to our everyday life. Seven thousand years ago, the ancient Chinese used lacquer generated from tree sap to protect wooden surfaces.[4] The detailed study of surfaces and interfaces became a bona fide scientific discipline during the 1970s. Since then it has been playing a forefront role in science. Surface and interface science is truly interdisciplinary, comprising the fields of physics, chemistry and analytical chemistry. Besides traditional coating applications, surface and interface science also relates closely to other areas such as heterogeneous catalysis, microelectronics, aviation, and biomedical devices.

The world of synthetic polymers is however not without its problems. The rising cost of oil has resulted in the increased production costs for many polymers. This fact, and the ever increasing interest in renewable materials and energy, has resulted in more time and resources being allocated to research in the renewable materials field.[5-7]

Among several of these renewable materials are glycopolymers, which can be defined in a general sense as synthetic polymers possessing a non-carbohydrate backbone but carrying carbohydrate (sugar) moieties as pendant or terminal groups.

Since the pioneering work of Horejsi et al.,[8] glycopolymers have raised an ever increasing interest as artificial materials for a number of biological and biomedical uses. This is mostly due to the expectation that polymers displaying complex functionalities, similar to those of natural glycoconjugates, might be able to mimic, or even exceed, their performance in specific applications (biomimetic approach).[9] For instance, studies have been published on the use of glycopolymers as macromolecular drugs,[10] drug delivery systems,[11] cell culture matrices,[12] matrices for encapsulation, stabilization and active ingredients release,[11] texture-enhancing food additives,[13] biosensitive[14] and biocatalytic hydrogels,[15] reverse osmosis membranes and stationary

phase for separation purposes,[16] surface modifiers,[17] artificial tissues and artificial organ substrates.[12]

One of the main goals in modern synthetic polymer chemistry is to prepare polymers with controlled molecular weight and well-defined architecture.[18] Free radical polymerization is the most important industrial process used to produce vinyl polymers,[19,20] but conventional free radical polymerization lacks control because of continuous initiation, chain transfer and termination processes.[20] Controlled/living radical polymerization (CRP) provides access to polymers with controlled molecular weight and narrow molecular weight distributions and with various architectures.[19,20] Atom transfer radical polymerization (ATRP) is one of the most efficient CRP methods and has been successfully applied to the synthesis of linear, (hyper)branched, comb-like, and star-like structures.[21,22] Densely grafted molecular brushes are among the most interesting macromolecular structures.

Molecular brushes are one-dimensional macromolecules that contain a high density of side chains (SCs) connected to a linear backbone.[23] Interest in molecular brushes comes from their compact structure and a persistent cylindrical shape.[24] The dense spacing of the side chains results in steric repulsion that induces an increase of the persistence length as well as the contour length of the polymer backbone.[25] Typically, polymer brushes are synthesized by living polymerization techniques, such as living anionic polymerization[26] and controlled/living radical polymerization (CRP).[20,27] Molecular brushes can be synthesized by one of three routes: "grafting onto",[28-31] "grafting through"[32-34] and "grafting from".[31,35,36] These methods can be combined with controlled polymerization techniques, which enable independent control of the molecular parameters i.e., degree of polymerization and polydispersity of main and side chain polymers, overall grafting density, and grafting uniformity.

The high density and proportion of relatively short side chains present in molecular brushes has an important effect on their resulting bulk properties. Due to the radial distribution and extended nature of the backbone, chain packing can be significantly hindered, leading to morphologies different from that expected for simple linear polymers with the same identity as the side chains.[37]

The chemical and topological chain complexity of the molecular brushes play an important role in the intra- and intermolecular interactions as well as in the structure formation and rheological properties of solutions and melts of such molecules.[38]

Rheological investigations of polymeric fluids have remained at the center of research activities due to their ability to connect macroscopic behaviour to molecular structure commonly known as structure-property relationships. Rheology not only offers guidelines to process materials but also yield key structural information that ultimately governs the final application. The evaluation of the rheological properties of polymer brushes can also provide valuable information related to the behaviour of a polymer under processing conditions prior to the formation of the final product.[39]
This dissertation describes the synthesis of well-defined glycopolymer brushes by the polymerization of a sugar-carrying methacrylate monomer using atom transfer radical polymerization (ATRP) and their extensive characterization.

1.2 Objectives

The basic motivation for this work was to synthesise novel hybrid glycopolymer brushes using well-defined macroinitiator backbones and a sugar-carrying methacrylate monomer. Glycopolymer brushes with different morphologies were synthesized via ATRP, and then their solution properties and mechanical properties studied and then compared to those of a linear glycopolymer. Such glycopolymer brushes have a high density of sugar moieties, resulting in enhanced biocompatibility and hydrophilicity. Therefore, one of the objectives of this study was to explore the easiest and more efficient pathway to prepare such glycopolymers.
The objectives of the study can be summarized as follows:

1. To synthesize the glycomonomer methyl 6-O-methacryloyl-α-D-glucoside (6-O-MMAGIc) in a good yield from the lipase-catalyzed, regioselective transesterification of vinyl methacrylate with methyl-α-D-glucoside, and also to synthesize a halogenated monomer 2-(2-bromoisobutyryloxy) ethyl methacrylate (BIEM) from 2-hydroxyethyl methacrylate (HEMA) and 2-bromoisobutyryl bromide.
2. To synthesize four well-defined multifunctional ATRP macroinitiators with different distribution of initiating sites along their backbones, namely P(2-(2-bromoisobutyryloxy) ethyl methacrylate (P(BIEM)), P(2-(2-bromoisobutyryloxy) ethyl methacrylate-co-methyl methacrylate) (P(BIEM-co-MMA)), P(2-(2-bromoisobutyryloxy) ethyl methacrylate-b-methyl methacrylate) (P(BIEM-b-MMA)) and P(4-vinylbenzyl chloride-alt-maleic

anhydride) (P(S_d-alt-MA) via reversible addition-fragmentation chain transfer (RAFT) mediated polymerization.

3. To use two different synthetic routes to synthesize eight of the above mentioned ATRP macroinitiators using the ATRP technique.
4. To use the ATRP process to control the grafting of unprotected 6-O-MMAGIc glycomonomer from these ATRP macroinitiators to prepare high molar mass and low PDI glycopolymer brushes with different grafting densities. The glycopolymer side chains will also be cleaved from the backbone and then characterized in order to estimate the grafting efficiency.
5. To characterize the glycopolymer brushes using various chromatographic and spectroscopic techniques and to study their thermal and mechanical properties.

1.3 Layout of the thesis

Chapter 1: Introduction and objectives

A brief introduction is given to the major areas relevant to this research, including glycopolymers and molecular brushes, and the objectives of the research project.

Chapter 2: Historical and theoretical background

Historical and theoretical aspects related to this research project are presented here. Included are important studies related to this research that have carried out by other researchers to date.

Chapter 3: Synthesis and characterization of novel glycopolymer brushes via a combination of RAFT and ATRP techniques

Chapter 3 addresses the organic synthesis that was required for this study as well as the synthesis and characterization of the first four glycopolymer brushes that have been used in this research.

Chapter 4: Synthesis and characterization of glycopolymer brushes initiated from different macroinitiators

This chapter covers the synthesis and characterization of a series of well-defined glycopolymer brushes with P(methyl 6-O-methacryloyl-α-D-glucoside) (P(6-O-MMAGIc)) side chains, using the "grafting from" approach, via ATRP.

Chapter 5: Structure and properties of high density glycopolymer brushes

The thermal and mechanical properties of the glycopolymer brushes with various degrees of polymerization of the backbone and various grafting densities are described in this chapter.

Chapter 6: General conclusions

Some general conclusions for the study are highlighted.

1.4 References

(1) Asua, J. *Prog. Polym. Sci.* **2002**, *27*, 1283-1346.

(2) Antonietti, M.; Landfester, K. *Prog. Polym. Sci.* **2002**, *27*, 689-757.

(3) Velasco, M.; Munoz, A.; Jimenez-Castellanos, M.; Castellano, I.; Gurruchaga, M. *Int. J. Pharm.* **1996**, *136*, 107-115.

(4) Advincula, R. C.; Brittain, W. J.; Caster, K. C.; Ruhe, J. *Polymer Brushes : Synthesis, Characterization, Applications*; Wiley-VCH: Weinheim, 2004.

(5) Lin, L.; Yao, Y.; Yoshioka, M.; Shiraishi, N. *Carbohydr. Polym.* **2004**, *57*, 123-129.

(6) Okada, M.; Tachikawa, K.; Aoi, K. *J. Polym. Sci. Part A: Polym. Chem.* **1997**, *35*, 2729-2737.

(7) Mosnacek, J.; Matyjaszewski, K. *Macromolecules* **2008**, *41*, 5509-5511.

(8) Djalali, R.; Hugenberg, N.; Fischer, K.; Schmidt, M. *Macromol. Rapid Comm.* **1999**, *20*, 444-449.

(9) Albertin, L.; Stenzel, M.; Barner-Kowollik, C.; Foster, L. J. R.; Davis, T. P. *Macromolecules* **2004**, *37*, 7530-7537.

(10) Choi, S.-K.; Mammen, M.; Whitesides, G. M. *J. Am. Chem. Soc.* **1997**, *119*, 4103-4111.

(11) Palomino, E. *Adv. Drug Deliv. Rev.* **1994**, *13*, 311-323.

(12) Karamuk, E.; Mayer, J.; Wintermantel, E.; Akaike, T. *Artif. Organs.* **1999**, *23*, 881-884.

(13) Cerrada, M. L.; Sanchez-Chaves, M.; Ruiz, C.; Fernandez-Garcia, M. *Eur. Polym. J.* **2008**, *44*, 2194-2201.

(14) Miyata, T.; Uragami, T.; Nakamae, K. *Adv. Drug Deliv. Rev.* **2002**, *54*, 79-98.

(15) Novick, S. J.; Dordick, J. S. *Chem. Mater.* **1998**, *10*, 955-958.

(16) Gruber, H.; Knaus, S. *Macromol. Symp.* **2000**, *152*, 95-105.

(17) Wulff, G.; Zhu, L.; Schmidt, H. *Macromolecules* **1997**, *30*, 4533-4539.

(18) Matyjaszewski, K.; Qin, S.; Boyce, J. R.; Shirvanyants, D.; Sheiko, S. S. *Macromolecules* **2003**, *36*, 1843-1849.

(19) Moad, G.; Solomon, D. *The Chemistry of Radical Polymerization*, 2nd ed.; Elsevier: Heidelberg, 2006.

(20) Matyjaszewski, K.; Davis, T. P. *Handbook of Radical Polymerization*; John Wiley and Sons: Canada, 2002.

(21) Wang, J.-S.; Matyjaszewski, K. *J. Am. Chem. Soc.* **1995**, *117*, 5614-5615.

(22) Matyjaszewski, K.; Xia, J. *Chem. Rev.* **2001**, *101*, 2921-2990.

(23) Hadjichristidis, N.; Pitsikalis, M.; Pispas, S.; Iatrou, H. *J. Am. Chem. Soc.* **2001**, *101*, 3747-3792.

(24) Gao, H.; Matyjaszewski, K. *J. Am. Chem. Soc.* **2007**, *129*, 6633-6639.

(25) Borner, H. G.; Duran, D.; Matyjaszewski, K.; da Silva, M.; Sheiko, S. S. *Macromolecules* **2002**, *35*, 3387-3394.

(26) Yagci, Y.; Atilla Tasdelen, M. *Prog. Polym. Sci.* **2006**, *31*, 1133-1170.

(27) Braunecker, W.; Matyjaszewski, K. *Prog. Polym. Sci.* **2007**, *32*, 93-146.

(28) Fredrickson, G. H. *Macromolecules* **1993**, *26*, 2825-2831.

(29) Subbotin, A.; Saariaho, M.; Ikkala, O.; ten Brinke, G. *Macromolecules* **2000**, *33*, 3447-3452.

(30) Muchtar, Z.; Schappacher, M.; Deffieux, A. *Macromolecules* **2001**, *34*, 7595-7600.

(31) Borner, H. G.; Beers, K.; Matyjaszewski, K.; Sheiko, S. S.; Moller, M. *Macromolecules* **2001**, *34*, 4375-4383.

(32) Yamada, K.; Miyazaki, M.; Ohno, K.; Fukuda, T.; Minoda, M. *Macromolecules* **1998**, *32*, 290-293.

(33) Neugebauer, D.; Zhang, Y.; Pakula, T.; Sheiko, S. S.; Matyjaszewski, K. *Macromolecules* **2003**, *36*, 6746-6755.

(34) Roos, S. G.; Müller, A. H. E.; Matyjaszewski, K. *Macromolecules* **1999**, *32*, 8331-8335.

(35) Beers, K. L.; Gaynor, S. G.; Matyjaszewski, K.; Sheiko, S. S.; Möller, M. *Macromolecules* **1998**, *31*, 9413-9415.

(36) Cheng, G.; Boker, A.; Zhang, M.; Krausch, G.; Müller, A. H. E. *Macromolecules* **2001**, *34*, 6883-6888.

(37) Rathgeber, S.; Pakula, T.; Wilk, A.; Matyjaszewski, K.; Beers, K. L. *J. Chem. Phys.* **2005**, *122*, 1-13.

(38) Tsujii, Y.; Ejaz, M.; Sato, K.; Goto, A.; Fukuda, T. *Macromolecules* **2001**, *34*, 8872-8878.

(39) Samakande, A.; Sanderson, R. D.; Hartmann, P. C. *Polymer* **2009**, *50*, 42-49.

Chapter 2: Historical and theoretical background

2.1 Glycopolymers

Numerous synthetic polymeric products have been produced over the past few decades in order to improve the quality of life of all the people who use them. In recent years, the preservation of limited mineral resources and the rising cost of oil have resulted in increased production cost of many polymers.[1] This fact, and the ever increasing interest in natural, environmentally friendly, biocompatible, and biodegradable materials, has resulted in the more effective utilization of renewable natural resources as precursors for the production of polymeric materials.[1-3]

Many researchers have therefore been carrying out investigations into the synthesis and manufacture of new biobased materials that are more environmentally acceptable.[2,4] Among several of these materials are the glycopolymers, which can be defined in a general sense as synthetic polymers possessing a non-carbohydrate backbone but carrying carbohydrate (sugar) moieties as pendant or terminal groups. This definition includes diverse macromolecular architectures such as glycopolymer brushes, comb-like copolymers, glycodendrimers, glycopolymer stars and hydrogels.[1,5-9] Glycopolymers and sugar-based monomers have become increasingly important in their use as artificial materials for a number of biological, pharmaceutical and biomedical uses.[5,10] This is mostly due to their role as biomimetic analogues, and to the presence of carbohydrate (sugar) moieties which impart to the glycopolymers specific properties to play an essential mediating role in a wide range of biomolecular recognition events.[6]

Glycopolymers have emerged as potentially important materials for the study of carbohydrate-protein interactions which are critical components of diverse biological processes.[11,12] Glycopolymers have also been investigated for various applications, including macromolecular drugs,[13] drug delivery systems,[14] cell culture matrices,[15] matrices for encapsulation, stabilization and active ingredients release,[14] texture-enhancing food additives,[8] biosensitive[16] and biocatalytic hydrogels,[17] reverse osmosis membranes and stationary phase for separation purposes,[18] surface modifiers,[19] artificial tissues and artificial organ substrates.[15]

2.1.1 Preparation of glycopolymers

Methods for the preparation of glycopolymers can roughly be classified into two main categories. The first method involves the polymerizations of sugar-based monomers and the second the chemical modification of preformed polymers with sugar-containing reagents.[20,21] In general, the latter method is much simpler and more convenient, mainly because the synthesis of sugar-based monomers involves tedious multistep reactions. However, the drawback of this approach is the incompletion of the reactions, mainly due to steric hindrance, resulting in polymers with less regular structures. Therefore, it is often better to use the former technique due to its advantage of allowing the synthesis of linear glycopolymers with well-defined architectures.[20] As a result, most of the glycopolymers reported to date in the literature have been synthesized by the polymerization of sugar-based monomers.[6]

Optimization of glycopolymer properties has required the utilization of controlled architectures and functionalities, which give the glycopolymers more sophisticated functions that may exceed those of natural glycoconjugates.[20] Moreover, the presence of suitable functional groups in a glycopolymer is usually not enough to bestow it with the biological properties required for a given application.[7] For these reasons, new well-defined synthetic glycopolymer architectures have been prepared using the recently discovered controlled/living free radical polymerization techniques such as nitroxide mediated polymerization (NMP),[20,22] atom transfer radical polymerization (ATRP),[4,20,23] and reversible addition-fragmentation chain transfer (RAFT) mediated polymerization.[5,21,24]

However, despite the increasing attention devoted to this wide range of tailored glycopolymers synthesized using these techniques, very few reports have appeared on the synthesis of well-defined glycopolymers without recourse to protecting group chemistry.[4,6,7] A particularly interesting example of this is the work published by Narain et al., on the ATRP of 2-gluconamidoethyl methacrylate (GAMA) and 2-lactobionamidoethyl methacrylate (LAMA) in methanol/water mixtures. They prepared controlled glycopolymers without the use of protective groups chemistry.[4,11] More recently, the first example of the polymerization of an unprotected sugar monomer via RAFT mediated polymerization was described by Lowe et al., who successfully

polymerized the commercially available 2-methacryloxyethyl glucoside directly in water.[21] The successful aqueous RAFT mediated polymerization of unprotected glycomonomer has also been described by Albertin et al,[5,7] who reported the lipase-catalyzed synthesis of methyl 6-O-methacryloyl-α-D-glucoside (6-O-MMAGlc) and its living radical polymerization in water via the RAFT process. These controlled/living radical polymerization techniques will be discussed in detail in the following sections (2.3).

2.2 Free radical polymerization

2.2.1 Introduction

Free radical polymerization has been an important research area in the preparation of synthetic polymers over the last hundred years.[25] It is one of the most important techniques used for producing polymers from vinyl monomers. It is used extensively in industry more than 70% of vinyl polymers, which themselves comprise 50% of all commercially made polymers, are synthesized via free radical polymerization.[26,27]

The polymerization can be performed in homogeneous (e.g. solution/bulk polymerization) and heterogeneous media (e.g. emulsion polymerization). One of the major advantages of free radical polymerization over other polymerization techniques is its relative tolerance to media impurities such as oxygen, water, additives and metal ions. The technique can be conducted at moderated temperature and pressure. Another advantage of this technique is its compatibility with a broad range of vinyl monomers.[27] Polystyrene, poly (methyl methacrylate), polybutadiene and branched polyethylene are examples of polymers made via free radical polymerization technique.[28]

However, free radical polymerization is inherently limited in its ability to synthesize multiblock copolymers, stars and graft copolymers. It is unable to control molar mass, and produces polymers with high polydispersity indexes (PDI > 1.5). It is difficult to control the polymerization stereochemistry in free radical polymerization as the technique produces only atactic or partially syndiotactic polymers.[29-31]

For a molecule to generate radicals, an amount of energy (bond dissociation energy) must be added to the system. The lower the amount of the energy needed to form a free radical, the more stable the free radical will be.[32]

$$CH_3^{\bullet} < R\text{-}CH_2^{\bullet} < R_2\text{-}CH^{\bullet} < R_3\text{-}C^{\bullet}$$

Least stable $\longrightarrow$ Most stable

The reactivity of vinyl monomers in a free radical polymerization depends on the ability of the substituents, R and X in Figure 2.1, to stabilize the propagating radical. For example, in styrene where the substituent X is H and R is a benzene ring, the radical formed upon addition to the propagating chain will be stable and have low reactivity compared to the vinyl chloride radical where R is Cl and X is H. As a result, the styrene monomer is more susceptible to radical addition. Thus different monomers have different radical reactivities and different propagation rate coefficients, depending on the substituent X. The reactivity of derived radicals is the opposite of their respective monomers. The more stable the monomer is, the more reactive the radical will be.[26,33]

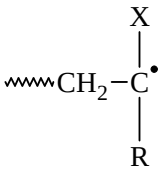

Figure 2.1: Propagating polymeric radical with substituents X and R.

2.2.2 Free radical polymerization kinetics

Free radical polymerization is generally described in three reaction steps: initiation, propagation and termination.

2.2.2.1 The initiation step

For a radical polymerization to occur, radicals need to be generated. This process is known as initiation. There are numerous classes of initiator compounds that have the ability to generate radical species upon decomposition.

The initiation step is considered to involve two reactions. The first step is the homolytic dissociation of an initiator molecule into one or more primary radicals (2.1). The second

step of the initiation involves the addition of the initiator derived (primary) radical to a single vinyl monomer molecule to form a chain initiating radical (2.2).

$$\text{I-I} \xrightarrow[h\nu]{k_d} 2\text{I}^{\bullet} \tag{2.1}$$

$$\text{I}^{\bullet} + \text{M} \xrightarrow{k_i} \text{R}_1^{\bullet} \tag{2.2}$$

The rate of dissociation of the initiator is described by the following equation:

$$-\frac{d[I]}{d[t]} = k_d[\text{I}] \tag{2.3}$$

Integration of equation (2.3) leads to equation (2.4) which describes the decrease of initiator concentration as a function of time:

$$[\text{I}] = [\text{I}]_0 \, e^{-k_d t} \tag{2.4}$$

where $[\text{I}]_0$ represents the initial initiator concentration, [I] represents the initiator concentration at time *t*, and k_d corresponds to the rate coefficient of initiator decomposition at a specific temperature.

In case two radicals are produced from the decomposition of one initiator molecule (not always the case), the rate of initiation R_i is given by equation (2.5).

$$R_i = 2\, k_d\, f\, [\text{I}] \tag{2.5}$$

The initiator efficiency *f* is the fraction of radicals that successfully initiates chains, which takes into account solvent cage effects and always has a value between zero and unity. As the monomer viscosity of the reaction medium increases, the diffusion of the radicals away from each other becomes difficult, hence the primary radicals remain in close proximity and recombination can occur. Typical values for *f* are between 0.5 and 0.8, and these values decrease as the reaction viscosity increases until it reaches the limiting value of zero.[26]

Different initiators have different properties. Each has its own unique requirement to decompose and to form a radical. The most common ways to generate radicals are via thermal initiation, chemical initiation (redox) and photoinitiation.[34]

Thermal initiation can be divided into two main classes: azo- and peroxy-type initiators (Figure 2.2).

Azo-initiator Peroxy-initiator

Figure 2.2: General structures of the azo and peroxy-type initiators.

These initiators decompose on addition of thermal energy to the system and are characterized by an initiator half-life ($t_{1/2}$), i. e. the time period during which half of the initiator molecules decompose.

In photoinitiated free radical polymerization the reaction temperature has almost no effect on the rate of decomposition of most photoinitiators. The rate of decomposition generally depends on the intensity of the UV light.[26] Photoinitiators decompose upon irradiation with visible or UV light source. The most commonly used photoinitiators contain a benzoyl group.

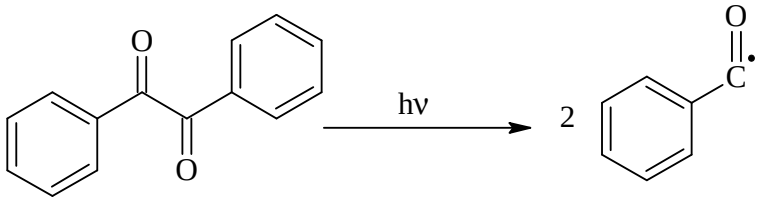

Benzil Benzil radical

Scheme 2.1: Formation of a benzil radical.

In a redox initiation process radicals are generated by the reaction between a reducing agent and an oxidizing agent. These radicals can initiate a free radical polymerization process (see Scheme 2.2).

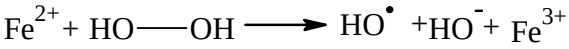

Scheme 2.2: A typical redox initiation system.

Other initiating techniques, which are less commonly used, include high intensity ultrasonic initiation, high energy radiation (γ-radiation), plasma initiation, self-initiation and electroinitiation.[26]

The molecular structure, nature and solubility of the initiators must be considered when choosing an initiator. The selection of a specific initiator for a particular polymerization system depends on the reaction conditions.[35]

2.2.2.2 The propagation step

After the reaction has been initiated, the radical formed in the initiation step is capable of adding successive monomer units to yield growing polymer chains as shown, in Scheme 2.3.

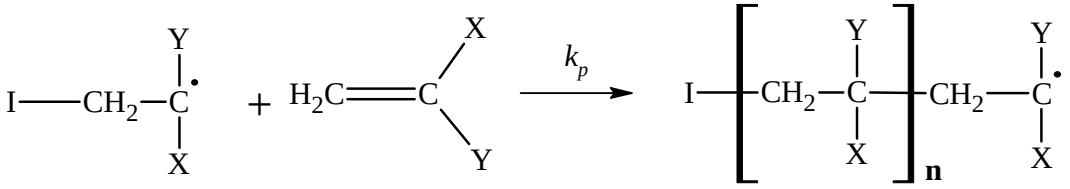

Scheme 2.3: Propagation of a radical by subsequent monomer addition.

Scheme 2.3 illustrates the multiple monomer additions that take place during propagation of the polymer chain. The rate at which addition of monomer to propagating radicals takes place is affected by the nature of the monomer unit and the reactivity of the propagating radical.[26,33] The substituents X and Y play important roles in determining both the reactivity of the monomer and the reactivity of the radical species in a polymerization reaction.

The rate of monomer consumption is expressed as:

$$\frac{-d[M]}{dt} = k_p[M^{\bullet}][M] \qquad (2.6)$$

where $[M^{\bullet}]$, [M] and k_p are the propagating radical concentration, monomer concentration at time t, and propagation rate coefficient. These values can be determined by means of methods such as calorimetry and pulsed laser photolysis.[36] It was proposed by Olaj et al.[37] that the propagation rate coefficient depends on the reaction temperature and the chain length, especially for the first few addition steps, where k_p is higher compared to the long chain propagation rate constant.[26]

In free radical polymerization the entire propagation reaction usually takes place within a fraction of a second. Thousands of monomer units are added to the growing chain within

this time period. The entire propagation process will continue until some termination process occurs. However, the polymerization carries on because the radicals are continuously generated by the decomposition of the initiator, as described in equation (2.4). Polymerization continues until it is limited by other factors such as the viscosity of the reaction medium or depletion of monomer and initiator.

2.2.2.3 The termination step

Termination refers to any step in which radicals are consumed and no new radicals are produced. Theoretically, in free radical polymerization the chain growth should continue until chain termination occurs. The most common termination is bimolecular reaction of propagating radicals that leads to the deactivation of the propagating radical chain ends. The two dominating bimolecular reactions are known as coupling (combination) and disproportionation, as illustrated in Scheme 2.4. These are however not the only possible methods by which termination can take place. Reaction between propagating radicals and inhibitors (e.g. oxygen, phenol, quinone) will also terminate the chain.

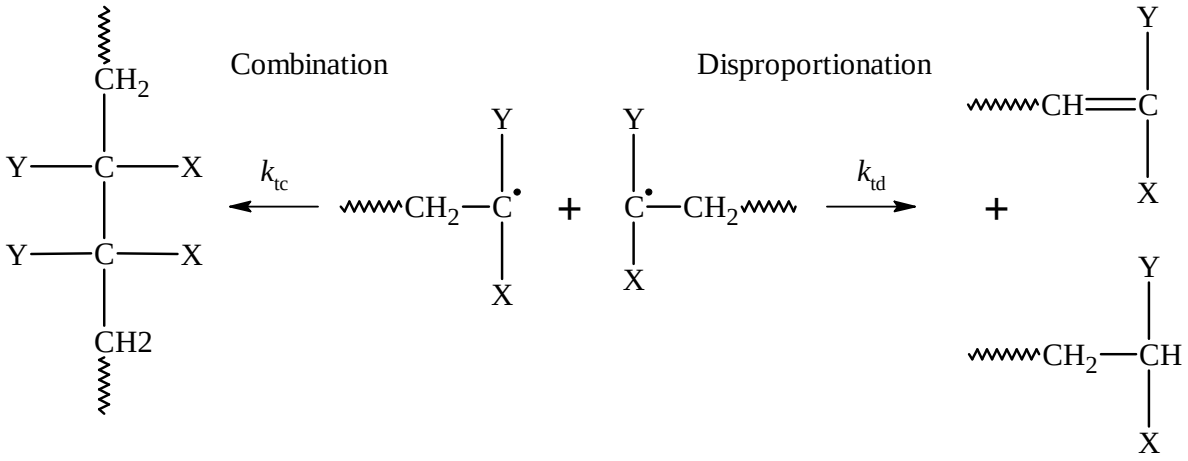

Scheme 2.4: Termination pathways for free radical polymerization.

The coupling reaction occurs between two growing polymer chains that react with each other to form a single terminated (dead) polymer chain of length equal to the sum of the lengths of the original growing chains. In a disproportionation reaction two radicals meet but, instead of coupling, a proton is exchanged to give two terminated (dead) polymer

chains. One is saturated and the other has a terminal double bond, each with a length equal to one of the original growing chains.

The rate of termination is usually determined by the rate of diffusion of the polymer chain.[38] As the molar mass of the chains increase there is a decrease in the diffusion rate of the radical chain ends. The diffusivity of these ends is dependent on the viscosity of the medium and the chain size and shape, and thus it can be deduced that termination is a chain length dependent process.[38-41] The rate of termination is given by:

$$\frac{-d[M^{\bullet}]}{dt} = 2k_t[M^{\bullet}]^2 \qquad (2.7)$$

where $[M^{\bullet}]$ and k_t are the propagating radical concentration and termination rate coefficient, respectively. In this relationship, the termination rate coefficient k_t is a linear combination of the rate coefficient for coupling (k_{tc}) and rate coefficient for disproportionation (k_{td}).[42]

$$k_t = k_{tc} + k_{td}$$

2.2.2.4 Chain transfer reactions

Chain transfer reactions refer to the processes whereby the active site is transferred to an independent molecule such as a monomer, initiator, polymer, solvent or chain transfer agent. Chain transfer is not formally a chain terminating reaction because the overall radical concentration is not reduced.[29] However, it has the tendency to limit the molar mass of polymer chains. Transfer is also a chain length and viscosity dependent process.[43]

The general chain transfer constant C is given by:

$$C = \frac{k_{tr}}{k_p} \qquad (2.8)$$

where k_{tr} is the chain transfer rate coefficient and k_p is the propagation rate coefficient.

The chain transfer constant is the ratio of the chain transfer and propagation rate coefficients.

If the free radical is transferred to a monomer then the original growing chain becomes a dead chain and a new radical begins to grow:

$$P_n^{\bullet} + M \xrightarrow{k_{tm}} P_n + P_1^{\bullet}$$

In a similar reaction, the solvent (S) can serve to transfer a radical:

$$P_n^{\bullet} + S \xrightarrow{k_{ts}} P_n + S^{\bullet}$$

A chain transfer agent *T* can be added to the reaction to enhance radical transfer and thereby reduce the molar mass:

$$P_n^{\bullet} + T \xrightarrow{k_{tt}} P_n + T^{\bullet}$$

The solvent radical $S^{\bullet}$ or the transfer agent radical $T^{\bullet}$ can initiate a new polymer chain by adding monomer units. If the chain end radical abstracts an atom from the backbone of another chain, the result is a new radical that can reinitiate to form a branch.

$$P_n^{\bullet} + P_m \xrightarrow{k_{tp}} P_n + P_i \dot{P} P_j$$

where 1 + j + i= m

If an inhibitor such as hydroquinone (In) is present in the reaction, then the free radical will be converted to the unreactive form Q.

$$P_n^{\bullet} + In \xrightarrow{k_{In}} P_n + Q$$

In principle, transfer can occur to any species in the polymerization system, and for this reason it is very important to choose solvents with transfer properties that are suitable for the target system. The chain transfer constants depend on different factors such as temperature, solvent or monomer.

The number average degree of polymerization DP_n is given by the Mayo equation[38]:

$$\frac{1}{DP_n} = \frac{(1+\lambda)(k_t)[P^{\bullet}]}{k_p[M]} + C_m + C_s\frac{[S]}{[M]} \qquad (2.9)$$

where λ is the fraction of termination by disproportionation, k_t is the termination rate coefficient, $[P^{\bullet}]$ is the overall radical concentration, [M] is the monomer concentration,

C_m is the chain transfer coefficient for chain transfer to monomer, and [S] is the concentration of chain transfer agent in the form of solvent.

2.3 Living radical polymerization (LRP)

The term living polymerization was first used to described a polymerization process in which the chain could propagate and grow without undergoing irreversible termination or chain transfer.[44] In the last few years, considerable effort has been expanded to develop radical processes that display the characteristics of living polymerization.[45-47] The current definition of living radical polymerization is still under debate, but is generally accepted to be a polymerization system that is capable of controlling the molar mass and the structure of the polymers.

Living/controlled radical polymerization (LRP) processes have drawn significant attention from both industry and academia.[26,48] This research area has recently become one of the most rapidly growing areas of polymer chemistry. Through the use of living radical polymerization techniques one is able to maintain the advantages of traditional free radical polymerization. These advantages include the compatibility with a range of vinyl monomers and insensitivity to small traces of impurities, while minimizing the disadvantages such as producing polymers with a wide molar mass distribution. LRP is a viable route to obtain polymers with low polydispersity index (PDI) and controlled molar mass under simple reaction conditions.[45-47] It also offers control over the chain-end functionality of the synthesized polymer, and most importantly gives polymer products that can be reactivated for chain extension with either the same or another monomer. This opens the way to the synthesis of blocks, stars, multiblock copolymers or other polymers of more complex architectures.

Ideally, LRP provides a tool to the design and production of a wide variety of existing as well as new materials that have the potential of revolutionizing the polymer industry. Potential applications of these materials range from novel surfactants, coatings, dispersants, adhesives, and biomaterials, to application in drug delivery.[49] In the past, this was only possible by means of living ionic polymerization techniques, which require stringent reaction conditions such as high vacuum, an inert atmosphere, absence of impurities, and the technique was limited to a relatively small number of monomers.[25]

Several LRP techniques have been developed over the past few decades, and all of them are based either on a reversible termination reaction such as NMP, which is also referred to as Stable Free Radical Mediated Polymerization (SFRP)[50,51] and ATRP[52,53], or based on a reversible chain transfer reaction such as RAFT mediated polymerization.[54,55]

If a living chain undergoes successive activation/deactivation cycles over a period of polymerization time, all living chains will be given an equal chance to grow, yielding a polymer with a low PDI.[26,56] Ideally, all chains are initiated simultaneously and the initiator should be consumed during the early stages of polymerization. The rate of initiation and the rate of exchange between species of various reactivity should be at least as fast as propagation.[26] A few chains are active at any time and the majority of the chains should be dormant. In this way an equilibrium between active species and dormant species is formed, resulting in controlled growth and a final polymer with a low PDI value. This equilibrium is shown in Scheme 2.5.

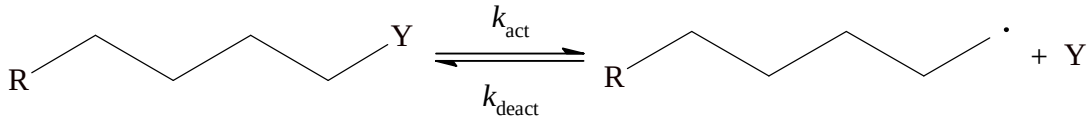

Scheme 2.5: General formation of a dormant species in LRP.

2.3.1 Nitroxide Mediated Polymerization (NMP)

The ability of nitroxide stable radicals to react with carbon centered radicals and to act as radical inhibitors has been known since the beginning of the 1980s.[26,51] However, it was only in 1993 when Georges et al.[57] showed the ability of nitroxides to react reversibly with growing polymer chains that nitroxides became useful for the preparation of polymers with low PDI values. The basic principle of NMP, as described by Hawker,[50,58] is that the carbon oxygen bond of the dormant alkoxyamine is unstable, and undergoes thermal fragmentation to yield a carbon centered radical and a stable nitroxide radical as shown in Scheme 2.6. The carbon centered radical can initiate polymerization to yield a polymeric radical, while the nitroxide radical reacts with the polymeric radical to yield the dormant unreactive species. This results in a low concentration of radicals, and therefore minimizes the termination rate for the polymerization.

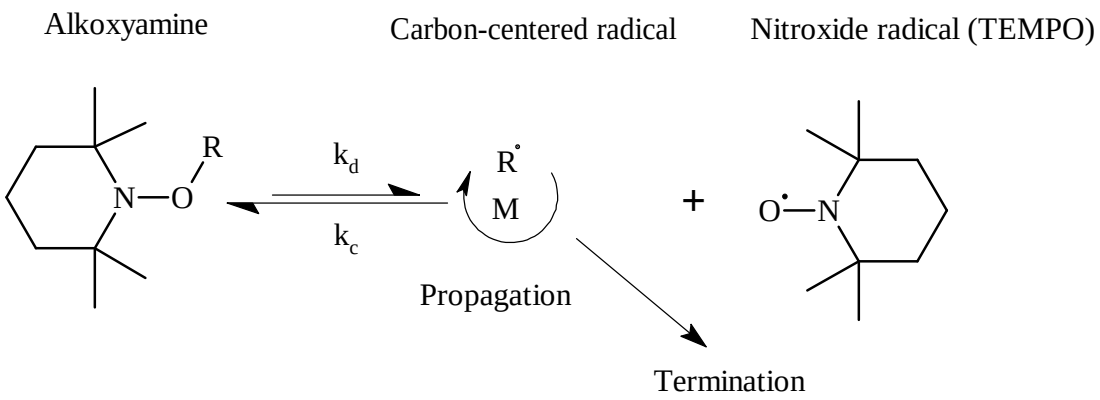

Scheme 2.6: Schematic representation of the NMP process.

Some common nitroxide mediators used in NMP are: 2,2,6,6-tetramethyl-l-piperdinyloxy (TEMPO),[45,46] di-tert-butylnitroxide (DBN),[26,59,60] and N-tert-butyl-N-(1-diethylphosphono-2,2 dimethylpropyl) nitroxide (DEPN).[26,61] See Figure 2.3

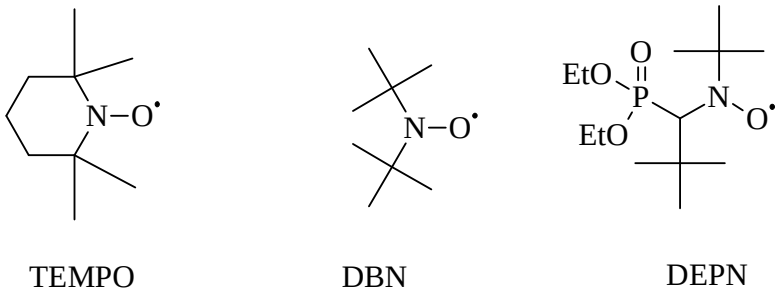

Figure 2.3: Examples of nitroxide mediators.

Among these, TEMPO is by far the most widely used, although it has very limited applicability to monomers other than styrene. Benoit et al.[62] developed α-hydrido alkoxyamines that are a more flexible alternative for NMP. These nitroxides react in much the same way as TEMPO, however, the difference in structure alters the equilibrium position (to the right side) and therefore allows for the polymerization of different monomers, such as acrylates and acrylamides, and provides fast rates of reaction.[26,62] NMP can be successfully used for making block copolymers based on styrene and its derivatives.[63] A major disadvantage of NMP is that the required optimum temperatures are usually high. The C-O bond formed between the nitroxide compound and the propagating radical is relatively stable and a substantial amount of energy is required to break it.[50]

2.3.2 Atom Transfer Radical Polymerization (ATRP)

The term atom transfer radical polymerization comes from the fundamental atom transfer step, which controls the uniform growth of the polymeric chains.[26,64] The concept of using a transition metal complex to mediate radical polymerization has been developed from Atom Transfer Radical Addition (ATRA) reactions, which is a modification of the Kharasch addition reaction, which used light or conventional radical initiators to generate a radical.[65-67]

ATRP is one of the most efficient controlled radical polymerization systems, which provides a route to a wide range of useful polymer architectures, including block copolymers, graft copolymers and star polymers.[26,68-70] It has been very widely applied because of the robustness of the chemistry involved and the commercial availability of many initiators, catalysts and ligands.[71] However, the requirement for a metal catalyst during polymerization is a disadvantage of the ATRP technique, where the catalyst acts as an impurity in the final polymer. Removal of the metal catalyst is typically expensive, but is often necessary before the polymer can be utilized in its final application. In addition, the catalyst is sensitive to other redox processes, and for this reason ATRP has a number of problems in aqueous or acidic media. This is because carboxylic acid based monomers, such as methacrylic acid or acrylic acid form an insoluble complex with the catalyst when ATRP is attempted in aqueous media. Nonetheless, many techniques have been successfully developed and applied to overcome these problems.[64,72,73]

ATRP was discovered independently by Matyjazewski[53] and Sawamoto[52] in 1995. Matyjazewski used the term ATRP whereas Sawamoto called the process transition metal catalyzed radical polymerization. ATRP is in many ways a complex multicomponent system, which includes monomer, initiator with a transferable halogen, catalyst (transition metal compound and a suitable ligand) and can additionally include solvent and various additives.[52,53,64,74,75]

The general mechanism for ATRP is shown in Scheme 2.7, where X represents the halide atom, M_t is the metal atom, L represents the ligand, $P^{\bullet}_m$ is the propagating radical, and n is the oxidation state of the metal.[25,76]

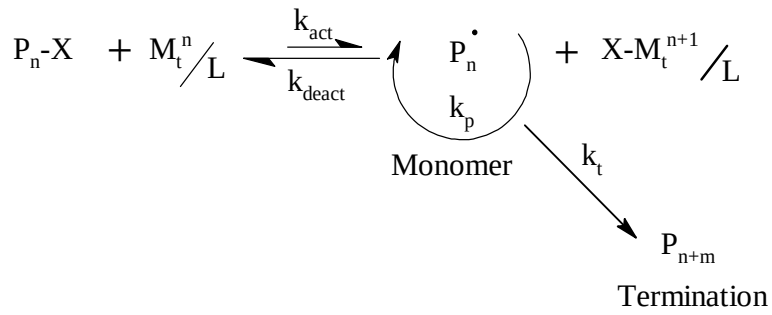

Scheme 2.7: Activation-deactivation equilibrium in ATRP.

ATRP is based on the reversible transfer of a halogen between a dormant alkyl halide (P-X) and a transition metal catalyst (activator, M_t^n/ligand) by redox chemistry. The transition metal catalyst (activator) is responsible for the homolytic cleavage of the alkyl halide bond (with a rate constant of activation k_{act}), which generates the growing radical ($P^{\bullet}$) as well as the corresponding higher oxidation state metal halide complex (deactivator, X-M_t^{n+1}/ligand). Polymer chains grow by the addition of monomer to the growing radicals in a similar manner to conventional free radical polymerization. The growing radical ($P^{\bullet}$, with a rate constant of deactivation, k_{deact}) reacts reversibly with the oxidized metal complex (X-M_t^{n+1}/ligand) to form the halide-capped dormant polymer chain (P_m-X) and the transition metal catalyst (M_t^n/ligand).[26,64,74,77]

In the ATRP process, oxidized metal complexes, the deactivators (X-M_t^{n+1}/ligand), are formed. They behave as persistent radicals to reduce the stationary concentration of the growing radicals; therefore the equilibrium constant ($K_{eq} = k_{act}/k_{deact}$) becomes strongly shifted towards the dormant species, thereby minimizing the termination rate of the polymerization.[76,78-81] As in a typical living polymerization, the number average degree of polymerization (DP_n) can be determined by the ratio of consumed monomer and initiator. The molar mass increases linearly with monomer conversion and can be predicted at any conversion by using equation 2.10.[26]

$$DP_n = \frac{[M]_0}{[I]_0} \text{ x conversion} \qquad (2.10)$$

where $[M]_0$ is the initial monomer concentration and $[I]_0$ is the initial initiator concentration.

In summary, a successful ATRP will have uniform growth of all the chains, which is achieved by fast initiation and rapid, reversible deactivation. Both activating and deactivating components must be simultaneously present in the system. Other factors, such as temperature, solvent, reaction time, additives, and solubility of all components, must also be taken into consideration.[65] A brief outline of these factors will be discussed, with close reference to the reagents used in this study.

2.3.2.1 Initiators

In ATRP, the main role of the initiator is to determine the number of growing polymer chains. The initiator in ATRP is usually a low molar mass alkyl halide (R-X), where the halide group X must be able to migrate between the growing chain and transition metal complex in a rapid and selective manner. It has been found that tertiary alkyl halides are more active than secondary alkyl halides, which in turn are more active than primary alkyl halides.[25] Halogens like chlorine, bromine and iodine, have been used in ATRP polymerization. Thus far, the best molar mass control is achieved when X is either chlorine or bromine.[82] Iodine is used less extensively, but it has been found to work in the controlled polymerization of styrene in rhenium based ATRP.[83] In choosing an initiator, the strength of the R-X bond in the initiator should be considered. Fluorine is therefore not used because the C-F bond is too strong to undergo homolytic cleavage. The general order of bond strength in the alkyl halides is R-Cl > R-Br > R-I.[25] The basic requirement for a good ATRP initiator is that it should have a reactivity that is at least comparable to that of the subsequently formed growing chains.

When the initiating moiety is attached to macromolecular species, macroinitiators are formed and can be used to synthesise block or graft copolymers.

In the past decade, various structural features of initiators have been reported, including: allyl halides,[84] sulfonyl halides,[85] functional (carboxylic acid group),[26] multifunctional star[86] and chloro-telechelic.[87]

2.3.2.2: Catalysts and ligands

The catalyst is arguably the most important component of a ATRP reaction because the choice of catalyst system will ultimately determine the position of atom transfer equilibrium and the dynamics of the interchange between the dormant and active

species.[64] Different types of catalysts have been used, but all can be considered as one electron oxidants/reductants.[26] The main prerequisites for a suitable catalyst include it having a metal center with at least two readily accessible oxidation states separated by one electron and affinity toward halogens. Also, the coordination sphere around the metal should, upon oxidation be able to accommodate a halogen [25,64]

In this study the focus is on the use of a copper complex catalyst, because complexes of copper have been found to be the most efficient catalysts in ATRP for a broad range of monomers in diverse media.[53,74-76] However, many other type of catalysts are also effective under appropriate reaction conditions including ruthenium,[52,64] iron,[64,88-90] nickel,[64,91] palladium,[64] manganese,[26,64] rhenium,[26,82] rhodium, molybdenum[26,64] and chromium.[64]

The selection of a suitable ligand is critical, in order to conduct a controlled ATRP. The ligand determines the solubility of the catalyst complex in the organic medium and adjusts the redox potential of the metal center for appropriate activity. Better solubility of the catalyst complex is often achieved by adding long alkyl substituents to the ligand.[76,92,93] Nitrogen based ligands have been widely used in copper mediated ATRP where bidentate and multidentate nitrogen ligands work best.[94,95] Cyclic and bridged ligands yield more active catalysts than linear ligands do. The activity of nitrogen based ligands for copper mediated ATRP is related to their structure and follows the following order: tetradentate (cyclic-bridged) > tetradentate (branched) > tetradentate (cyclic) > tridentate > tridentate (linear) > bidentate ligands. Activities of copper complexes strongly depend on the ligand structure, and even small structural changes may lead to large differences in their activity.[94] Examples of some nitrogen based ligands successfully used in copper mediated ATRP are: 2,2'-bipyridine(bpy); 4,4'-di(5-nonyl)-2,2'-bipyridine (dNbpy); N,N,N',N',N"pentamethyldiethylenetriamine (PMDETA); 1,1,4,7,10,10-hexamethyltriethylenetetramine (HMTETA), N-(n-propyl)-2-pyridylmethanimine (n-Pr-1); and tris(2-(dimethylamino)ethyl)amine (Me_6TREN).[94]

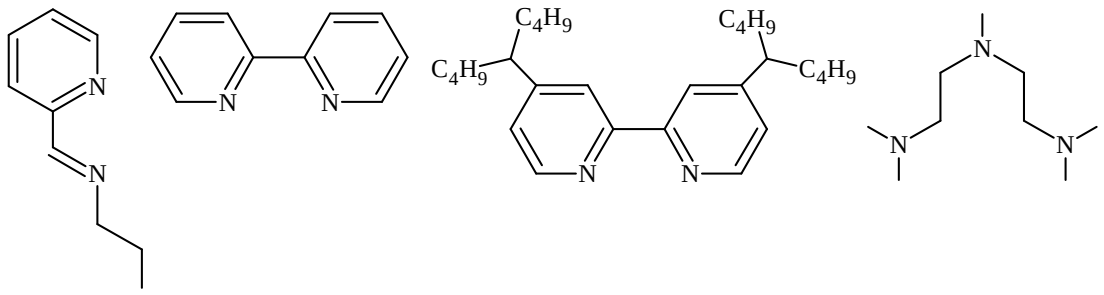

Figure 2.4: Examples of nitrogen based ligands used in copper mediated ATRP.

In this study a simple Schiff base ligand (n-Pr-1) was used. The latter was studied by Haddleton et al.[93] and found to be very effective in the copper mediated ATRP of methacrylate monomers. Bidentate ligands (bpy) and (dNbpy) were also used.

2.3.2.3 Monomers and solvents

Many different monomers have been successfully polymerized using ATRP to yield controlled, well-defined polymers. Typical types of monomers include styrenes, acrylates, methacrylates, dienes and other relatively reactive monomers such as acrylamides, acrylonitrile and vinylpyridine. Most monomers which contain substituents (e.g., phenyl or carbonyl) that can stabilize the propagating radicals are polymerizable via ATRP.[26,64] However, it is still difficult to homopolymerize some less stabilized monomers such as halogenated alkenes, alkyl substituted olefins and vinyl esters, although their copolymerization has been successful in some cases. In addition, acidic monomers should be protected, otherwise they interfere with the initiator by protonation of the ligand, and reduce catalyst reactivity.[26]

Typically, ATRP can be performed in bulk, but sometimes a solvent is necessary in the case of polymers that are insoluble in their monomers (e.g. polyacrylonitrile).[64] Many different solvents, mostly nonpolar, have been used for solution polymerization, such as benzene, p-xylene, diphenyl ether, ethyl acetate, toluene and many other for different monomers.[64] Some polar solvents, such as alcohols, water, dimethylformamide, dimethylsulfoxide and ethylene carbonate have been used successfully.[96-98] Several factors affect the solvent choice. Interaction between solvent and catalyst should be

considered and chain transfer to solvent must be minimized. Catalyst poisoning by solvent must be avoided.[64,99]

2.3.2.4 Temperature and additives

Reaction temperatures used in ATRP are generally in the range of 60-120 °C, although some polymerizations do proceed at lower temperature.[100] The higher the temperature the faster the reaction rate, because both the propagation rate constant and the atom transfer equilibrium constant increase with temperature.[99,101] This can lead to better control, although, chain transfer, decomposition of catalyst and side reactions become more pronounced at elevated temperatures.[91,92] The optimum temperature depends on many factors, including the monomer, the catalyst and the target molar mass.[64]

Ideally, oxygen should be removed from the polymerization reaction because oxygen can rapidly oxidize transition metal catalysts used in ATRP. However, a small amount of oxygen can be tolerated, particularly if a sufficient amount of reducing agent (e.g., Cu (0) or ascorbic acid) is present in the polymerization. Moreover, the addition of zerovalent metal or organic reducing agents in the form of monosaccharides[102] (e.g., glucose, galactose and mannose), or aluminumalkoxides[103] and phenol,[104,105] will reduce the oxidized metal complex (deactivator) to regenerate the transition metal catalyst (activator). Therefore the rate of polymerization will be enhanced, while the necessary control over molar mass and molar mass distribution is maintained.[26,64,102,103,105]

2.3.3 Reversible Addition-Fragmentation Chain Transfer (RAFT) mediated polymerization

Recent trends show that polymers are being increasingly used in sensitive biological and medical applications. It has therefore, become increasingly significant to have control over the length and functionality of the polymer chains. However, when using LRP techniques the choice of the monomer remains a challenge because it is difficult to apply some techniques such as NMP to monomers such as methacrylates. Similarly vinyl acetate cannot be polymerized via the ATRP technique.[25,64,106] In 1998, Rizzardo et al.[54] reported a new LRP technique that has the distinction of being applicable to a vast range of monomers bearing various functional groups, under a wide range of conditions. It is based on reversible addition-fragmentation chain transfer, and it is designated as the RAFT process.

RAFT mediated polymerization has now become one of the most rapidly developing areas in polymer science.[107] This can be ascribed to its ability to control polymer chain length, architecture (di-, tri- or multiblock copolymers, star-shaped polymers, graft copolymers, etc.),[47,108-111] composition and functionality of various polymers under conditions similar to those used in conventional free radical polymerization (i, e. monomers, initiators, solvents and temperature).[24,112] RAFT mediated polymerization is usually carried out by the addition of a small quantity of a chain transfer agent (RAFT agent) to a conventional free radical polymerization mixture.

The RAFT agent/monomer combination should be compatible and correctly chosen (appropriate choice of R- and Z- groups) for a successful RAFT mediated polymerization.[113,114] RAFT agents are simple organic compounds, possessing a thiocarbonyl thio moiety of the general structure Z-C(=S)-S-R, which imparts the living behaviour to free radical polymerization. Z refers to the stabilizing group that governs the reactivity of the C=S toward radical addition, and R refers to the free radical homolytic leaving group that is capable of reinitiating the polymerization.[25,26,115,116]

There are five common classes of thiocarbonyl thio RAFT agents, with different efficiencies towards different monomers, depending on the nature of the Z group. They are classified as follows:

- dithioesters (where Z is aryl or alkyl)[26,117-120]
- trithiocarbonates (where Z is substituted sulphur)[26,109,115,121,122]
- dithiocarbamates (where Z is substituted nitrogen)[26,123]
- xanthates (where Z is substituted oxygen)[26,123,124]
- phosphoryl (where Z is substituted phosphorus).[125,126]

2.3.3.1 Important aspects of Z and R groups

The degree of control exhibited in the RAFT process and the end-functionality of the resulting chains will greatly depend on the structure of the RAFT agent. The selection of the stabilizing Z-group and the leaving R-group are important to determine both the addition and fragmentation rates, and thus the effectiveness of the RAFT agent.[113,114] Transfer constants are also strongly dependent on the Z-group and R-group substituents.

The Z-group should be correctly chosen to stabilize the intermediate radical and to activate the C=S double bond towards the propagating polymeric radical addition in the RAFT polymerization. It is also essential to choose the right Z-group in RAFT mediated polymerization, because different Z-groups have different effects on the rate of radical addition to the C=S double bound.[26,113] The effects of the Z-group on a series of RAFT mediated polymerizations of styrene have been proposed by Chiefari et al.[114] where the chain transfer coefficient decreases in the series where Z is aryl (Ph) > alkyl (CH_3) ~ alkylthio (SCH_2Ph,SCH_3) ~ N-pyrrole > aryloxy (OC_6H_5) > alkoxy > dialkylamino. Examples of Z groups includes[26]:

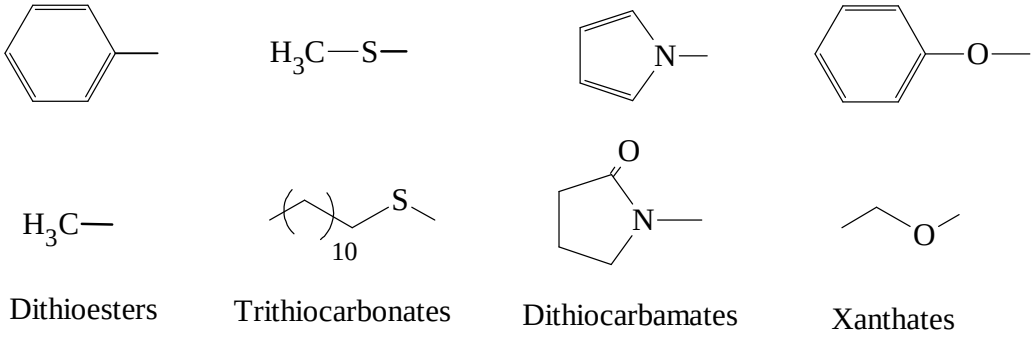

Figure 2.5: Examples of different RAFT agent Z-groups

Similar considerations must be taken into account with regard to the nature of the R-group of the RAFT agent. R groups are commonly related to the monomer being used

or to the initiators that have previously been shown to work successfully in conventional free radical polymerization.[116,123,127] The R-group should be a good free radical leaving group (relative to the growing polymeric chain), which readily fragments upon the formation of an intermediate radical, and is capable of reinitiating polymerization.[25,26,114,128] The R group must be chosen such that its stability is appropriate to the monomer that is to be polymerized. An inappropriate choice of the R-group can lead to significant retardation and uncontrolled polymerization.[24,26,129] A number of factors such as steric factors, radical stability and polar factors appear to be important in determining the leaving group ability of radicals. The more stable, more electrophilic, and more bulky radicals are better leaving groups. The leaving group ability decreases in the series R = tertiary > secondary > primary, because there is a difference in stability of these types of radicals.[113,130]

Examples of R-groups commonly used in RAFT mediated polymerization include:[26]

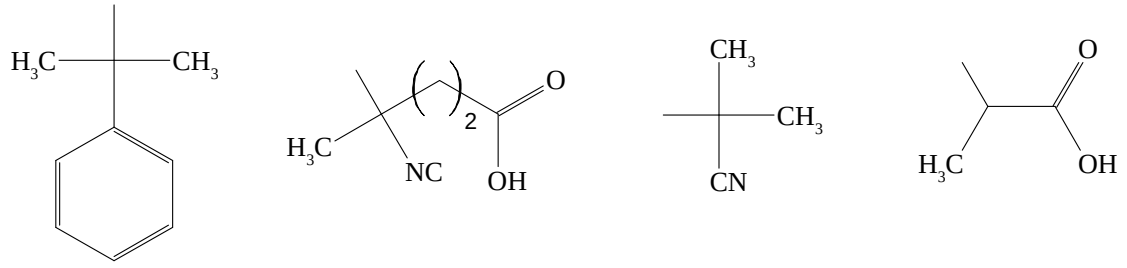

Cumyl | Cyanovaleric acid | Cyanoisopropyl | Propionic acid

Figure 2.6: Examples of different RAFT agent R-groups.

2.3.3.2 Mechanism of RAFT

Evidence for the RAFT mechanism has been obtained using techniques such as Nuclear Magnetic Resonance spectroscopy (NMR),[131] Ultraviolet- visible spectroscopy (UV-vis)[54] and Electron Spin Resonance spectroscopy (ESR).[132]

The general mechanism of RAFT-mediated polymerization as proposed by Rizzardo and coworkers is illustrated in Scheme 2.8:[108]

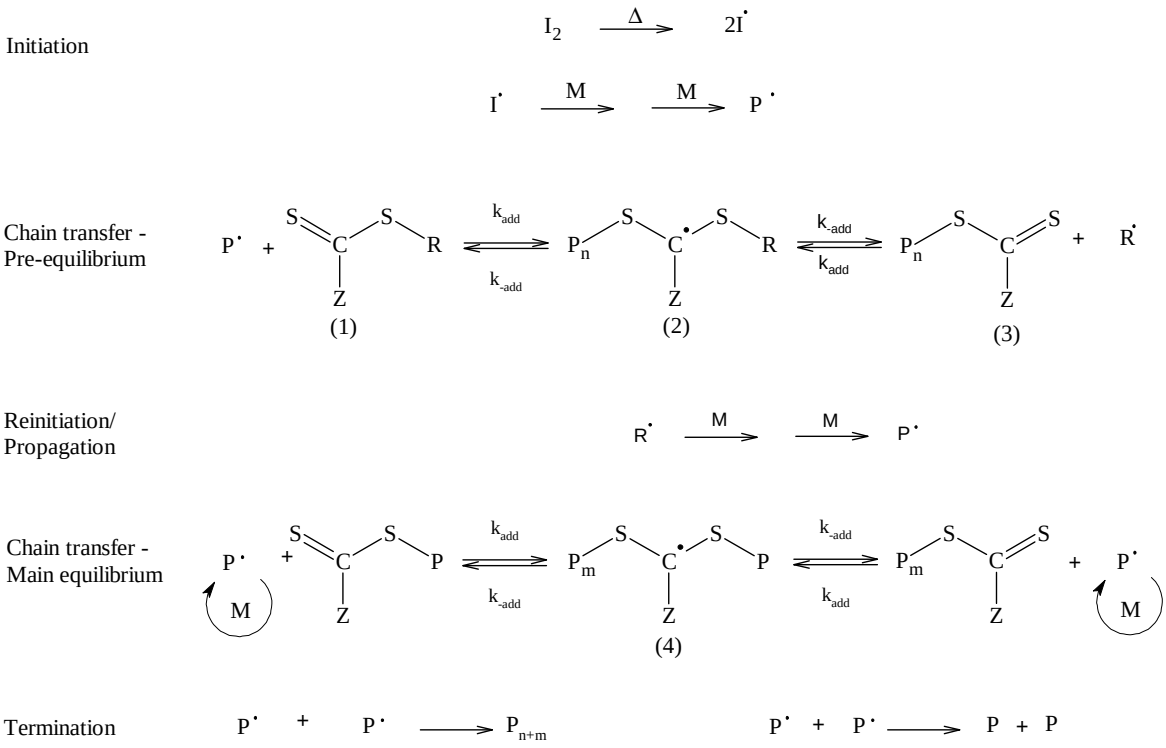

Scheme 2.8: Schematic representation of the mechanism of RAFT mediated polymerization.

RAFT mediated polymerization is initiated by the decomposition of an initiator such as 2,2'-azobis(isobutyronitrile) (AIBN) to form radicals. These radicals tend to undergo addition to the monomer unit, to produce propagating radicals $P^{\bullet}_n$, or react with the (C=S) double bond of the initial RAFT agent at a rate similar to or greater than the rate of addition to the monomer.[55] An intermediate radical is formed upon each addition of radical to the RAFT agent. This intermediate radical (species 2 in Scheme 2.8) undergoes

fragmentation in either of two ways. First, it can fragment back to the original radical species and the initial RAFT agent or, second, it can fragment to yield a leaving group radical $R^{\bullet}$ and a dormant polymeric thiocarbonyl thio compound, which is also called a macro-RAFT agent (species 3 in Scheme 2.8). The leaving group radical $R^{\bullet}$ will propagate (reinitiate) to form a new polymeric radical $P^{\bullet}_{m}$ and then add again to the macro-RAFT agent, forming an intermediate radical (species 4 in Scheme 2.8), which will then fragment, releasing any one of the dormant polymeric thiocarbonyl thio compounds, and the process continues in this manner.

For stepwise growth of polymer chains, the addition rate constant of propagating radicals to the (C=S) double bond in a thiocarbonyl thio compound should be higher than the propagation rate constant of the monomer ($k_{add} > k_p$).[55] This provides an equal probability for all chains to grow, leading to living characteristics and low PDI.

As in all radical polymerizations, some termination always occurs via radical-radical coupling. However, termination is reduced in RAFT mediated polymerization by the low concentration of active radicals with respect to the dormant polymer species.

In the RAFT process, when the polymerization is complete, the great majority of the polymer chains should contain the thiocarbonyl thio moiety as the end group, which allows for the synthesis of various advanced architectures, such as di-, tri- or multiblock copolymers, star-shaped polymers, graft copolymers, etc.

One of the characteristics of the RAFT process is that the molar mass is controlled by the stoichiometry of the reaction and it increases in a linear manner with monomer conversion. Molar mass can be predicted theoretically using equation 2.11, if it is assumed that all the RAFT agents have reacted.[55,108,109,133]

$$M_{n,\,th} = \frac{x[M]_0}{[RAFT]_0} MW_M + MW_{RAFT} \qquad (2.11)$$

where $[M]_0$ and $[RAFT]_0$ are the initial concentrations of the monomer and the RAFT agent, MW_M and MW_{RAFT} are the molar masses of the monomer and the RAFT agent, x is the fractional conversion, and $M_{n,th}$ is the theoretical number average molar mass of the formed polymer.

In most cases, polymers synthesized by RAFT mediated polymerization are coloured. The polymer chains contain the thiocarbonyl thio moiety as the end group, which may decompose to produce odorous byproducts.[25] This might not be desirable from an industrial point of view, and as a result various techniques have been used to remove the RAFT end group once the synthesis of the polymer is complete.[134]

2.4 Graft copolymers

Along with the increasing scientific and technological capabilities of the global society, a growing demand for materials with novel properties for specific applications is evident. Graft copolymers are attractive because they usually retain the unique properties of their individual components and offer the possibility to combine two different and unusual properties that are desirable for a particular application in one polymer structure.[26]

Graft copolymers are a special type of branched copolymer that contain a long sequence of one monomer referred to as the backbone polymer and one or more branches or grafts of long sequences of usually another monomer.[26,135] The chemical nature and composition of the branches and the backbone differ in most cases.[135] Grafted chains (branches) generally possess a degree of polymerization that is less than that of the main chain (backbone). Branches are usually distributed randomly along the backbone, although recent advances in synthetic methods allow the preparation of better defined structures.[135] The simplest case of a graft copolymer can be represented by Scheme 2.9.

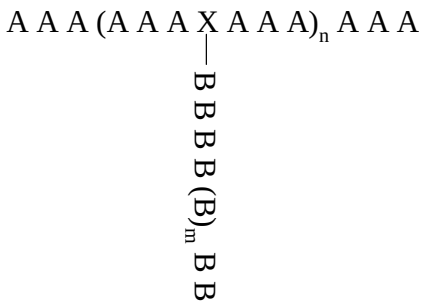

Scheme 2.9: General structure of a simple graft copolymer.

Sequence A represents the main polymer chain or the backbone, sequence B is the grafted or side chain, and X is the unit in the backbone where the graft is attached.

2.4.1 Polymer brushes (densely grafted copolymers)

The study of polymer brushes is of great interest because of their unique properties and potential application in the surface modification of materials.[136,137] This has led to applications in many areas of science and technology, such as the stabilization of colloidal suspensions,[138] lubrication,[139] bioactive surfaces,[140] adhesive,[137]

compatibilizers,[137] composite materials,[137] drug delivery,[137] and in chemical gating for smart materials.[141] The term polymer brushes can be described as assemblies of polymer chains that are tethered by one anchor points to a surface of a planar or spherical solid or to a linear polymer chain, where the graft density of the polymer is high enough such that the chains become crowded, and are forced to stretch away from the surface in order to avoid segmental overlapping.[137,142,143] Thus, molecular brushes are a specific class of graft copolymers containing a high density of polymer side chains that are attached to a polymer backbone at an approximate density of one chain per backbone monomer unit.[25,26,143]

When the distance between two anchored polymers is larger than the size of the surface-attached polymer molecule, so that the polymer side chains do not interact with each other, two cases can be distinguished, depending on the interaction between the polymer side chains and the substrate surface (see Figure 2.7). If there is a strong attractive force between the polymer chains and the surface; the polymer chains are flattened out to a pancake-like conformation.[137,144] However, if the interaction between the polymer chains and the surface is weak, or even repulsive, the polymer chains are attached to the surface through a short stem and form a typical random coil, yielding a mushroom-like conformation.[137]

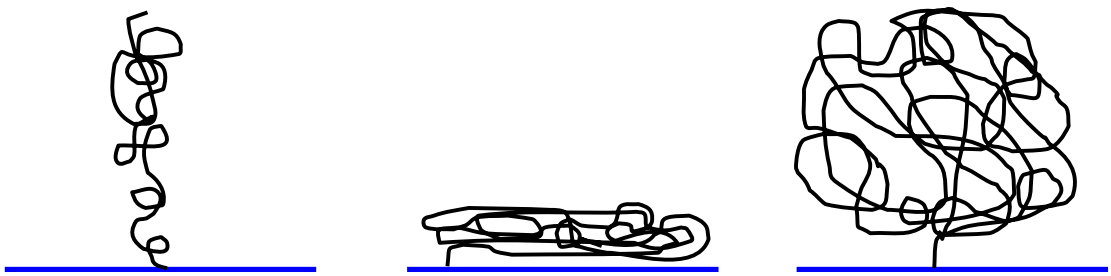

Figure 2.7: Conformations of tethered polymer chains: (A) brush (B) pancake (C) mushroom.

Depending on the substrates, if they are linear polymer chains, planar surfaces, or spherical particles, polymer brushes can be classified as one-dimensional, two-dimensional, and three-dimensional brushes, respectively.[143] Polymer brushes with a much longer backbone than side chain are shown to exhibit the form of cylindrical brush

polymers with the backbone in the core, from which the side chains emanate radially.[137,143] Conversely, molecular brushes with backbones of the order of the length of the side chains yield mostly polymers of spherical or star-like architecture because the main chain hardly exceeds the length of the side chain.[145-147]

2.4.2 Structure of cylindrical polymer brushes

The architecture of cylindrical polymer brushes can be varied by being densely or loosely grafted, having flexible or stiff side chains. In terms of chemical composition, polymer brushes can be classified as homopolymer brushes, mixed homopolymer brushes, branched polymer brushes, and copolymer brushes.[143] Homopolymer brushes refer to an assembly of grafted polymer chains consisting of one type of repeat unit. Block copolymer brushes refer to an assembly of grafted polymer chains consisting of two or more homopolymer chains covalently connected to each other at one end.[137] As shown in Figure 2.8, the structures of cylindrical copolymer brushes can be classified into two broad categories, depending on the direction of chemical heterogeneity of the side chains. If the brushes (side chains) consist of block or statistical copolymer structures along the length of the backbone or the side chains the results are linearly distributed copolymer brushes and radially distributed copolymer brushes, respectively.[137,143]

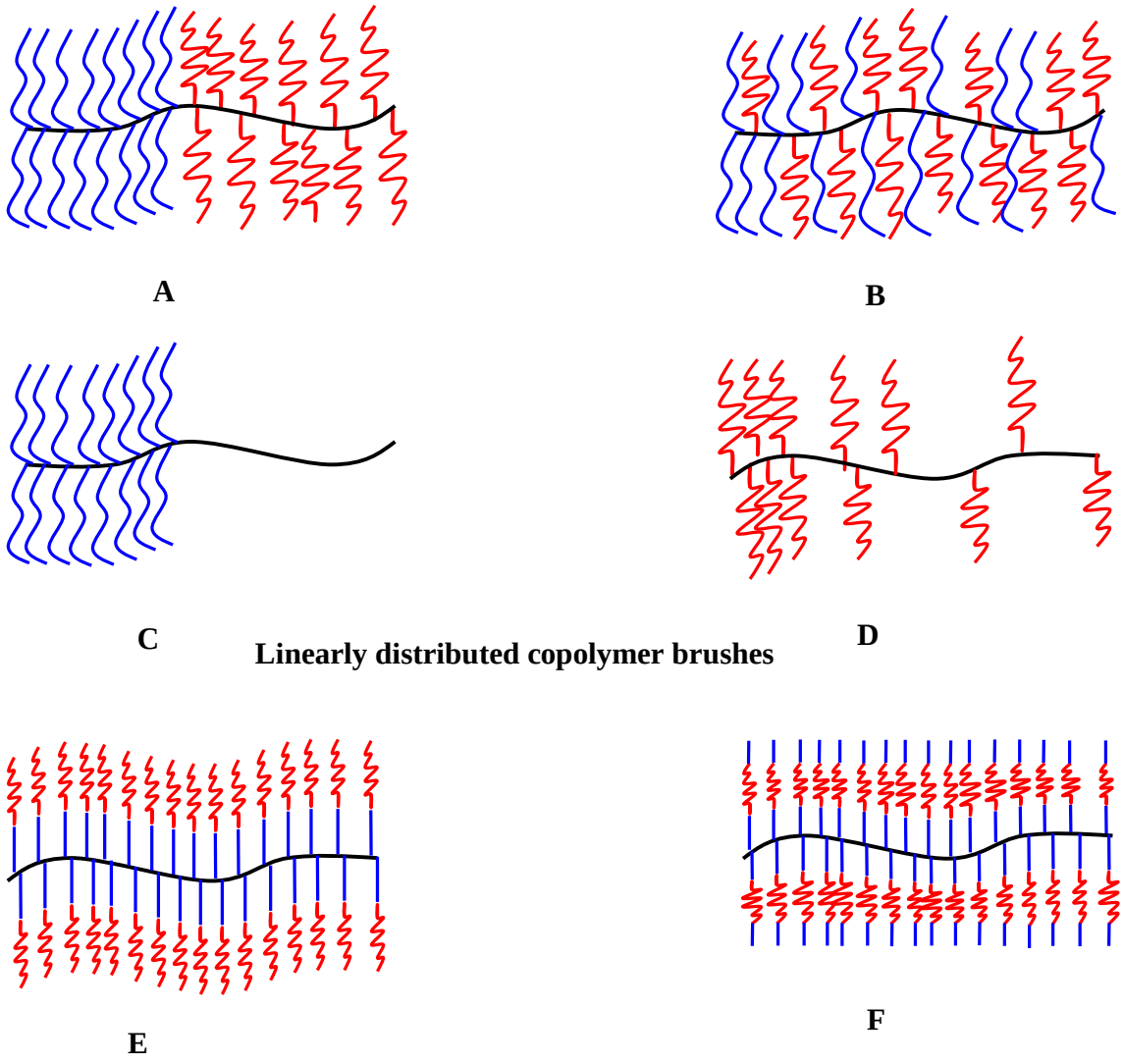

Figure 2.8: Brush copolymer structures with the monomer composition varied linearly or radially. (A) brush-block-brush copolymer, (B) heterograft brush copolymer, (C) brush-coil copolymer or brush-block-linear; (D) gradient brush copolymer; (E) core-shell brush copolymer, (F) triblock copolymer side chains.

2.4.2.1 Linearly distributed copolymer brushes

If a cylindrical polymer brush consist of two types of chemically different homopolymer side chains, which are distributed in a completely asymmetric fashion along the block

copolymer backbone in which both blocks contain side chains, brush-block-brush copolymers are obtained, as seen in Figure 2.8A. A combination of grafting through and grafting from is usually used to prepare brush-block-brush copolymers.[148,149] However, depending on the distribution of the two different side chains along the backbone, alternating or random, and the nature of the solvent, a Janus cylinder brush type or heterograft brush copolymer type are obtained, respectively (Figure 2.8B). These types of polymer brushes can be obtained by copolymerization of macromonomers or by copolymerization of a macromonomer with a low molecular weight monomer containing an initiator precursor functionality.[143,150,151] Yet another different architecture can be envisioned, where the side chains are present in a discontinuous fashion along the backbone, such that at least one block of the backbone has side chains and another section does not, brush-block-linear or brush coil copolymers are formed (Figure 2.8C). There are several examples of molecular brushes with block copolymer backbones reported in the literature in which one block is a cylindrical brush, while the other is composed of a linear polymer.[152] Gradient copolymer brushes (Figure 2.8D) are usually produced when the grafting density of non-randomly distributed side chains are varied gradually along the backbone. In order to vary the spacing between the grafting sites, incorporation of non-initiating side groups into a backbone is necessary. Depending on the reactivity ratios, copolymerization of one monomer with a non initiating pendant group and the second carrying initiating centers will lead to a gradient of active initiating sites along the macroinitiator.[137,153]

2.4.2.2 Radially distributed copolymer brushes

In the radially distributed copolymer brushes the side chains are composed of more than one type of monomer repeat unit. If the side chains consist of block copolymers, cylindrical polymer brushes will have a core-shell structure (Figure 2.8E).[154] On the other hand, when the side chains are prepared of statistical copolymers, the result is cylindrical polymer brushes with statistical copolymer side chains (Figure 2.8F). Cylindrical polymer brushes with soft cores and hard shells were prepared by grafting from, using the ATRP technique.[155]

2.4.3 Synthesis of cylindrical polymer brushes

Regular graft copolymers exhibit the structure of cylindrical brushes if the side chains are densely grafted, that is, each monomer unit of the backbone carries a side chain, and the backbone is much longer than the side chains.[137,156] There are generally two techniques used to tether polymer chains onto a substrate; either physically by physisorption or chemically through covalent attachment. A physisorbed brush typically consists of a two component polymer chain where one part of the polymer chains strongly adheres to the surface, leaving the chains of the other part to stretch away from the surface. A disadvantage to physisorbed brushes is that they are unstable towards solvents or thermal treatment due to the relatively weak Van der Waals forces or hydrogen bonding that anchors them to the surface. Another problem with physisorption is that attachment of more polymer chains is hindered by a diffusion barrier created by the already attached chains, thus resulting in poor control over the grafting density.[137,157] Alternatively as shown in Scheme 2.10,[143] cylindrical polymer brushes possessing densely grafted side chains covalently bonded to a linear backbone can be synthesized by three different strategies (*i*) grafting through method, (*ii*) grafting onto method or (*iii*) grafting from method.[143] Each method has its own advantages and disadvantages in terms of reaching high grafting density and degree of control over the length of the side chains.

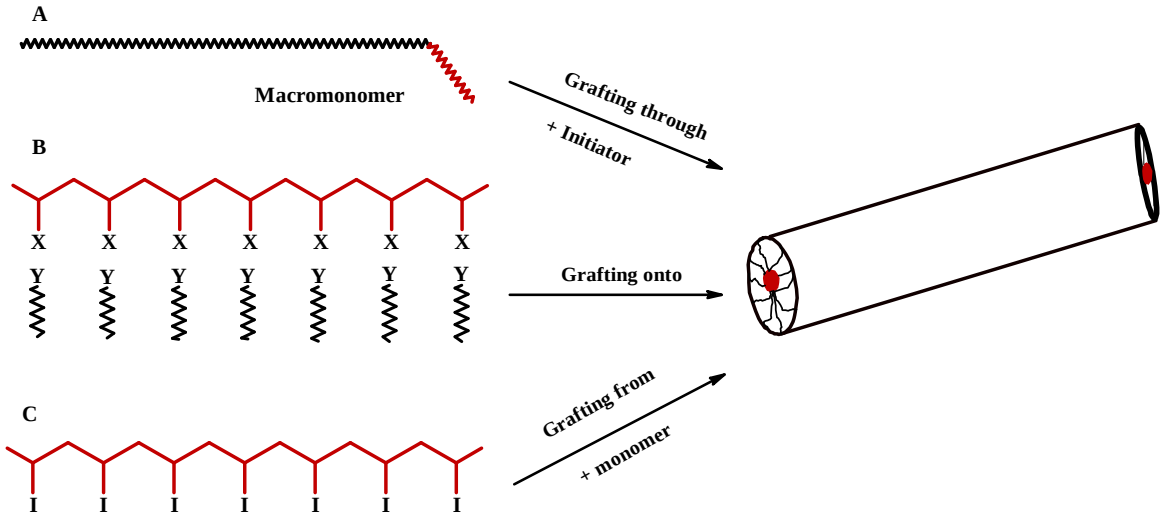

Scheme 2.10: Strategies for the synthesis of cylindrical polymer brushes: (A) grafting through, (B) grafting onto (X and Y are functional groups capable of coupling), (C) grafting from (I is an initiating group).

In this study the focus is on the use of grafting from via the ATRP technique for the synthesis of cylindrical polymer brushes.

2.4.3.1 Grafting through method

The grafting through method is also known as the macromonomer method, which is the homopolymerization or copolymerization of vinyl terminated macromonomers. Grafting through has been applied for the synthesis of cylindrical polymer brushes for more than a decade.[137] In the past, conventional radical polymerization of macromonomers was widely used, producing polymer brushes with a broad chain length distribution. Although macromonomers can be synthesized via LRP techniques, and thus can be well-defined, the resulting polymer brushes often have broad molecular weight distributions.[148,158]

The grafting through method has found widespread use as the physical properties of the arms can be characterized prior to the synthesis of the polymer brushes.[159] Major limitations associated with the radical polymerization of macromonomers are however, the poor size control of the resulting polymer brushes. In addition the incomplete conversion of the macromonomer can lead to the requirement of tedious purification, since fractionation or dialysis would be required to remove unreacted macromonomer.[148]

It has also been difficult to synthesize polymer brushes with a high degree of polymerization, because of the inherently low concentration of polymerizable groups and the steric hindrance of side chains.[160] Nevertheless, a wide variety of polymer brush architectures can be readily synthesized by the grafting through copolymerization of different macromonomers.[135,143]

2.4.3.2 Grafting onto method

In the grafting onto method, preformed, end-functionalized polymer chains are reacted with a functionalized polymer backbone on each monomer unit to generate cylindrical polymer brushes.[137,161] One advantage of this method is that both the backbone and the side chains are prepared via different polymerization techniques, independently, and hence they can be characterized separately before coupling.[137,143] The resulting polymer brushes are therefore well-defined with respect to their backbone and side chains. The covalent attachment makes the polymer layer relatively more thermally and solvolytically stable than physisorbed polymers.[137] However, relatively low grafting densities and very

thin polymer layers are obtained due to the required diffusion of long polymer chains to reactive surface sites. It is also due to steric crowding of already attached chains on the surface that hinder diffusion of more chains to reactive sites.[137] It is therefore difficult to achieve the complete substitution of reactive sites on the backbone by the side chains.[137,143] Typically, an excess of side chains is used in order to obtain a high grafting density. While this approach can successfully lead to an increase in the grafting density, purification becomes problematic when trying to remove the unreacted side chains.[135,137,143,162]

2.4.3.3 Grafting from method

The third method, grafting from, has received much attention recently as a new pathway for the preparation of well-defined cylindrical polymer brushes from a multifunctional macroinitiator backbone.[154,155,163] In the grafting from method the polymerization is directly initiated from a surface immobilized initiator to generate a polymer brush.[137,143]

In the grafting from method, controlled polymerization of the backbone monomer is very important, since the PDI of a brush polymer is governed by that of the macroinitiator. Therefore, various LRP techniques have been utilized to make the backbone (macroinitiator), including ATRP,[68,154] NMP,[50,58] and RAFT mediated polymerization.[164,165] Often, further functionalization (e.g., esterification of hydroxy groups) is needed to achieve the attachment of initiating groups to the backbone.[68,154,163]

ATRP has proven to be a valuable polymerization technique for the preparation of polymer brushes, as both the composition and the degree of polymerization of the backbone and side chains can be precisely controlled.[143] The grafting from approach was adapted to ATRP to synthesize a variety of molecular architectures, such as block copolymer brushes, star like brushes, and gradient brushes.[53,64,154,166] There have been several reports in the literature of molecular brushes synthesized by grafting from via ATRP of styrenic, acrylate and methacrylate monomers.[68,151,154]

One advantages of the technique is the possibility to obtain high grafting densities and thick polymer films, because the propagation of polymer chain only requires the diffusion of small monomer molecules which simultaneously grow in a progressive fashion.[137,143] Moreover, the purification of the resulting polymer brushes is much simpler than in the

case of the other two grafting methods.[137,163] The method also facilitates low radical concentrations which causes inter- and intramolecular termination events to be significantly suppressed, since inter- and intramolecular termination can lead to macroscopic gelation.[56,64,166] Among the different LRP techniques that are available, grafting from via ATRP has been most extensively used to produce polymer brushes.[162]

2.5 References

(1) Okada, M.; Tachikawa, K.; Aoi, K. *J. Polym. Sci. Part A: Polym. Chem.* **1997**, *35*, 2729-2737.

(2) Mosnacek, J.; Matyjaszewski, K. *Macromolecules* **2008**, *41*, 5509-5511.

(3) Fang, J.; Fowler, P. *J. Food, Agric. & Environ.* **2003**, *1*, 82-84.

(4) Narain, R.; Armes, S. P. *Chem. Commun.* **2002**, *23*, 2776-2777.

(5) Albertin, L.; Stenzel, M. H.; Barner-Kowollik, C.; Foster, L. J. R.; Davis, T. P. *Macromolecules* **2005**, *38*, 9075-9084.

(6) Bernard, J.; Hao, X.; Davis, T. P.; Barner-Kowollik, C.; Stenzel, M. H. *Biomacromolecules* **2006**, *7*, 232-238.

(7) Albertin, L.; Stenzel, M.; Barner-Kowollik, C.; Foster, L. J. R.; Davis, T. P. *Macromolecules* **2004**, *37*, 7530-7537.

(8) Cerrada, M. L.; Sanchez-Chaves, M.; Ruiz, C.; Fernandez-Garcia, M. *Eur. Polym. J.* **2008**, *44*, 2194-2201.

(9) Brandenburg, K.; Andrae, J.; Mueller, M.; Koch, M. H. J.; Garidel, P. *Carbohydr. Res.* **2003**, *338*, 2477-2489.

(10) You, L. C.; Lu, F. Z.; Li, Z. C.; Zhang, W.; Li, F. M. *Macromolecules* **2003**, *36*, 1-4.

(11) Narain, R.; Armes, S. P. *Biomacromolecules* **2003**, *4*, 1746-1758.

(12) Ladmiral, V.; Melia, E.; Haddleton, D. M. *Eur. Polym. J.* **2004**, *40*, 431-449.

(13) Choi, S.-K.; Mammen, M.; Whitesides, G. M. *J. Am. Chem. Soc.* **1997**, *119*, 4103-4111.

(14) Palomino, E. *Adv. Drug Deliv. Rev.* **1994**, *13*, 311-323.

(15) Karamuk, E.; Mayer, J.; Wintermantel, E.; Akaike, T. *Artif. Organs.* **1999**, *23*, 881-884.

(16) Miyata, T.; Uragami, T.; Nakamae, K. *Adv. Drug Deliv. Rev.* **2002**, *54*, 79-98.

(17) Novick, S. J.; Dordick, J. S. *Chem. Mater.* **1998**, *10*, 955-958.

(18) Gruber, H.; Knaus, S. *Macromol. Symp.* **2000**, *152*, 95-105.

(19) Wulff, G.; Zhu, L.; Schmidt, H. *Macromolecules* **1997**, *30*, 4533-4539.

(20) Okada, M. *Prog. Polym. Sci.* **2001**, *26*, 67-104.

(21) Lowe, A. B.; Sumerlin, B. S.; McCormick, C. L. *Polymer* **2003**, *44*, 6761-6765.

(22) Grande, D.; Baskaran, S.; Chaikof, E. L. *Macromolecules* **2001**, *34*, 1640-1646.

(23) Ohno, K.; Tsujii, Y.; Fukuda, T. *J. Polym. Sci. Part A: Polym. Chem.* **1998**, *36*, 2473-2481.

(24) Albertin, L.; Cameron, N. R. *Macromolecules* **2007**, *40*, 6082-6093.

(25) Moad, G.; Solomon, D. *The Chemistry of Radical Polymerization*, 2nd ed.; Elsevier: Heidelberg, 2006.

(26) Matyjaszewski, K.; Davis, T. P. *Handbook of Radical Polymerization*; John Wiley and Sons, Inc.: Canada, 2002.

(27) Hong, K.; Zhang, H.; Mays, J. W.; Visser, A. E.; Brazel, S.; Holbrey, D.; Reichert, W. M.; Rogers, R. D. *Chem. Commun.* **2002**, 1368-1369.

(28) Moad, G.; Rizzardo, E.; Thang, S. H. *Aust. J. Chem.* **2005**, *58*, 379-410.

(29) Shipp, D. A. *J. Macromol. Sci.* **2005**, *45*, 171-194.

(30) Isobe, Y.; Fujioka, D.; Habaue, S.; Okamoto, Y. *J. Am. Chem. Soc.* **2001**, *123*, 7180-7181.

(31) Ray, B.; Isobe, Y.; Morioka, K.; Habaue, S.; Okamoto, Y.; Kamigaito, M.; Sawamoto, M. *Macromolecules* **2003**, *36*, 543-545.

(32) Morrison, R.; Boyd, R. *Organic Chemistry*, Third ed.; Allyn and Bacon: New York.

(33) Beuermann, S.; Buback, M. *Prog. Polym. Sci.* **2002**, *27*, 191-254.

(34) Bai, R.-K.; You, Y.-Z.; Pan, C.-Y. *Macromol. Rapid Comm.* **2001**, *22*, 315-319.

(35) Sandler, S.; Karo, W. *Polymer Syntheses*, Second ed.; Wasserman, H., Ed.; Academic Press.: London, 1992.

(36) Olaj, O. F.; Bitai, I.; Hinkelman, F. *Macromol. Chem.* **1987**, *188*, 1689-1702.

(37) Olaj, O. F.; Vana, P.; Zoder, M. *Macromolecules* **2002**, *35*, 1208-1214.

(38) Heuts, J. P. A.; Davis, T. P.; Russell, G. T. *Macromolecules* **1999**, *32*, 6019-6030.

(39) Russell, G. T.; Gilbert, R. G.; Napper, D. H. *Macromolecules* **1992**, *25*, 2459-2469.

(40) Russell, G. T.; Gilbert, R. G.; Napper, D. H. *Macromolecules* **1993**, *26*, 3538-3552.

(41) Scheren, P. A. G. M.; Russell, G. T.; Sangster, D. F.; Gilbert, R. G.; German, A. L. *Macromolecules* **1995**, *28*, 3637-3649.

(42) Powell, F.; Brooks, B. *Chem. Eng. Sci.* **1995**, *50*, 837-848.

(43) Casey, B. S.; Mills, M. F.; Sangster, D. F.; Gilbert, R. G.; Napper, D. H. *Macromolecules* **1992**, *25*, 7063-7065.

(44) Szwarc, M. *J. Polym. Sci. Part A: Polym. Chem.* **1998**, *36*, ix-xv.

(45) Pradel, J. L.; Boutevin, B.; Ameduri, B. *J. Polym. Sci. Part A: Polym. Chem.* **2000**, *38*, 3293-3302.

(46) Miura, Y.; Nakamura, N.; Taninguchi, I. *Macromolecules* **2001**, *34*, 447-455.

(47) De Brouwer, H.; Schellekens, M. A. J.; Klumperman, B.; Monteiro, M. J.; German, A. L. *J. Polym. Sci. Part A: Polym. Chem.* **2000**, *38*, 3596-3603.

(48) Perrier, S.; Takolpuckdee, P. *J. Polym. Sci. Part A: Polym. Chem.* **2005**, *43*, 5347-5393.

(49) Moad, G.; Chiefari, J.; Chong, B. Y.; Krstina, J.; Mayadunne, R. T.; Postma, A.; Rizzardo, E.; Thang, S. H. *Polym. Int.* **2000**, *49*, 993-1001.

(50) Hawker, C. J.; Bosman, A. W.; Harth, E. *Chem. Rev.* **2001**, *101*, 3661-3688.

(51) Moad, G.; Rizzardo, E.; Solomon, D. H. *Macromolecules* **1982**, *15*, 909-914.

(52) Kato, M.; Kamigaito, M.; Sawamoto, M.; Higashimura, T. *Macromolecules* **1995**, *28*, 1721-1723.

(53) Wang, J.-S.; Matyjaszewski, K. *J. Am. Chem. Soc.* **1995**, *117*, 5614-5615.

(54) Chiefari, J.; Chong, Y. K. B.; Ercole, F.; Krstina, J.; Jeffery, J.; Le, T. P. T.; Mayadunne, R. T. A.; Meijs, G. F.; Moad, C. L.; Moad, G.; Rizzardo, E.; Thang, S. H. *Macromolecules* **1998**, *31*, 5559-5562.

(55) Mayadunne, R. T. A.; Rizzardo, E.; Chiefari, J.; Chong, Y. K.; Moad, G.; Thang, S. H. *Macromolecules* **1999**, *32*, 6877-6980.

(56) Goto, A.; Fukuda, T. *Prog. Polym. Sci.* **2004**, *29*, 329-385.

(57) Georges, M. K.; Veregin, R. P. N.; Kazmaier, P. M.; Hamer, G. K. *Macromolecules* **1993**, *26*, 2987-2988.

(58) Hawker, C. J. *Acc. Chem. Res.* **1997**, *30*, 373-382.

(59) Goto, A.; Fukuda, T. *Macromolecules* **1999**, *32*, 618-623.

(60) Jousset, S.; Hammouch, S.; Catala, O. *Macromolecules* **1997**, *30*, 6685-6687.

(61) Farcet, C.; Lansalot, M.; Charleux, B.; Pirri, R.; Vairon, J.-P. *Macromolecules* **2000**, *33*, 8559-8570.

(62) Benoit, D.; Hawker, C. J.; Huang, E. E.; Lin, Z.; Russell, T. P. *Macromolecules* **2000**, *33*, 1505-1507.

(63) Yoshida, E.; Ishizone, T.; Hirao, A.; Nakaharna, S.; Takataj, T.; Endoj, T. *Macromolecules* **1994**, *27*, 3119-3124.

(64) Matyjaszewski, K.; Xia, J. *Chem. Rev.* **2001**, *101*, 2921-2990.

(65) Davis, K. A.; Matyjaszewski, K. *Statistical, Gradient, Block, and Graft Copolymers by Controlled/Living Radical Polymerizations*; Springer: Berlin / Heidelberg, 2002.

(66) Haddleton, D. M.; Kukulj, D.; Duncalf, D. J.; Heming, A. M.; Shooter, A. J. *Macromolecules* **1998**, *31*, 5201-5205.

(67) Gossage, R. A.; Van de Kuil, L. A.; Van Koten, G. *Acc. Chem. Res.* **1998**, *31*, 423-431.

(68) Beers, K. L.; Gaynor, S. G.; Matyjaszewski, K.; Sheiko, S. S.; Möller, M. *Macromolecules* **1998**, *31*, 9413-9415.

(69) Patten, T. E.; Matyjaszewski, K. *Adv. Mater.* **1998**, *10*, 901-915.

(70) Patten, T. E.; Matyjaszewski, K. *Acc. Chem. Res.* **1999**, *32*, 895-903.

(71) Venkataraman, S.; Wooley, K. L. *Macromolecules* **2006**, *39*, 9661-9664.

(72) Oh, J. K.; Min, K.; Matyjaszewski, K. *Macromolecules* **2006**, *39*, 3161-3167.

(73) Jakubowski., W.; Kirci-Denizli., B.; Gil., R. R.; Matyjaszewski, K. *Macromol. Chem. Phys.* **2008**, *209*, 32-39.

(74) Braunecker, W.; Matyjaszewski, K. *Prog. Polym. Sci.* **2007**, *32*, 93-146.

(75) Wang, J.-S.; Matyjaszewski, K. *Macromolecules* **1995**, *28*, 7901-7910.

(76) Matyjaszewski, K.; Patten, T. E.; Xia, J. *J. Am. Chem. Soc.* **1997**, *119*, 674-680.

(77) Percec, V.; Barboiu, B.; Kim, H.-J. *J. Am. Chem. Soc.* **1998**, *120*, 305-316.

(78) Fischer, H. *J. Polym. Sci. Part A: Polym. Chem.* **1999**, *37*, 1885-1901.

(79) Ohno, K.; Goto, A.; Fukuda, T.; Xia, J.; Matyjaszewski, K. *Macromolecules* **1998**, *31*, 2699-2701.

(80) Fischer., H. *Chemical Reviews* **2001**, *101*, 3581-3610.

(81) Tang, W.; Tsarevsky, N. V.; Matyjaszewski, K. *J. Am. Chem. Soc.* **2006**, *128*, 1598-1604.

(82) Kotani, Y.; Kamigaito, M.; Sawamoto, M. *Macromolecules* **1999**, *32*, 2420-2424.

(83) Kotani, Y.; Kamigaito, M.; Sawamoto, M. *Macromolecules* **2000**, *33*, 6746-6751.

(84) Nakagawa, Y.; Matyjaszewski, K. *Polymer* **1998**, *30*, 138-141.

(85) Wang, J.-L.; Grimaud, T.; Matyjaszewski, K. *Macromolecules* **1997**, *30*, 6507-6512.

(86) Kickelbick, G.; Miller, P. J.; Matyjaszewski, K. *Polym. Prepr.* **1998**, *39*, 284-285.

(87) Reining, B.; Keul, H.; Hocker, H. *Polymer* **1999**, *40*, 3555-3563.

(88) Teodorescu, M.; Gaynor, S. G.; Matyjaszewski, K. *Macromolecules* **2000**, *33*, 2335-2339.

(89) Ando, T.; Kamigaito, M.; Sawamoto, M. *Macromolecules* **1997**, *30*, 4507-4510.

(90) Matyjaszewski, K.; Wei, M.; Xia, J.; McDermott, N. E. *Macromolecules* **1997**, *30*, 8161-8164.

(91) Uegaki, H.; Kotani, Y.; Kamigaito, M.; Sawamoto, M. *Macromolecules* **1997**, *30*, 2249-2253.

(92) Percec, V.; Barboiu, B.; Neumann, A.; Ronda, J. C.; Zhao, M. *Macromolecules* **1996**, *29*, 3665-3668.

(93) Haddleton, D. M.; Crossman, M. C.; Dana, B. H.; Duncalf, D. J.; Heming, A. M.; Kukulj, D.; Shooter, A. J. *Macromolecules* **1999**, *32*, 2110-2119.

(94) Tang, W.; Matyjaszewski, K. *Macromolecules* **2006**, *39*, 4953-4959.

(95) Tang, H.; Arulsamy, N.; Radosz, M.; Shen, Y.; Tsarevsky, N. V.; Braunecker, W. A.; Tang, W.; Matyjaszewski, K. *J. Am. Chem. Soc.* **2006**, *128*, 16277-16285.

(96) Kricheldorf., H. R.; Nuyken., O.; Swift., G. *Handbook of Polymer Synthesis*, 2nd ed.; Marcel Dekker: New York, 2005.

(97) Iovu, M.; Maithufi, N.; Mapolie, S. *Macromol. Symp.* **2003**, *193*, 209-226.

(98) Teoh, R. L.; Guice, K. B.; Loo, Y.-L. *Macromolecules* **2006**, *39*, 8609-8615.

(99) Matyjaszewski, K.; Davis, K.; Patten, T. E.; Wei, M. *Tetrahedron* **1997**, *53*, 15321-15329.

(100) Odian., G. *Principles of Polymerization*, 4th ed.; John Wiley and Sons.: Hoboken, New Jersey, 2004.

(101) Matyjaszewski, K. *Macromol. Symp.* **1998**, *134*, 105-118.

(102) De Vries, A.; Klumperman, B.; de Wet-Roos, D.; Sanderson, R. D. *Macromol. Chem. Phys.* **2001**, *202*, 1645-1648.

(103) Guo, J.; Han, Z.; Wu, P. *J. Mol. Catal. A: Chem.* **2000**, *159*, 77-83.

(104) Gnanou., Y.; Hizal., G. *J. Polym. Sci. Part A: Polym. Chem.* **2004**, *42*, 351-359.

(105) Haddleton, D. M.; Clark, A. J.; Crossman, M. C.; Duncalf, D. J.; Heming, A. M.; Morsley, S. R.; Shooter, A. J. *Chem. Commun.* **1997**, *13*, 1173-1174.

(106) Shim, S. E.; Jung, H.; Lee, H.; Biswas, J.; Choe, S. *Polymer* **2003**, *44*, 5563-5572.

(107) Adamy, M.; Van Herk, A. M.; Destarac, M.; Monteiro, M. J. *Macromolecules* **2003**, *36*, 2293-2301.

(108) Chong, B. Y. K.; Le, T. P. T.; Moad, G.; Rizzardo, E.; Thang, S. H. *Macromolecules* **1999**, *32*, 2071-2074.

(109) Mayadunne, R. T. A.; Rizzardo, E.; Chiefari, J.; Krstina, J.; Moad, G.; Postma, A.; Thang, S. H. *Macromolecules* **2000**, *33*, 243-245.

(110) Perrier, S.; Takolpuckdee, P.; Westwood, J.; Lewis, D. M. *Macromolecules* **2004**, *37*, 2709-2717.

(111) Vosloo, J. J.; Tonge, M. P.; Fellows, C. M.; D'Agosto, F.; Sanderson, R. D.; Gilbert, R. G. *Macromolecules* **2004**, *37*, 2371-2382.

(112) Rizzardo, E.; Chiefari, J.; Chong, B. Y. K.; Ercole, F.; Krstina, J.; Jeffery, J.; Le, T. P. T.; Mayadunne, R. T. A.; Meijs, G. F.; Moad, C. L.; Moad, G.; Thang, S. H. *Macromol. Symp.* **1999**, *143*, 291-307.

(113) Chong, B. Y. K.; Krstina, J.; Le, T. P. T.; Moad, G.; Postma, A.; Rizzardo, E.; Thang, S. H. *Macromolecules* **2003**, *36*, 2256-2272.

(114) Chiefari, J.; Mayadunne, R. T. A.; Moad, C. L.; Moad, G.; Rizzardo, E.; Postma, A.; Skidmore, M. A.; Thang, S. H. *Macromolecules* **2003**, *36*, 2273-2283.

(115) Smulders, W.; Gilbert, R. G.; Monteiro, M. J. *Macromolecules* **2003**, *36*, 4309-4318.

(116) Bouhadir, G.; Legrand, N.; Quiclet-Sire, B.; Zard, S. Z. *Tetrahedron Lett.* **1999**, *40*, 277-280.

(117) Tonge, M. P.; McLeary, J. B.; Vosloo, J. J.; Sanderson, R. D. *Macromol. Symp.* **2003**, *193*, 289-304.

(118) Barner, L.; Quinn, J. F.; Barner-Kowollik, C.; Vana, P.; Davis, T. P. *Eur. Polym. J.* **2003**, *39*, 449-459.

(119) Perrier, S.; Davis, T. P.; Carmichael, A. J.; Haddleton, D. M. *Eur. Polym. J.* **2003**, *39*, 417-422.

(120) Prescott, S. W.; Ballard, M. J.; Rizzardo, E.; Gilbert, R. G. *Macromolecules* **2002**, *35*, 5417-5425.

(121) Stenzel, M. H.; Davis, T. P. *J. Polym. Sci. Part A: Polym. Chem.* **2002**, *40*, 4498-4512.

(122) You, Y.-Z.; Chun-Yan, H.; Bai, R.-K.; Pan, C.-Y.; Wang, J. *Macromol. Chem. Phys.* **2002**, *203*, 477-483.

(123) Thang, S. H.; Chong, Y. K. B.; Mayadunne, R. T. A.; Moad, G.; Rizzardo, E. *Tetrahedron Lett.* **1999**, *40*, 2435-2438.

(124) Quiclet-Sire, B.; Wilczewska, A.; Zard, S. Z. *Tetrahedron Lett.* **2000**, *41*, 5673-5677.

(125) Alberti, A.; Benaglia, M.; Laus, M.; Macciantelli, D.; Sparnacci, K. *Macromolecules* **2003**, *36*, 736-740.

(126) Laus, M.; Papa, R.; Sparnacci, K.; Alberti, A.; Benaglia, M.; Macciantelli, D. *Macromolecules* **2001**, *34*, 7269-7275.

(127) Tang, C.; Kowalewski, T.; Matyjaszewski, K. *Macromolecules* **2003**, *36*, 8587-8589.

(128) Rizzardo, E.; Chiefari, J.; Moad, G.; Thang, S. H. *ACS Symp. Ser.* **2000**, *786*, 278-296.

(129) Chernikova, E.; Morozov, A.; Leonova, E.; Garina, E.; Golubev, V.; Bui, C.; Charleux, B. *Macromolecules* **2004**, *37*, 6329-6339.

(130) Hawthorne, D. G.; Moad, G.; Rizzardo, E.; Thang, S. H. *Macromolecules* **1999**, *32*, 5457-5459.

(131) McLeary, J. B.; Calitz, F. M.; McKenzie, J. M.; Tonge, M. P.; Sanderson, R. D.; Klumperman, B. *Macromolecules* **2004**, *37*, 2383-2394.

(132) Calitz, F. M.; Tonge, M. P.; Sanderson, R. D. *Macromolecules* **2003**, *36*, 5-8.

(133) Vana, P.; Davis, T. P.; Barner-Kowollik, C. *Macromol. Theory Simul.* **2002**, *11*, 823-835.

(134) Postma, A.; Davis, T. P.; Evans, R. A.; Li, G.; Moad, G.; O'Shea, M. S. *Macromolecules* **2006**, *39*, 5293-5306.

(135) Hadjichristidis, N.; Pitsikalis, M.; Pispas, S.; Iatrou, H. *J. Am. Chem. Soc.* **2001**, *101*, 3747-3792.

(136) Halperin, A.; Tirrell, M.; Lodge, T. P. *Adv. Polym. Sci.* **1992**, *100*, 31-71.

(137) Advincula, R. C.; Brittain, W. J.; Caster, K. C.; Ruhe, J. *Polymer Brushes : Synthesis, Characterization, Applications*; Wiley-VCH: Weinheim, 2004.

(138) Pincus, P. *Macromolecules* **1991**, *24*, 2912-2919.

(139) Joanny, J. F. *Langmuir* **1992**, *8*, 989-995.

(140) Tiller, J. C.; Lee, S. B.; Lewis, K.; Klibanov, A. M. *Biotechnol. Bioeng* **2002**, *79*, 465-471.

(141) Ito, Y.; Ochiai, Y.; Park, Y. S.; Imanishi, Y. *J. Am. Chem. Soc.* **1997**, *119*, 1619-1623.

(142) Sumerlin, B. S.; Neugebauer, D.; Matyjaszewski, K. *Macromolecules* **2005**, *38*, 702-708.

(143) Zhang, M.; Müller, A. H. E. *J. Polym. Sci. Part A: Polym. Chem.* **2005**, *43*, 3461-3481.

(144) De Gennes, P. G. *Macromolecules* **2002**, *13*, 1069-1075.

(145) Djalali, R.; Li, S.-Y.; Schmidt, M. *Macromolecules* **2002**, *35*, 4282-4288.

(146) Muthukrishnan, S.; Zhang, M.; Burkhardt, M.; Drechsler, M.; Mori, H.; Müller, A. H. E. *Macromolecules* **2005**, *38*, 7926-7934.

(147) Ito, K.; Kawaguchi, S. *Adv. Polym. Sci.* **1999**, *142*, 129-178.

(148) Qin, S.; Matyjaszewski, K.; Xu, H.; Sheiko, S. S. *Macromolecules* **2003**, *36*, 605-612.

(149) Ishizu, K.; Satoh, J.; Sogabe, A. *J. Colloid Interface Sci.* **2004**, *274*, 472-479.

(150) Liu, Y.; Abetz, V.; Müller, A. H. E. *Macromolecules* **2003**, *36*, 7894-7898.

(151) Neugebauer, D.; Zhang, Y.; Pakula, T.; Matyjaszewski, K. *Polymer* **2003**, *44*, 6863-6871.

(152) Neiser, M. W.; Muth, S.; Kolb, U.; Harris, J. R.; Okuda, J.; Schmidt, M. *Angew. Chem. Int. Ed.* **2004**, *43*, 3192-3195.

(153) Borner, H. G.; Duran, D.; Matyjaszewski, K.; da Silva, M.; Sheiko, S. S. *Macromolecules* **2002**, *35*, 3387-3394.

(154) Cheng, G.; Boker, A.; Zhang, M.; Krausch, G.; Müller, A. H. E. *Macromolecules* **2001**, *34*, 6883-6888.

(155) Borner, H. G.; Beers, K.; Matyjaszewski, K.; Sheiko, S. S.; Moller, M. *Macromolecules* **2001**, *34*, 4375-4383.

(156) Ishizu, K.; Toyoda, K.; Furukawa, T.; Sogabe, A. *Macromolecules* **2004**, *37*, 3954-3957.

(157) Belder, G. F.; ten Brinke, G.; Hadziioannou, G. *Langmuir* **1997**, *13*, 4102-4105.

(158) Mori, H.; Müller, A. H. E. *Prog. Polym. Sci.* **2003**, *28*, 1403-1439.

(159) Jha, S.; Dutta, S.; Bowden, N. B. *Macromolecules* **2004**, *37*, 4365-4374.

(160) Gerle, M.; Fischer, K.; Roos, S.; Müller, A. H. E.; Schmidt, M.; Sheiko, S. S.; Prokhorova, S.; Moller, M. *Macromolecules* **1999**, *32*, 2629-2637.

(161) Lee, H.; Matyjaszewski, K.; Yu, S.; Sheiko, S. S. *Macromolecules* **2005**, *38*, 8264-8271.

(162) Barbey, R.; Lavanant, L.; Paripovic, D.; SchuIwer, N.; Sugnaux, C.; Tugulu, S.; Klok, H.-A. *Chem. Rev.* **2009**, *109*, 5437-5527.

(163) Zhang, M.; Breiner, T.; Mori, H.; Müller, A. H. E. *Polymer* **2003**, *44*, 1449-1458.

(164) Qin, S.; Borner, H. G.; Matyjaszewski, K.; Sheiko, S. S. *Polym. Prepr. (Am. Chem. Soc., Div. Polym. Chem.)* **2002**, *43*, 237-238.

(165) Venkatesh, R.; Klumperman, B. *Macromol. Chem. Phys.* **2004**, *205*, 2161-2168.

(166) Kamigaito, M.; Ando, T.; Sawamoto, M. *Chem. Rev.* **2001**, *101*, 3689-3745.

Chapter 3: Synthesis and characterization of novel glycopolymer brushes via a combination of RAFT and ATRP techniques

Abstract

The synthetic pathways that were investigated for the preparation of 2-(2-bromoisobutyryloxy) ethyl methacrylate monomer, N-(n-propyl)-2-pyridylmethanimine ligand and methyl 6-O-methacryloyl-α-D-glucoside glycomonomer are described. The focus is largely on the synthesis and characterization of novel glycopolymer brushes, namely P(2-(2-bromoisobutyryloxy) ethyl methacrylate))-g-P(methyl 6-O-methacryloyl-α-D-glucoside) (P(BIEM)-g-P(6-O-MMAGIc)), P(2-(2-bromoisobutyryloxy) ethyl methacrylate-co-methyl methacrylate)-g-P(methyl 6-O-methacryloyl-α-D-glucoside) (P(BIEM-co-MMA)-g-P(6-O-MMAGIc)), P(2-(2-bromoisobutyryloxy) ethyl methacrylate-b-methyl methacrylate)-g-P(methyl 6-O-methacryloyl-α-D-glucoside) (P(BIEM-b-MMA)-g-P(6-O-MMAGIc)) and P(4-vinylbenzyl chloride-alt-maleic anhydride)-g-P(methyl 6-O-methacryloyl-α-D-glucoside) (P(S_d-alt-MA)-g-P(6-O-MMAGIc)). Reversible Addition-Fragmentation Chain Transfer (RAFT) mediated polymerization was used to syntheses four well-defined ATRP macroinitiators. These Atom Transfer Radical Polymerization (ATRP) macroinitiators were subsequently used in the "grafting from" approach to prepare high molar mass and low PDI glycopolymer brushes with different grafting densities along the backbone. The number average molar masses of the glycopolymer brushes were determined using SEC-MALLS chromatography and further characterization was conducted using ^{1}H-NMR spectroscopy. The results confirmed that glycopolymer brushes were successfully synthesized via a combination of RAFT and ATRP techniques.

3.1 Introduction

Polymer brushes have generated much interest due to their unique properties and their ability to alter the surface properties of materials.[1] It is known that the solution and bulk properties of polymers are significantly influenced by their chain architecture.[2] Their properties depend on a variety of molecular parameters, including the degree of polymerization of the backbone and side chains, grafting density, main chain topology and chemical composition.[3]

A polymer brush is defined as an assembly of polymer chains which are densely tethered by one end to a surface or an interface. Due to the high steric crowding the chains are forced to stretch away from the surface to avoid segmental overlap.[1,4,5] The architecture of polymer brushes can be varied by then being densely or loosely grafted, having flexible or stiff side chains, being homopolymers or copolymers.[4,6] Three synthetic routes for the preparation of polymer brushes are described in the literature:[3,6-8] (I) "grafting onto" (attachment of side chains to the backbone), (II) "grafting through" (homo- and copolymerization of macromonomers) and (III) "grafting from" (growing side chains from the backbone). To achieve high grafting density, grafting from, using the macroinitiator via the ATRP, technique has proved particularly beneficial.[9-12]

The macroinitiator can be prepared in different ways, for example, Hawker et al.[13] and Matyjaszewski et al.[14] prepared ATRP macroinitiators by NMP and ATRP respectively. Another interesting example is the work reported by Klumperman et al.,[3] where the RAFT technique was used directly to prepare ATRP macroinitiators without having to resort to protecting group chemistry on the ATRP initiator moiety.

Recently glycopolymers, synthetic sugar-containing polymers, are becoming increasingly attractive to polymer chemists because of their role as biomimetic analogues and their potential for commercial applications.[15-17] Glycopolymers of different structures confer high hydrophilicity and water solubility and can therefore be used for specialized applications, such as artificial materials for a number of biological, pharmaceutical and biomedical uses.[18-21] Glycopolymers can be prepared via two different approaches, the first method involves the polymerizations of sugar-based monomers, whereas the second

method entails the chemical modification of preformed polymers with sugar-containing reagents.[22,23]

Here we report the synthesis and characterization of various ATRP macroinitiators using the RAFT technique, without the need to use protecting group chemistry on the ATRP initiator moiety. Glycopolymer brushes comprising methyl 6-O-methacryloyl-α-D-glucoside (6-O-MMAGlc) side chains were then prepared using the grafting from approach, via ATRP. The polymer brushes were characterized using ^{1}H-NMR spectroscopy and size exclusion chromatography (SEC).

Glycopolymers can be defined in a general sense as synthetic polymers possessing a non-carbohydrate backbone but carrying carbohydrate (sugar) moieties as pendant or terminal groups.[15,24] In this work the first method was used, where the glycomonomer was synthesized using an enzymatic approach to regioselectively functionalize the primary hydroxyl group. However, introducing the vinyl functionality in this position has been found to eliminate the biological activity of the resulting glycopolymer.[25]

3.2 Experimental details

3.2.1 Chemicals

2-Hydroxyethyl methacrylate 98% (Sigma-Aldrich), triethylamine 99.5% (Sigma-Aldrich), dichloromethane 98% (Merck), 2-bromoisobutyryl bromide 98% (Sigma-Aldrich), sodium hydrogen carbonate 99% (Fluka), sodium chloride 98% (Sigma-Aldrich), distilled deionized water was obtained from a Millipore Milli-Q purification system, magnesium sulphate (anhydrous) 99% (Saarchem), n-propylamine 99% (Alfa Aesar), pyridine-2-carboxaldehyde 99% (Sigma-Aldrich), diethyl ether 99.7%(Sigma-Aldrich), methyl α-D-glucoside 99% (Sigma-Aldrich), Novozym 435 (a commercially available immobilized lipase; kindly donated by Novozymes (Pty) Ltd; South Africa), vinyl methacrylate 98% (Sigma-Aldrich), acetonitrile anhydrous 99.8% (Sigma-Aldrich), methanol 98% (Alfa Aesar), ethyl acetate (Sasol Class3), ethanol and heaxane (Kimix CP), p-xylene 99% (Merck), 1,4-dioxane 99% (Saarchem uniLAB), methyl ethyl ketone 99.7% (Sigma-Aldrich), maleic anhydride 99% (Acros Organics), 4-vinylbenzyl chloride

90% (Sigma-Aldrich), copper (I) bromide 99% (Sigma-Aldrich), ethyl α-bromoisobutyrate 98% (Fluka) and N,N-dimethylformamide 97% (Fluka) were all used as received without further purification. Methyl methacrylate 99% (Sigma-Aldrich) was purified by passing through a column of basic aluminum oxide to remove inhibitor. 2,2 azobis(isobutyronitrile) (Riedel de Haën) was re-crystallized twice from ethanol and dried under vacuum before use. For column chromatography, silica gel (Fluka), particle size 0.063-0.2 mm, Brockmann 2-3) was used.

3.2.2 Analyses

3.2.2.1 Nuclear magnetic resonance spectroscopy (NMR)

^{1}H-NMR and ^{13}C-NMR spectra were obtained using a Varian VXR 400 MHz instrument equipped with a Varian magnet (7.0 T), or a 600 MHz Varian Unity Inova spectrometer equipped with an Oxford magnet (14.09 T). Depending on the solubility of the synthesized compounds, deuterated chloroform ($CDCl_3$) and deuterated dimethyl sulfoxide (DMSO-d6) were used as solvents. All chemical shifts are reported in ppm downfield from tetramethylsilane (TMS), used as an internal standard (δ = 0 ppm).

3.2.2.2 Size exclusion chromatography (SEC)

Molar masses and molar mass distributions were measured using size exclusion chromatography (SEC). The SEC instrument consisted of a Waters 117 plus auto-sampler, Waters 600, E system controller (run by Millennium^{32} V 3.05 software) and a Waters 610 fluid unit. A Waters 410 differential refractometer and Waters 2487 dual wavelength absorbance detector were used. A laser photometer miniDAWN (Wyatt Technology Corporation, Santa Barbara, CA) multi-angle laser light scattering with ASTRA software (Wyatt Technology Corporation) was used. The system was equipped with 50 x8 mm guard column and three 300x8 mm linear columns (PSS, $3x10^3$, 10^2, and $3x10^3$ Å pore size; 10μm particle size). N,N-dimethylacetamide (DMAc) (HPLC grade, 0.03% w/v, LiCl, 0.05% BHT) was used as eluent at a flow rate of 1 mL/min, while the column oven was kept at 40 °C. 100 μL of polymer solutions of 5 mg/mL were injected.

The system was calibrated with narrow PMMA standards ranging from 800 to 2 x 10^6 g/mol. All molar masses are reported as PMMA equivalents.

3.2.2.3 Atomic force microscopy (AFM)

AFM measurements were performed with a Easy Scan II AFM (Nanosurf). The microscope was operated in tapping mode at a resonance frequency of 360 kHz and at ambient conditions.

3.2.3: Synthesis of RAFT agent, ATRP ligand and monomers

3.2.3.1 Synthesis of 2-cyanoprop-2-yl dithiobenzoate (CIPDB)

The synthesis of 2-cyanoprop-2-yl dithiobenzoate (CIPDB) was carried out in a similar fashion according to the method of Moad et al.[26] and purified by successive liquid chromatography on silica using hexane/diethyl ether (9:1) as an eluent system. After removal of solvent under reduced pressure the product was stored below -10°C. The purity of the RAFT agent was estimated via ^{1}H-NMR spectroscopy to be 96%.

3.2.3.2 Synthesis of 2-(2-bromoisobutyryloxy) ethyl methacrylate (BIEM)

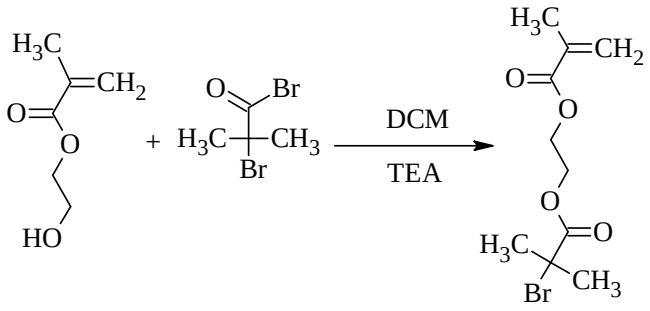

2-Hydroxyethyl methacrylate 2-(2-Bromoisobutyryloxy)ethyl methacrylate

Scheme 3.1: Synthesis of 2-(2-bromoisobutyryloxy) ethyl methacrylate.

The monomer was synthesized according to a procedure available in the literature.[3,27] Under argon, a solution of 2-hydroxyethyl methacrylate (HEMA, 10.0 g, 0.07 mol) and triethylamine (TEA, 15.6 g, 0.15 mol) in dichloromethane (DCM, 50 mL) was stirred at 0 °C for 45 min. A solution of 2-bromoisobutyryl bromide (21.2 g, 0.09 mol) in DCM (25 mL) was added dropwise over a period of 30 min. The mixture was stirred at 0 °C for 6 h

under an argon atmosphere and then filtered to remove the formed solids. The solids were washed with DCM. The filtrate was then washed with deionized water (2 x 100 mL), 0.5 M $NaHCO_3$ (2 x 100 mL) and saturated NaCl (2 x 100 mL) solutions. Sodium sulphate was added to remove traces of water, and then filtered off. The DCM was removed at 25 °C under vacuum. The purity of the obtained product was checked by ^{1}H-NMR spectroscopy and estimated to be 99.0%. The yield was 94%.

^{1}H-NMR ($CDCl_3$): δ (ppm) = 6.1 (m, 1H), 5.56 (m, 1H, CH_2=C), 4.39 (m, 4H, -O-CH_2–CH_2–O-), 1.91 (q, 3H, α–CH_3), 1.89 (s, 6H, –C(Br)(CH_3)$_2$). ^{13}C-NMR ($CDCl_3$): δ (ppm) = 171.5 (–O-C=O), 167 (O=C-O-), 135.69 (CH_2=C), 126.1 (CH_2=C), 63.44 (CH_2-O), 61.93 (O-CH_2), 55.43 (–C(Br)(CH_3)$_2$), 30.5 (–C(Br)(CH_3)$_2$), 18.67 (α–CH_3). ESI-MS m/z calcd for $C_{10}H_{16}BrO_4$, 280.12; found: 281 ($M+H^+$).

3.2.3.3 Preparation of N-(n-propyl)-2-pyridylmethanimine (n-Pr-1)

The synthesis of n-Pr-1 was carried out according to the method of Haddleton et al.[28] An excess of n-propylamine (2.95 g, 0.05 mol) was added dropwise to a cooled stirred solution of pyridine-2-carboxaldehyde (4.5 g, 0.042 mol) in diethyl ether (5 mL). After complete addition of the amine, anhydrous magnesium sulphate (4 g) was added and the slurry stirred for 5 h at 25 °C. The solution was filtered, and the solvent removed to afford a golden yellow oil. Yield: 5.9 g (94.7%). ^{1}H-NMR ($CDCl_3$): δ (ppm) = 8.60 (m, 1H), 8.38 (s, 1H), 7.97 (m, 1H), 7.69 (m, 1H), 7.27 (m, 1H), 3.62 (t, 2H), 1.71 (m, 2H), 0.94 (t, 3H). ^{13}C-NMR ($CDCl_3$): δ (ppm) = 161.7, 154.6, 149.3, 136.4, 124.5, 121.1, 63.3, 23.8, 11.8.

3.2.3.4 Synthesis of methyl 6-O-methacryloyl-α-D-glucoside (6-O-MMAGlc)

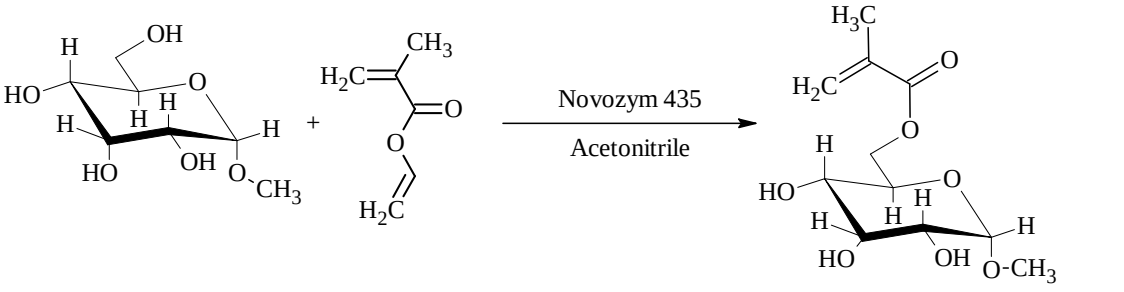

Methyl-α-D-glucoside Vinyl methacrylate Methyl 6-O-methacryloyl-α-D-glucoside

Scheme 3.2: Synthesis of methyl 6-O-methacryloyl-α-D-glucoside.

6-O-MMAGlc monomer was prepared according to the method of Albertin et al.,[15,29] with some modifications. A conical flask was charged with methyl α-D-glucoside (8.0 g, 0.041 mol), Novozym 435 (4.0 g), vinyl methacrylate (4.4 g, 0.039 mol) and dry acetonitrile (40 mL). Novozym 435 was chosen as the catalyst because of its ability to catalyze regioselective esterification and transesterification reactions in a number of organic solvents.

The flask was sealed with a stopper and the suspension stirred at 200 rpm and 50 °C for 7 days before stopping the reaction by filtering off the enzyme. The filtrate was washed with methanol (100 mL) and the collected organic phases were rotary evaporated to dryness to yield a yellow-brown syrup. Ethyl acetate (100 mL) was then added to the syrup in order to precipitate the unreacted methyl α-D-glucoside. The product was purified by column chromatography on silica using volume ratios of 7:2:1 ethyl acetate:hexane:ethanol as an eluent system. The collected fractions were checked by TLC for the presence of the 6-O-MMAGlc monomer (Rf 0.34). The plates were immersed in a solution of sulphuric acid: ethanol (2:8 volume ratio) and then heated with a hot air blower for spots detection. The fractions were then rotary evaporated at room temperature (to avoid polymerization). A clear syrup of 6-O-MMAGlc monomer was obtained, 64% yield with respect to methyl α-D-glucoside.

^{1}H-NMR ($CDCl_3$): δ (ppm) =1.92 (s, 3H, H-11), 3.33 (d, 1H, H-4), 3.37 (s, 4H, H-7 and dd, H-2), 3.52 (dd, 1H, H-3), 3.72 (m, 1H, H-5), 4.09 (dd, 1H, H-6), 4.31 (dd, 1H, H-6),

4.43 (d, 1H, H-1), 4.72 (d, 1H, H-10), 5.55 (t, 1H, H-10). ^{13}C-NMR ($CDCl_3$): δ (ppm) = 18.28 (C-11), 55.08 (C-7), 64.04 (C-6), 69.73 (C-5), 70.45 (C-4), 71.97 (C-2), 74.11 (C-3), 99.40 (C-1), 126.12 (C-10), 136.02 (C-9), 167.57 (C-8). ESI-MS m/z calcd for $C_{11}H_{22}O_7N$, 280.14; found 280 ($M + NH_4^+$).

3.2.3.5 Synthesis of ATRP macroinitiators via the RAFT process

ATRP macroinitiators with different distributions of initiating sites along the backbone were prepared by the RAFT process. A general synthesis of the macroinitiators is outlined in Scheme 3.1.

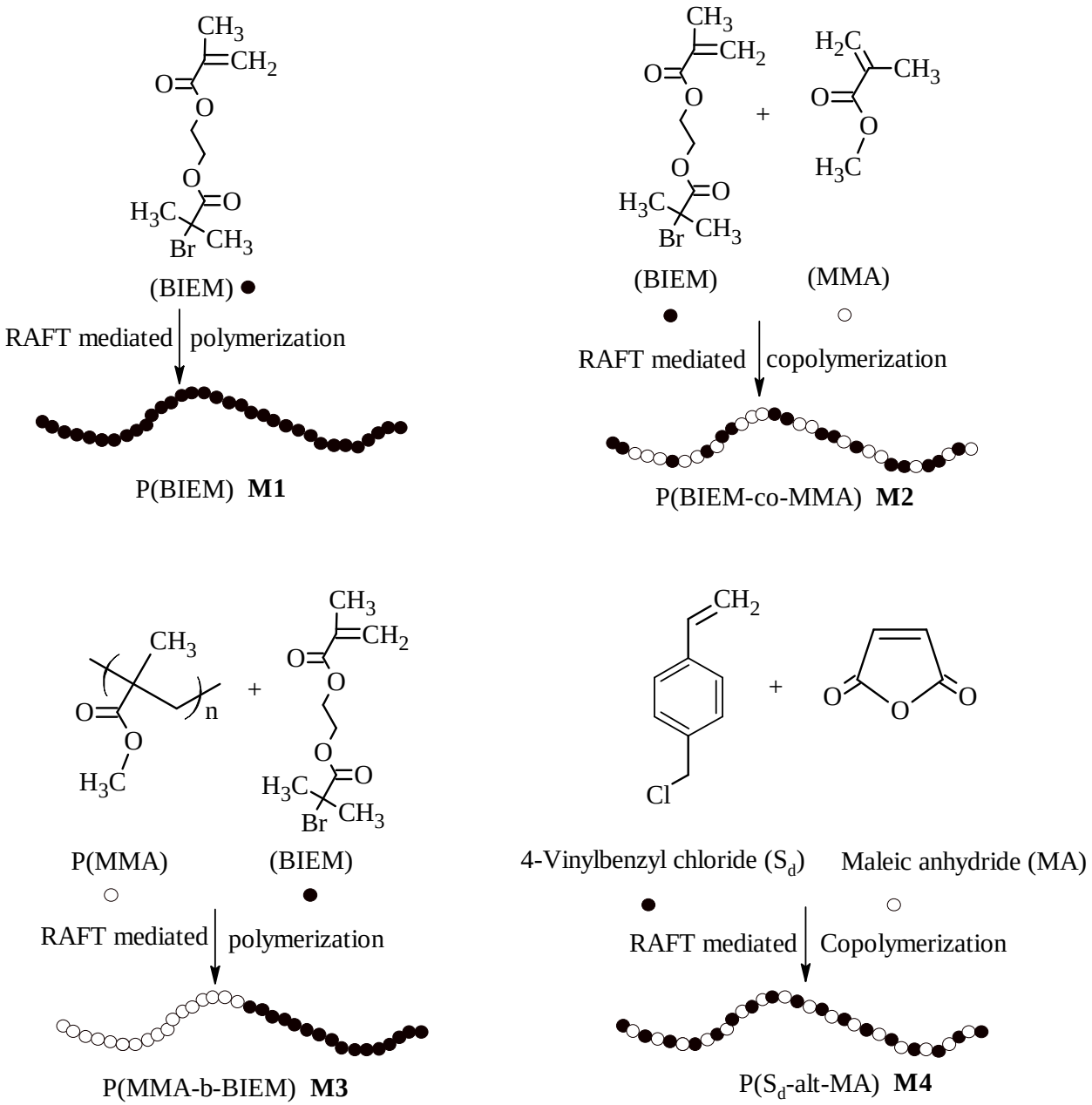

Scheme 3.3: General synthesis of ATRP macroinitiators.

3.2.4 Polymerization procedures

All polymerizations were carried out in a pear-shaped 50 mL Schlenk flask heated in an oil bath. The polymerization reaction mixture was degassed using a minimum of three freeze-pump-thaw cycles followed by the introduction of high purity argon. The molar ratio of monomer to RAFT agent was calculated from equation 2.11. Typical polymerizations were performed as follows:

3.2.4.1 RAFT-mediated polymerization of 2-(2-bromoisobutyryloxy) ethyl methacrylate (BIEM) (M1)

A stock solution for the polymerization in a Schlenk flask was prepared by accurately weighing the monomer BIEM (2 g, 7.0 x 10^{-3} mol), RAFT agent (CIPDB, 0.02 g, 9.03 x 10^{-5} mol), AIBN (2.9 x 10^{-3} g, 1.8 x 10^{-5} mol) and the solvent p-xylene (4 g). The stock solution was degassed via three freeze-pump-thaw cycles, immersed in a thermostated oil bath preheated at 60 °C and stirred using a magnetic stirrer. After 24 h reaction time the P(BIEM) was isolated by precipitation in methanol. After filtration the solvent was removed and the polymer was dried under vacuum for 24 h. The polymer was analyzed by SEC and ^{1}H-NMR spectroscopy: M_n = 13.0 x10^3 g/mol, PDI = 1.12.

3.2.4.2 RAFT-mediated copolymerization of BIEM and methyl methacrylate (M2)

A stock solution of BIEM (1 g, 3.5 x 10^{-3} mol), MMA (0.35 g, 3.5 x 10^{-3} mol), RAFT agent (CIPDB, 0.014 g, 6.2 x 10^{-5} mol), AIBN (0.002 g, 1.26 x 10^{-5} mol), and 1,4-dioxane (3 g) was prepared and degassed by three freeze-pump-thaw cycles . The Schlenk flask was immersed in a thermostated oil bath preheated at 60 °C. After 24 h of reaction under magnetic stirring, P(BIEM-co-MMA) was isolated by precipitation in methanol. After filtration the solvent was removed and the polymer was dried under vacuum for 24 h. The polymer was analyzed via SEC and ^{1}H-NMR spectroscopy: M_n = 10.0 x 10^3 g/mol, PDI = 1.14. The copolymer resulted in a random distribution in composition along the backbone due to their reactivity ratios.[6]

3.2.4.3 RAFT-mediated block copolymerization of P(MMA) and BIEM (M3)

A 50 mL Schlenk flask was charged with, BIEM (1 g, 3.5 x 10^{-3} mol), AIBN (0.003 g, 1.8 x 10^{-5} mol) and 1,4-dioxane (5 g). A stock solution of macroRAFT agent P(MMA) (0.35 g, M_n 5.0 x10^3 g/mol, PDI 1.12, prepared according to a procedure available in the literature[26]) in 1,4-dioxane was added to the mixture in the Schlenk flask and degassed three times using three freeze-pump-thaw cycles, after which the flask was immersed in a thermostated oil bath preheated at 60 °C. After 24 h reaction under magnetic stirring the P(MMA-b-BIEM) was isolated by precipitation in methanol. The product was dried in a vacuum oven for 24 h and then analyzed by SEC and ^{1}H-NMR spectroscopy: M_n = 9.0 x 10^3 g/mol, PDI = 1.21.

3.2.4.4 RAFT-mediated copolymerization of 4-vinylbenzyl chloride and maleic anhydride (M4)

In a typical RAFT polymerization procedure a stir bar was placed in a 50 mL Schlenk flask along with maleic anhydride (0.98 g, 0.01 mol), 4-vinylbenzyl chloride (2 g, 0.01 mol), RAFT agent (CIPDB, 0.03 g, 1.36 x 10^{-4} mol), AIBN (0.004 g, 2.7 x 10^{-5} mol) and methyl ethyl ketone (MEK) (6 g). The solution was degassed by three freeze-pump-thaw cycles. The Schlenk flask was immersed in a thermostated oil bath preheated at 60 °C. After 24 h of reaction under magnetic stirring P(S_d-alt-MA) was isolated by precipitation in diethyl ether. The copolymer was dried in a vacuum oven for 24 h and then analyzed by SEC and ^{1}H-NMR spectroscopy: M_n = 15.0 x 10^3 g/mol, PDI = 1.16.

It is known that RAFT mediated radical polymerization of styrene and maleic anhydride results in the formation of a close to alternating copolymer.[30,31] A similar trend is expected for the current maleic anhydride and 4-vinylbenzyl chloride system.[32]

3.2.5 Synthesis of glycopolymer brushes

A series of glycopolymer brushes with approximately constant length of the side chains and different grafting densities were prepared by using the grafting from approach. All polymerizations were carried out in a pear-shaped 50 mL Schlenk flask heated in an oil bath. The polymerization mixture was degassed by a minimum of three freeze-pump-thaw cycles followed by the introduction of high purity argon. Monomer conversion for

graft polymerization was determined gravimetrically, based on monomer consumption. The degree of polymerization of the side chains was calculated using equation 2.10, based on monomer conversion, assuming quantitative initiation from each Br or Cl atom. A typical polymerization was performed as follows:

3.2.5.1 Synthesis of P(BIEM)-g-P(6-O-MMAGIc)

A stock solution for the graft polymerization was prepared in a 50 mL Schlenk flask by accurately weighing the PBIEM (0.04 g, 0.14 x 10^{-3} mol of initiating α-bromoester group), Cu(I)Br (0.01 g, 0.07 x 10^{-3} mol) and n-Pr-1 ligand (0.02 g, 0.14 x 10^{-3} mol). The mixture was stirred in DMF (4 g) for 15 min to dissolve the macroinitiator completely. A homogenous mixture was obtained due to the polar nature of DMF. A solution of 6-O-MMAGlc monomer (2 g, 7.0 x 10^{-3} mol) in DMF (2 g) was then added and the reaction mixture was degassed by three freeze-pump-thaw cycles followed by the introduction of high purity argon. The flask was sealed with a rubber septum and placed in a preheated thermostated oil bath at 60 °C. The polymerization was stopped after 1 h by cooling to room temperature and opening the flask to the air. The polymerization solution, which was very viscous even at such a low conversion, was diluted with DMF and passed though a column of neutral aluminum oxide three times to remove any traces of the catalyst, followed by precipitation in diethyl ether twice to remove unreacted monomer. The yield was 0.8 g of isolated polymer. The product was characterized by ^{1}H-NMR spectroscopy and SEC. According to SEC using PMMA calibration, the molar mass was determined to be M_n = 85.0 x 10^3 g/mol and the PDI = 1.21. The monomer conversion was 40%.

3.2.5.2 Synthesis of P(MMA-co-BIEM)-g-P(6-O-MMAGIc)

The polymerization procedure used here was the same as described above. A 50 mL Schlenk flask, PMMA-co-PBIEM (0.09 g, 0.14 x 10^{-3} mol of initiating α-bromoester group, from ^{1}H-NMR spectroscopy), Cu(I)Br (0.01 g, 0.07 x 10^{-3} mol), n-Pr-1 ligand (0.02 g, 0.14 x 10^{-3} mol) and DMF (4 g) was added. A solution of 6-O-MMAGlc monomer (2 g, 7.0 x 10^{-3} mol) in DMF (2 g) was then added to the reaction mixture. The flask was sealed with a rubber septum and placed in a preheated thermostated oil bath at

60 °C. The polymerization was stopped after 90 min by cooling to room temperature and opening the flask to the air. The yield was 1.1 g of isolated polymer; and the monomer conversion was 55%. According to SEC using PMMA calibration the molar mass and polydispersity were M_n = 55.0 x 10^3 g/mol and PDI = 1.25, respectively.

3.2.5.3 Synthesis of (P(MMA-b-BIEM))-g-P(6-O-MMAGIc)

In a typical synthesis, a magnetic stirrer bar was placed in a 50 mL Schlenk flask together with P(MMA-b-BIEM) (0.08 g, 0.14 x 10^{-3} mol of initiating α-bromoester group, obtained from ^{1}H-NMR spectroscopy), Cu(I)Br (0.01 g, 0.07 x 10^{-3} mol), n-Pr-1 ligand (0.02 g, 0.14 x 10^{-3} mol) and DMF as solvent (4 g). The solution was stirred until a homogenous mixture was obtained. A solution of 6-O-MMAGlc monomer (2 g, 7.0 x 10^{-3} mol) in DMF (2 g) was then added to the reaction mixture. The reaction mixture was degassed by three freeze-pump-thaw cycles followed by the introduction of high purity argon. The flask was sealed with a rubber septum and placed in a preheated thermostated oil bath at 60 °C. The polymerization was stopped after 90 min by cooling to room temperature and opening the flask to the air.

The polymerization solution was very viscous, and therefore diluted with DMF then this is passed though a column of neutral aluminum oxide three times to remove the catalyst, followed by precipitation in diethyl ether twice to remove unreacted monomer. The yield was 0.9 g of isolated polymer and the conversion was 45% of 6-O-MMAGlc. SEC with PMMA calibration was used to determine the molar mass and polydispersity: M_n = 47.0 x 10^3 g/mol and PDI = 1.29.

3.2.5.4 Synthesis of P(S_d-alt-MA)-g-P(6-O-MMAGIc)

The polymerization procedure used here was the same as described above. A 50 mL Schlenk flask, P(S_d-alt-MA) (0.05 g, 0.15 x 10^{-3} mol of initiating α-bromoester group, obtained from ^{1}H-NMR spectroscopy), Cu(I)Br (0.01 g, 0.07 x 10^{-3} mol), n-Pr-1 ligand (0.02 g, 0.15 x 10^{-3} mol) and DMF (4 g). A solution of 6-O-MMAGlc monomer (2 g, 7.0 x 10^3 mol) in DMF (2 g) was then added to the reaction mixture. The polymerization was stopped after 90 min by cooling to room temperature and opening the flask to the air. The yield was 0.7 g of isolated polymer; and the monomer conversion was 35%. SEC with

PMMA calibration was used to determine the molar mass and polydispersity: M_n = 63.0 x 10^3 g/mol and PDI = 1.32.

3.3 Results and discussion

3.3.1 Synthesis and characterization of P(6-O-MMAGlc) via ATRP (test reaction)

In order to find appropriate reaction conditions for the synthesis of densely grafted glycopolymers via ATRP, we initially investigated the influence of the catalyst system solvent and temperature on the homopolymerization of 6-O-MMAGlc (see Scheme 3.4).

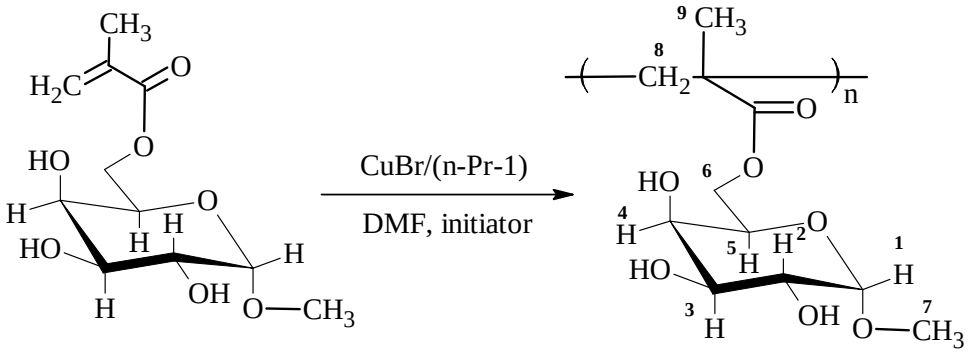

Scheme 3.4: Synthesis of P(6-O-MMAGlc) homopolymer via ATRP (position numbering as used for ^{1}H-NMR assignments).

In this study we used the CuBr/ (n-Pr-1) catalyst system for ATRP to prepare well-defined monodisperse linear and densely grafted glycopolymers. The use of CuBr/(n-Pr-1) as the catalyst system in conjunction with ethyl α-bromoisobutyrate as initiator has proven to be an efficient ATRP system for the controlled polymerization of methacrylates.[33-36]

Unfortunately P(6-O-MMAGlc) is only soluble in extremely polar solvents such as water, DMSO and DMF, none of which have been shown to be particularly successful as solvents for ATRP.[29,37] For an ideal synthesis of densely grafted glycopolymers (glycopolymer brushes), living radical polymerization systems are required to avoid crosslinking reactions and gelation due to chain transfer or recombination reactions.[38,39] One of the main advantages in using the living radical polymerization techniques is the

high functional group tolerance, which allows unprotected sugar monomers to be used.[40-42] Hence, the important step was to find suitable conditions for the controlled homo- and copolymerization of the sugar-carrying methacrylate monomer 6-O-MMAGlc.

In preliminary experiments, the homopolymerization of 6-O-MMAGlc was conducted under various reaction conditions aiming to prepare well-defined, monodisperse, linear P(6-O-MMAGlc). These conditions include the use of different concentrations of the catalyst system, different solvents and different temperatures. The polymerization of 6-O-MMAGlc that was carried out in water at 60 °C and 95 °C gave bimodal molar mass distribution curves and, as a result, the MMD was quite broad, as shown in Figure 3.1A and Figure 3.1B. Alternatively, the polymerization was carried out in DMF at 100 °C, which led to a decrease of the reaction rate, but also afforded polymer with a fairly broad monomodal molar mass distribution (Figure 3.1C). The bimodal distribution could be due to termination by recombination at higher temperatures. It was noted that when water was used as the solvent, the rate of polymerization was very high and 6-O-MMAGlc homopolymer was obtained in a quantitative yield. This is probably due to the more active nature of the Cu(I) catalyst in the presence of water.[43] However, in a few cases, the polymer could not be dissolved in good solvents, which suggests that some degree of cross-linking occurred during the polymerization, possibly due to transesterification.[39]

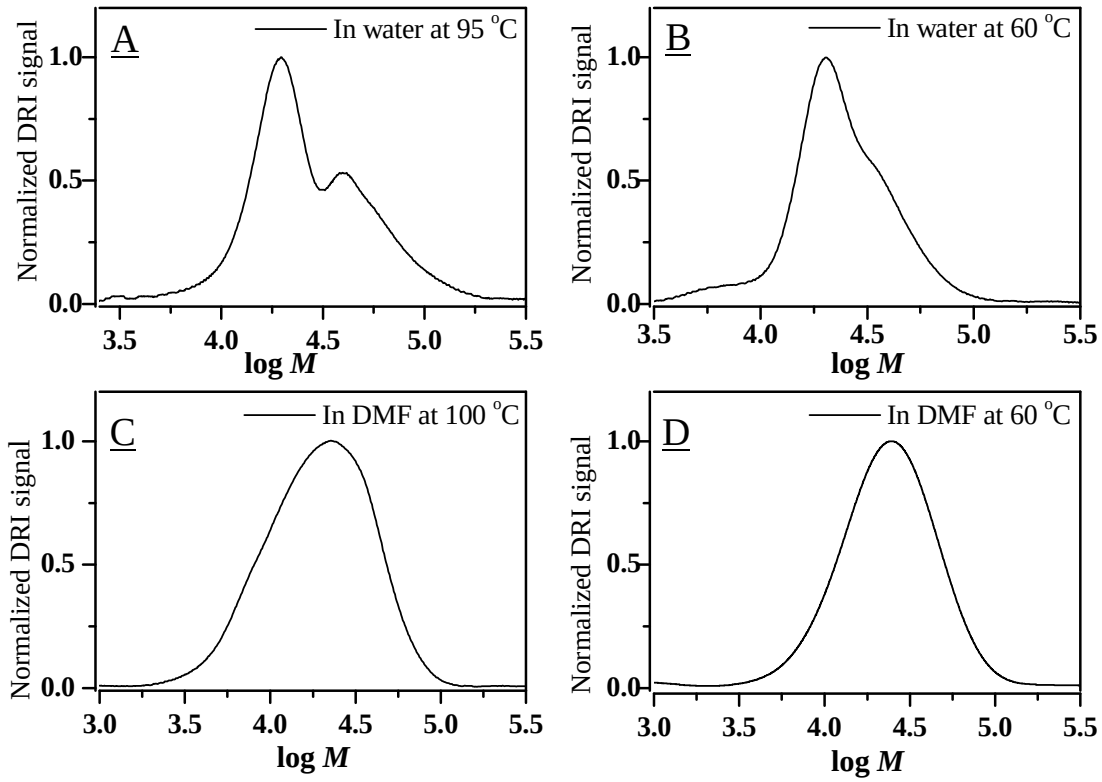

Figure 3.1: Molar mass distributions of linear P(6-O-MMAGlc), where ($[M]_0/[I]_0$ = 55), (A) in water at 95 °C ($[I]_0$:$[CuBr]_0$:$[ligand]_0$:1:1:2), (B) in water at 60 °C ($[I]_0$:$[CuBr]_0$:$[ligand]_0$:1:0.5:1), (C) in DMF at 100 °C ($[I]_0$:$[CuBr]_0$:$[ligand]_0$:1:1:2), (D) in DMF at 60 °C ($[I]_0$:$[CuBr]_0$:$[ligand]_0$:1:0.5:1).

Hence, an appropriate concentration of initiator and catalyst system, namely $[I]_0$:$[CuBr]_0$:$[ligand]_0$:1:0.5:1 at 60 °C in DMF, was found to be suitable system for the controlled polymerization of 6-O-MMAGlc.

The monomer conversion during the polymerization was determined gravimetry by drying to constant weight in a vacuum oven at 40 °C.[8,11] For most polymerizations a conversion of approximately 95% was achieved after 3 h. The molar mass increased linearly with conversion and the PDI was low (PDI < 1.2). Moreover, the molar mass of P(6-O-MMAGlc) determined by SEC was nearly twice the theoretical molar mass, based on the ratio of monomer consumed to initial initiator concentration ($DP_n = \Delta[M]/[I]_0$). This suggests that either the efficiency of initiation is only 50% or the hydrodynamic volume of P(6-O-MMAGlc) and PMMA standard at the same molar masses are not the

same. This could not be confirmed by NMR, because the end group resonances overlap with resonances of the polymer repeat units. Therefore, SEC with a multi-angle laser light scattering detector (MALLS) was used to determine the absolute molar mass of the P(6-O-MMAGlc). The refractive index increment (dn/dc) value used was calculated from ASTRA software. A dn/dc value of 0.092 ± 0.004 mL/g was used for molar mass calculations, determined from repeated injections of pure P(6-O-MMAGlc) solution of known concentration. Furthermore the P(6-O-MMAGlc) was characterized by ^{1}H-NMR spectroscopy. ^{1}H-NMR (DMSO-d6, 40 °C): δ (ppm): 0.76 and 0.94 (CH_2 chain), 1.8 (11-H), 3 (4-H), 3.38 (H-7), 3.57 (2-H), 4.18 (3-H), 4.58 (5-H), 4.77 (6-H), 4.91 (6-H), 5.12 (1-H). The peak assignments were made after comparison with the spectrum of homopolymer P(6-O-MMAGlc).[29]

3.3.2 Synthesis and characterization of ATRP macroinitiators and their corresponding glycopolymer brushes

The RAFT homopolymerization and copolymerization of BIEM with MMA monomers and S_d with MA monomers for the preparation of macroinitiators were investigated. Further, the synthesis and characterization of glycopolymer brushes with P(6-O-MMAGIc) side chains will be discussed. The thermal and mechanical properties of these polymer brushes will be discussed in the next chapter (chapter 5).

The synthesis of a macroinitiator with a narrow PDI is crucial because the molar mass distribution (MMD) of the polymer brushes is largely dependent on the MMD of the backbone.[2,3] For the synthesis of macroinitiators, 2-cyanoprop-2-yl dithiobenzoate was used as the RAFT agent, because it is known from literature that it controls the polymerization of MMA, as a result of its high chain transfer coefficient coupled with the fact that the cyanoisopropyl group is a good initiating species for MMA polymerization.[26] It was expected that by using the RAFT technique for the synthesis of ATRP macroinitiators the need to use protective group chemistry on the ATRP initiator moiety would be avoided.[3]

ATRP macroinitiators with different distributions of initiating species along the backbone were prepared by the RAFT process, according to Scheme 3.3. Since these

macroinitiators were going to function as the polymer brush backbones they were extensively characterized in order to provide data information on the initiator density and its distribution along the backbone (see Table 3.1). The actual number of initiating groups along the backbone was calculated from the DP of the backbone, and the molar fraction of BIEM units in the backbones, which was determined by ^{1}H-NMR spectroscopy.

Table 3.1: Data pertaining to ATRP macroinitiators synthesized via the RAFT process

Macro-initiator	Conversion[a] (%)	$M_{n,th}$ (g/mol)[b]	$M_{n,SEC}$ (g/mol)[c]	$M_{n,NMR}$ (g/mol)	Molar fraction of initiating moiety[d]	DP_n[e]	PDI
M1	60	22 x 10^3	13 x 10^3	12 x 10^3	1	43	1.12
M2	57	22 x 10^3	10 x 10^3	14 x 10^3	0.45	77	1.14
M3	62	22 x 10^3	9 x 10^3	12.5 x10^3	0.51	65	1.21
M4	55	22 x 10^3	15 x 10^3	11 x 10^3	0.49	88	1.16

a) Calculated via gravimetry

b) $M_{n,th} = \{x[M]_0/[RAFT]_0\}MW_M + MW_{RAFT}$

c) From SEC, calibrated with PMMA standards

d) Molar fraction of BIEM and S_d in the macroinitiators calculated from ^{1}H-NMR (see Figure 3.2)

e) Number average degree of polymerization of the backbone (macroinitiator) was calculated as $DP_n = M_n/[(1-x)M_{MMA} + x\ M_{BIEM}$, where M_{MMA} = 100.11 and M_{BIEM} = 279.12, and x is molar fraction of initiator BIEM unites in the backbone. The DP_n of M4 macroinitiator was obtained in a similar way

The ^{1}H-NMR spectrum of the macroinitiator M1, in Figure 3.2A, clearly shows two typical peaks at 4.22 and 4.38 ppm (peak b), which represent the methylene protons between the two ester groups of the macroinitiator.[2]

For macroinitiators M2 and M3 (Figure 3.2B and Figure 3.2C) the integration area of the $-OCH_3$ protons at 3.6 ppm (peak c) from MMA and the four protons from BIEM 4.22

and 4.38 ppm (peak b), were compared to determine the final copolymer composition. The ratio between BIEM and MMA in macroinitiators M2 and M3 was calculated, based on the integration areas, to be 45:55 and 51:49, respectively.[6]

The ^{1}H-NMR spectrum of macroinitiator M4 is shown in Figure 3.2D, the poorly resolved resonance peaks at 6.1–7.5 ppm is ascribed to the protons of the benzene ring in 4-vinylbenzyl chloride, while the peak at 2.31 ppm is associated with the protons of the maleic anhydride backbone.[44,45] The calculation based on integration area revealed that the ratio between 4-vinylbenzyl chloride and maleic anhydride was 49:51.

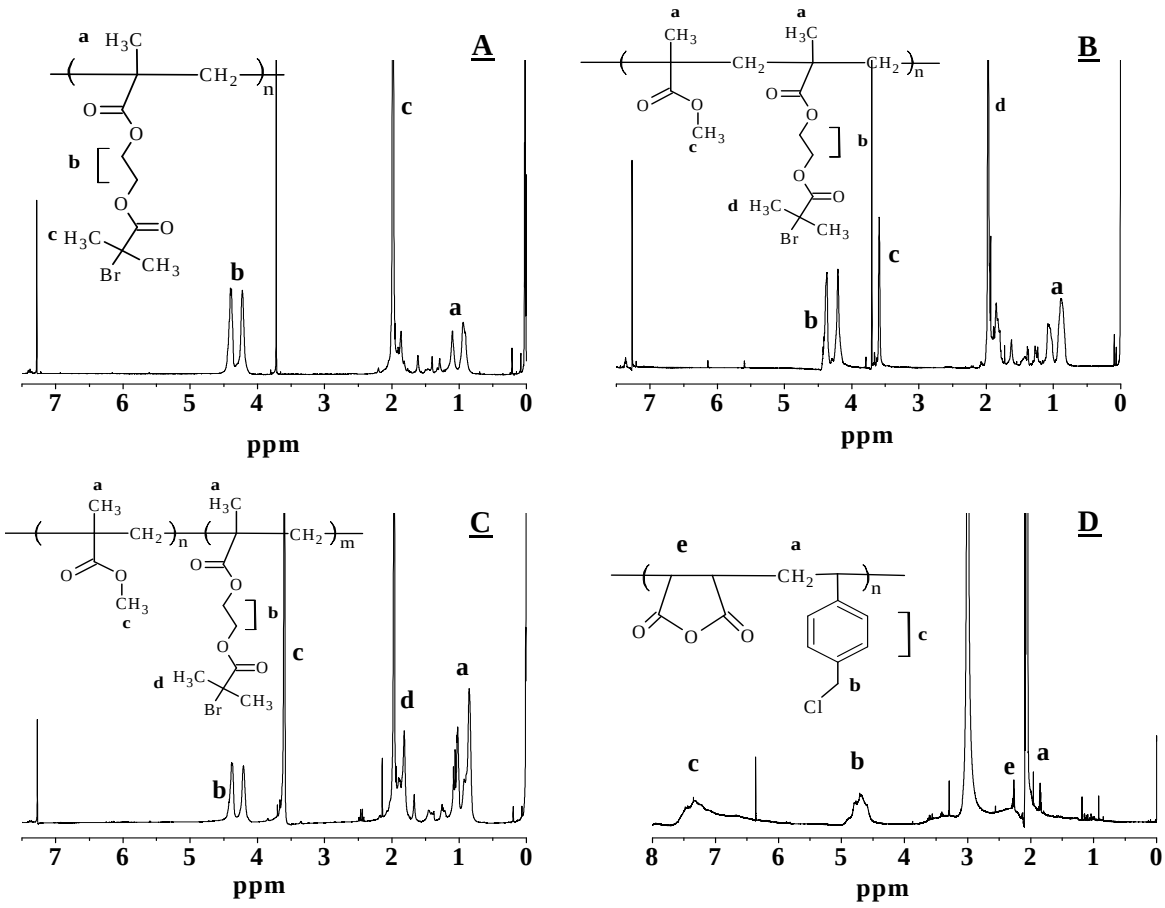

Figure 3.2: ^{1}H-NMR spectra of ATRP macroinitiators: (A) P(BIEM) (M1), (B) P(BIEM-co-MMA) (M2), (C) P(BIEM-b-MMA) (M3), (D) P(S_d-alt-MA) (M4).

When polymer brushes are synthesized by "grafting from" via a radical method, it is necessary to ensure a low concentration of active species due to the tendency for termination to take place by both intra- and intermolecular coupling, which leads to cross-linked polymers or polymers with multimodal distributions.[11] Therefore, low temperatures and low active species [Cu(I)] concentration were used to reduce the concentration of radicals during the polymerization. An increase in the viscosity at higher conversions is avoided, as the weight ratio of solvent to monomer was 3:1.

Glycopolymer brushes were synthesized with an approximately similar DP of side chains by grafting 6-O-MMAGlc monomer from the four macroinitiators via ATRP. Although there are several polymerization variables that can be considered, we used conditions (temperature, solvent, catalyst system) similar to those used for the synthesis of well-defined P(6-O-MMAGlc) (refer to Figure 3.1).

The evaluation of experimental molar masses and molar mass distributions of the macroinitiators and their corresponding glycopolymer brushes were investigated by SEC analysis. Figure 3.3 shows that each chromatogram exhibits a narrow monomodal molar mass distribution (PDI < 1.4). The SEC traces shift to higher molar mass, indicating that high molar mass glycopolymer brushes were formed. There was no significant tailing or shoulder formation observed, indicating that intermolecular coupling (brush-brush coupling) reactions during the polymerization were negligible.[46] The brush syntheses appeared to proceed in a controlled fashion since the PDI for all the glycopolymer brushes remained comparable to that of the macroinitiators.[6] It was noticed that the polymerization of 6-O-MMAGlc was very fast and it went to relatively high conversion, as can be seen in Table 3.2. This is expected, since 6-O-MMAGlc acts as a reducing agent, which will reduce the deactivator to regenerate the activator, and therefore the rate of polymerization will be enhanced.[47]

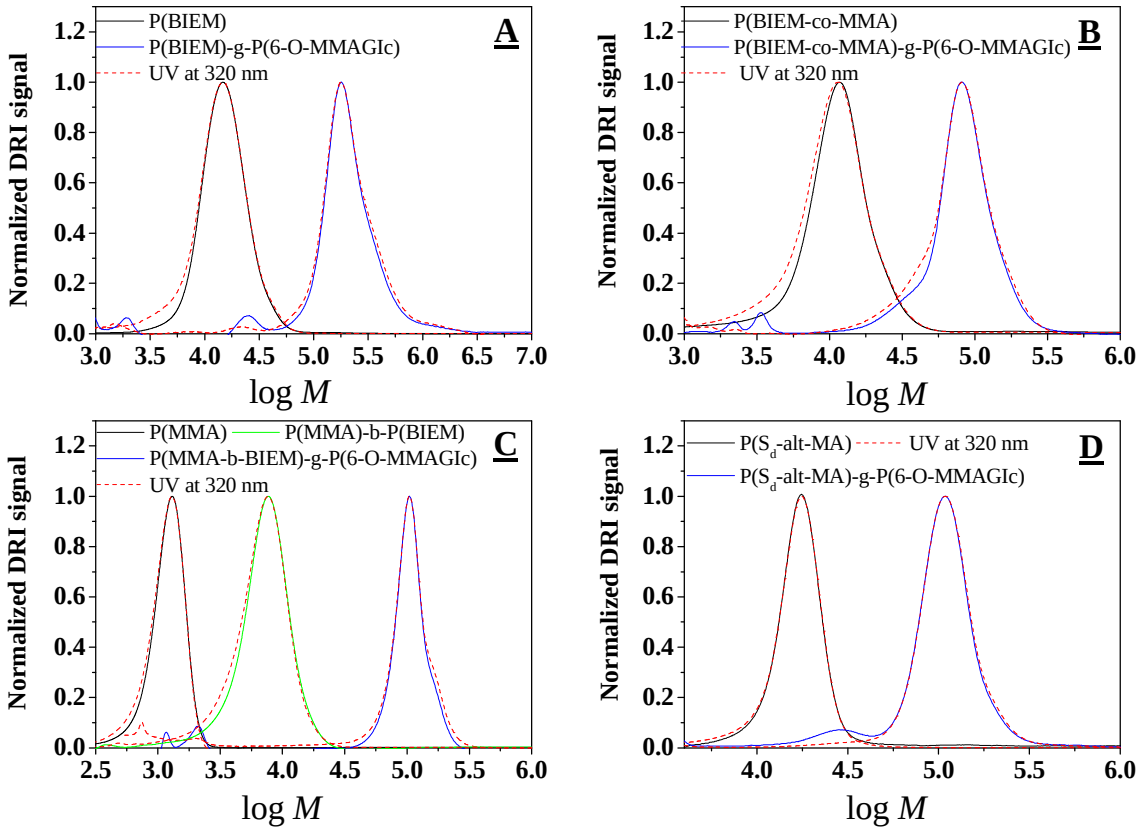

Figure 3.3: SEC chromatograms of macroinitiators and their corresponding glycopolymer brushes, measured in DMAc.

The M_n values obtained from SEC data analysis using refractive index detection relative to PMMA standards are just apparent ones. The lower values of experimental M_n observed for glycopolymer brushes could be due to the fact that the glycopolymer brushes have lower hydrodynamic volumes than the equivalent linear polymers. As a result, the glycopolymer brushes will elute later during SEC analysis compared to their linear polymers. In order to obtain more accurate estimate of M_n and PDI of the glycopolymer brushes, SEC with a MALLS detector was performed in DMAc. The dn/dc value used (0.092 mL/g) was based on the composition of the side chains (P(6-O-MMAGlc)) since they comprised the bulk of the material (> 95%).[14] The absolute molar mass values from these measurements are tabulated in Table 3.2. It is clear that the true molar masses are significantly higher than the apparent ones. This is in accordance with

the general phenomenon that polymer brushes are more compact than linear chains with identical molar masses.[3]

Table 3.2. Reaction conditions and results for grafting of 6-O-MMAGlc from ATRP macroinitiators.[a]

Macro-initiator	$[M]_0$:$[I]_0$:$[CuBr]_0$:$[L]_0$ [b]	Time (min)	Conv.[c] (%)	$M_{n,SEC}$ (g/mol)[d]	$M_{n,abs}$ (g/mol)[e]	DP_n [f]	PDI
M1	50:1:0.5:1	60	40	85 x 10^3	121 x10^3	10	1.21
M2	50:1:0.5:1	90	55	55 x 10^3	70 x 10^3	6	1.25
M3	50:1:0.5:1	90	45	47 x 10^3	68 x 10^3	7	1.29
M	50:1:0.5:1	90	35	63 x 10^3	75 x 10^3	6	1.32

a) Solution polymerization in DMF (75 Wt % to 6-O-MMAGIc) at 60 °C

b) $[I]_0$ is defined as the molar amount of Br or Cl in the macroinitiator

c) Calculated gravimetry

d) Determined from SEC, calibrated with PMMA standards

e) Determined by SEC-MALLS in DMAc

f) Calculated from $M_{n,abs}$ assuming a 100% initiation efficiency according to $DP_{sc} = (M_{n,brush} - M_{n,macroinitiator})/(x \times DP_{n,\ macroinitiator} \times M_{n,6\text{-}O\text{-}MMAGIc})$, where $M_{n,6\text{-}O\text{-}MMAGIc}$ = 262 g/mol and *x* is molar fraction of initiator BIEM unites in the backbone

The presence of RAFT agent end-group moieties can be examined using dual detection for SEC. UV and RI detectors were used to determine whether the polymer chains contained the RAFT agent as an end group. The UV detector was set at 320 nm, as the thiocarbonyl thio moiety (-S(C=S)-) of the RAFT agent absorb strongly at this wavelength.[48] Overlay comparisons of the two signals indicate whether the RAFT agent functionality is homogeneously or heterogeneously distributed throughout the molar mass distribution curve. The graphs in Figure 3.3 show that the RAFT moiety was homogenously distributed in most of the polymer chains. The delay between RI and the UV detectors has been compensated for so that both signals overlap at their peak maximum. A small fraction of the RI signal at higher molar mass does not completely overlap with UV signal (Figure 3.3C). This can either be explained by the interaction of

the polymer with the SEC column or that there are a few chains at the high molar mass side that do not contain the RAFT agent as an end group. At low molar mass the observed UV signal is very strong due to the fact that the chains are small, resulting in a high concentration of RAFT agent per mass of chain.[49]

Figure 3.4 shows the ^{1}H-NMR spectra of the glycopolymer brushes. A broad peak attributed to anomeric hydroxyl groups of the sugar moieties (2.9-3.6 ppm) appears, and the characteristic peaks for the macroinitiators are to be in the spectra. This demonstrates the successful formation of molecular brushes with glycopolymer side chains.

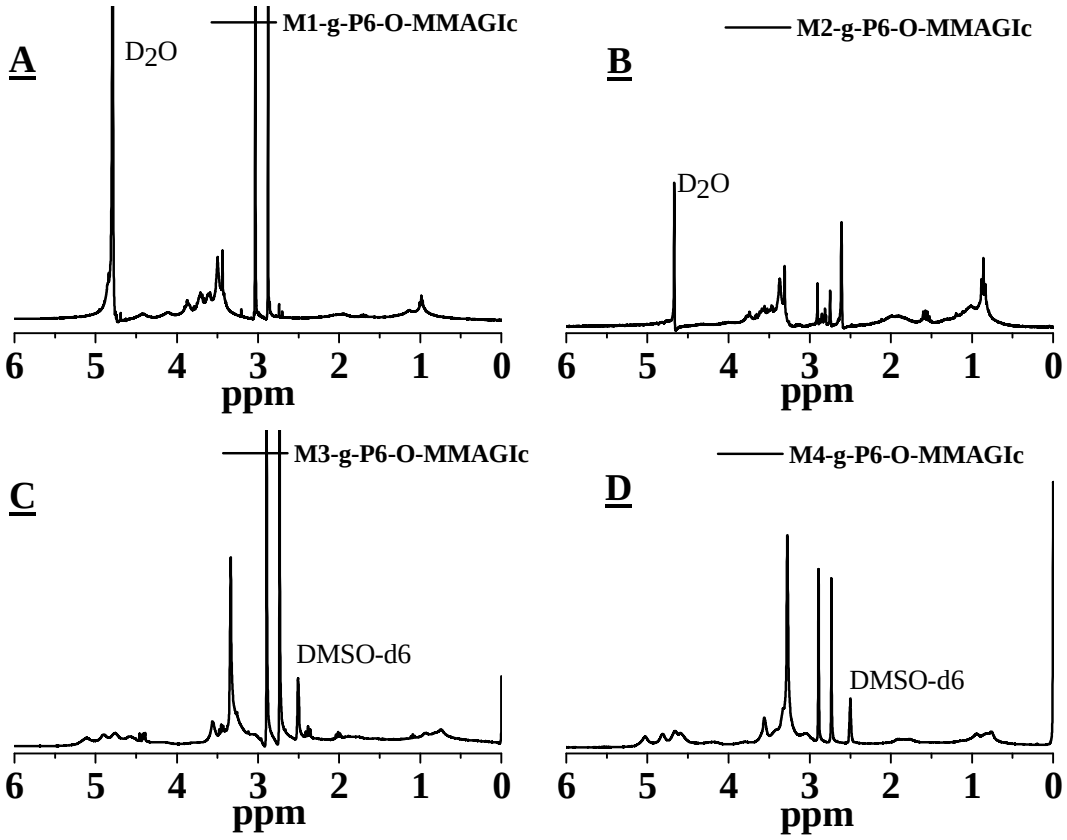

Figure 3.4: ^{1}H-NMR spectra of glycopolymer brushes: (A) P(BIEM)-g-P(6-O-MMAGIc), (B) P(BIEM-co-MMA)-g-P(6-O-MMAGIc), (C) P(BIEM-b-MMA)-g-P(6-O-MMAGIc), (D) P(S_d-alt-MA)-g-P(6-O-MMAGIc).

3.3.3 Visualization of glycopolymer brushes by AFM

The glycopolymer brushes were further characterized by AFM in order to visualize the polymer morphology. Previous studies showed that molecular brushes could be visualized as single molecules by using tapping mode AFM.[7,50] Even the backbone and the side chains were clearly observed due to the high spatial resolution and strong material contrast of tapping mode AFM.[7,51] All samples for AFM studies were prepared by spin casting from dilute aqueous solutions of concentrations varying from 0.1 mg/mL to 0.2 mg/mL. Polymers were spin coated at room temperature at 2000 rpm on freshly cleaved mica. Figure 3.5 shows the AFM images of the P(BIEM)-g-P(6-O-MMAGIc) and P(BIEM-co-MMA)-g-P(6-O-MMAGIc) glycopolymer brushes.

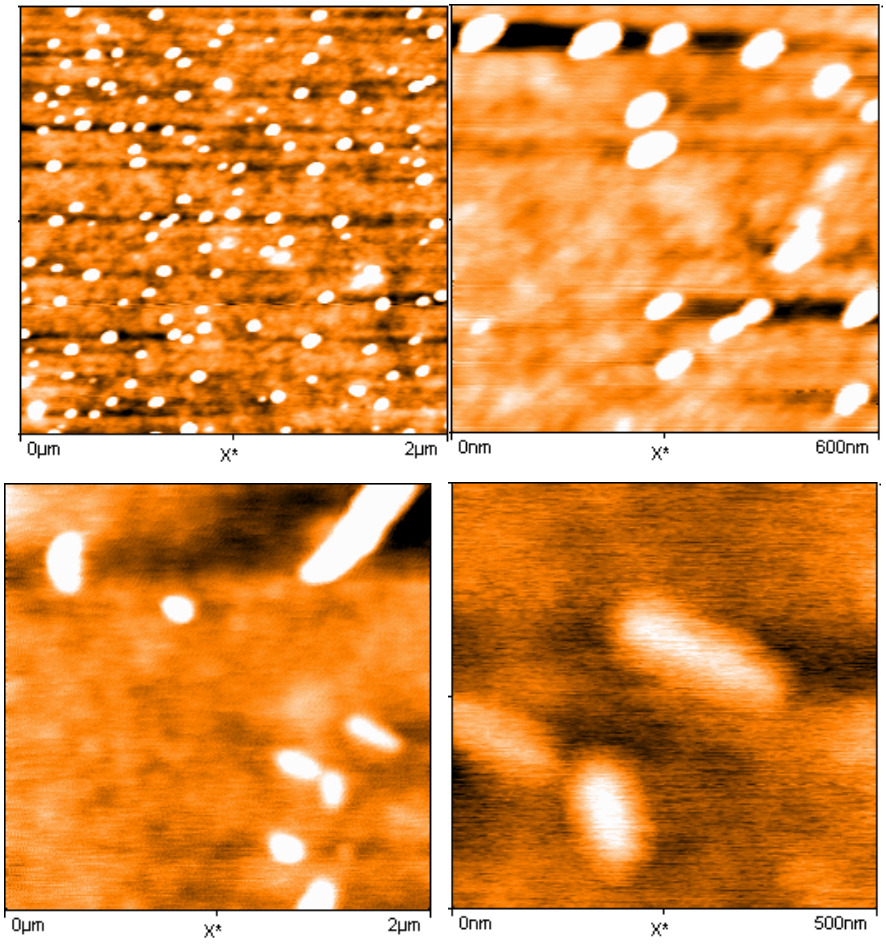

Figure 3.5: Tapping-mode AFM images for: (top) P(BIEM)-g-P(6-O-MMAGIc) brush polymer, (bottom) P(BIEM-co-MMA)-g-P(6-O-MMAGIc) spin coated from a dilute aqueous solution onto mica. Shown are hight images.

In the images, only islands of polymer molecules are visible; single molecules are not observed. This may be attributed to the fact that brushes are not completely stretched due to the low DP of the backbone. It is, therefore, speculated that the backbone tends to coil and form these islands.[52] Furthermore the grafting density of the glycopolymer brushes might be low, hence repulsion between adsorbed side chains is reduced, resulting in the contraction of the backbone.[6] Polymer aggregation due to strong interaction between glycopolymer and polar mica substrate could be another reason.[3] Furthermore, the polymer was spin coated from water, and it is reported in literature that an increase in humidity could rearrange polymer molecules to form clusters of several molecules on a mica surface.[53]

3.4 Conclusion

A successful combination of RAFT mediated polymerization and ATRP techniques were applied for the synthesis of short novel glycopolymer brushes. This work clearly shows the ability of the RAFT process to control the polymerization of halogenated monomer, where 2-cyanoprop-2-yl dithiobenzoate RAFT agent was successfully used for the synthesis of four well-defined ATRP macroinitiators. However, a deviation of the molar masses of the macroinitiators from the theoretical values, as well as polydispersity index in the range of 1.6 to 2.2 was observed for high targeted molar mass polymerization. Radical transfer to the halogen in the monomers (ATRP initiator moiety) is thought to be responsible for this limitation.[54] This suggests that protective group chemistry on the ATRP initiator moiety is needed in order to obtain well-defined, higher molar mass macroinitiators. Alternative methods for the synthesis of ATRP macroinitiators with higher molar masses will be discussed in the next chapter.

The four ATRP macroinitiators prepared here were subsequently used to then prepare high molar mass and low polydispersity index glycopolymer brushes with difference in grafting density along the backbone. This work demonstrated that the CuBr/n-Pr-1 catalyst system could successfully be used for the polymerization of unprotected 6-O-MMAGIc in the "grafting from" process, leading to well-defined glycopolymer brushes. AFM revealed that the molecular brushes adsorbed on a mica surface, and only islands of polymer molecules were visible as opposed to individual brushes in earlier study.

3.5 References

(1) Zhang, M.; Müller, A. H. E. *J. Polym. Sci. Part A: Polym. Chem.* **2005**, *43*, 3461-3481.

(2) Zhang, M.; Breiner, T.; Mori, H.; Müller, A. H. E. *Polymer* **2003**, *44*, 1449-1458.

(3) Venkatesh, R.; Klumperman, B. *Macromol. Chem. Phys.* **2004**, *205*, 2161-2168.

(4) Barbey, R.; Lavanant, L.; Paripovic, D.; SchuIwer, N.; Sugnaux, C.; Tugulu, S.; Klok, H.-A. *Chem. Rev.* **2009**, *109*, 5437-5527.

(5) Advincula, R. C.; Brittain, W. J.; Caster, K. C.; Ruhe, J. *Polymer Brushes : Synthesis, Characterization, Applications*; Wiley-VCH: Weinheim, 2004.

(6) Lee, H.; Matyjaszewski, K.; Yu, S.; Sheiko, S. S. *Macromolecules* **2005**, *38*, 8264-8271.

(7) Mori, H.; Müller, A. H. E. *Prog. Polym. Sci.* **2003**, *28*, 1403-1439.

(8) Borner, H. G.; Duran, D.; Matyjaszewski, K.; da Silva, M.; Sheiko, S. S. *Macromolecules* **2002**, *35*, 3387-3394.

(9) Borner, H. G.; Beers, K.; Matyjaszewski, K.; Sheiko, S. S.; Moller, M. *Macromolecules* **2001**, *34*, 4375-4383.

(10) Neugebauer, D.; Sumerlin, B. S.; Matyjaszewski, K.; Goodhart, B.; Sheiko, S. S. *Polymer* **2004**, *45*, 8173-8179.

(11) Sumerlin, B. S.; Neugebauer, D.; Matyjaszewski, K. *Macromolecules* **2005**, *38*, 702-708.

(12) Neugebauer, D.; Zhang, Y.; Pakula, T.; Matyjaszewski, K. *Polymer* **2003**, *44*, 6863-6871.

(13) Hawker, C. J.; Bosman, A. W.; Harth, E. *Chem. Rev.* **2001**, *101*, 3661-3688.

(14) Beers, K. L.; Gaynor, S. G.; Matyjaszewski, K.; Sheiko, S. S.; Möller, M. *Macromolecules* **1998**, *31*, 9413-9415.

(15) Albertin, L.; Stenzel, M. H.; Barner-Kowollik, C.; Foster, L. J. R.; Davis, T. P. *Macromolecules* **2005**, *38*, 9075-9084.

(16) You, L. C.; Lu, F. Z.; Li, Z. C.; Zhang, W.; Li, F. M. *Macromolecules* **2003**, *36*, 1-4.

(17) Bernard, J.; Hao, X.; Davis, T. P.; Barner-Kowollik, C.; Stenzel, M. H. *Biomacromolecules* **2006**, *7*, 232-238.

(18) Novick, S. J.; Dordick, J. S. *Chem. Mater.* **1998**, *10*, 955-958.

(19) Palomino, E. *Adv. Drug Deliv. Rev.* **1994**, *13*, 311-323.

(20) Wulff, G.; Zhu, L.; Schmidt, H. *Macromolecules* **1997**, *30*, 4533-4539.

(21) Karamuk, E.; Mayer, J.; Wintermantel, E.; Akaike, T. *Artif. Organs.* **1999**, *23*, 881-884.

(22) Okada, M. *Prog. Polym. Sci.* **2001**, *26*, 67-104.

(23) Lowe, A. B.; Sumerlin, B. S.; McCormick, C. L. *Polymer* **2003**, *44*, 6761-6765.

(24) Okada, M.; Tachikawa, K.; Aoi, K. *J. Polym. Sci. Part A: Polym. Chem.* **1997**, *35*, 2729-2737.

(25) Granville, A. M.; Quémener, D.; Davis, T. P.; Barner-Kowollik, C.; Stenzel, M. H. *Macromol. Symp.* **2007**, *255*, 81-89.

(26) Moad, G.; Chiefari, J.; Chong, B. Y.; Krstina, J.; Mayadunne, R. T.; Postma, A.; Rizzardo, E.; Thang, S. H. *Polym. Int.* **2000**, *49*, 993-1001.

(27) Matyjaszewski, K.; Gaynor, S. G.; Kulfan, A.; Podwika, M. *Macromolecules* **1997**, *30*, 5192-5194.

(28) Haddleton, D. M.; Crossman, M. C.; Dana, B. H.; Duncalf, D. J.; Heming, A. M.; Kukulj, D.; Shooter, A. J. *Macromolecules* **1999**, *32*, 2110-2119.

(29) Albertin, L.; Stenzel, M.; Barner-Kowollik, C.; Foster, L. J. R.; Davis, T. P. *Macromolecules* **2004**, *37*, 7530-7537.

(30) Moad, G.; Rizzardo, E.; Thang, S. H. *Aust. J. Chem.* **2005**, *58*, 379-410.

(31) Germack, D. S.; Harrisson, S.; Brown, G. O.; Wooley, K. L. *J. Polym. Sci. Part A: Polym. Chem.* **2006**, *44*, 5218-5228.

(32) Zhang, Y.; Huang, J.; Chen, Y. *Macromolecules* **2005**, *38*, 5069-5077.

(33) Haddleton, D. M.; Kukulj, D.; Duncalf, D. J.; Heming, A. M.; Shooter, A. J. *Macromolecules* **1998**, *31*, 5201-5205.

(34) Haddleton, D. M.; Clark, A. J.; Crossman, M. C.; Duncalf, D. J.; Heming, A. M.; Morsley, S. R.; Shooter, A. J. *Chem. Commun.* **1997**, *13*, 1173-1174.

(35) Haddleton, D. M.; Waterson, C.; Derrick, P. J.; Jasieczek, C. B.; Shooter, A. J. *Chem. Commun.* **1997**, *10*, 683-684.

(36) Haddleton, D. M.; Jasieczek, C. B.; Hannon, M. J.; Shooter, A. J. *Macromolecules* **1997**, *30*, 2190-2193.

(37) Beers, K. L.; Boo, S.; Gaynor, S. G.; Matyjaszewski, K. *Macromolecules* **1999**, *32*, 5772-5776.

(38) Simanek, E. E.; McGarvey, G. J.; Jablonowski, J. A.; Wong, C.-H. *Chem. Rev.* **1998**, *98*, 833-862.

(39) Robinson, K. L.; Khan, M. A.; de Paz Banez, M. V.; Wang, X. S.; Armes, S. P. *Macromolecules* **2001**, *34*, 3155-3158.

(40) Geng, J.; Mantovani, G.; Tao, L.; Nicolas, J.; Chen, G.; Wallis, R.; Mitchell, D. A.; Johnson, B. R. G.; Evans, S. D.; Haddleton, D. M. *J. Am. Chem. Soc.* **2007**, *129*, 15156-15163.

(41) Ladmiral, V.; Melia, E.; Haddleton, D. M. *Eur. Polym. J.* **2004**, *40*, 431-449.

(42) Miura, Y. *J. Polym. Sci. Part A: Polym. Chem.* **2007**, *45*, 5031-5036.

(43) Wang, X.-S.; Armes, S. P. *Macromolecules* **2000**, *33*, 6640-6647.

(44) Wang, T.-L.; Lee, H.-M.; Kuo, P.-L. *J. App. Polym. Sci.* **2000**, *78*, 592-602.

(45) Saad, G. R.; Morsi, R. E.; Mohammady , S. Z.; Elsabee, M. Z. *J. Polym. Res.* **2008**, *15*, 115-123.

(46) Cheng, G.; Boker, A.; Zhang, M.; Krausch, G.; Müller, A. H. E. *Macromolecules* **2001**, *34*, 6883-6888.

(47) De Vries, A.; Klumperman, B.; de Wet-Roos, D.; Sanderson, R. D. *Macromol. Chem. Phys.* **2001**, *202*, 1645-1648.

(48) Russum, J.; Jones, C. W.; Schork, F. J. *Macromol. Rapid Comm.* **2004**, *25*, 1064-1068.

(49) Fleet, R.; McLeary, J. B.; Grumel, V.; Weber, W. G.; Matahwa, H.; Sanderson, R. D. *Macromol. Symp.* **2007**, *255*, 8-19.

(50) Djalali, R.; Li, S.-Y.; Schmidt, M. *Macromolecules* **2002**, *35*, 4282-4288.

(51) Sheiko, S. S.; Moller, M. *Chem. Rev.* **2001**, *101*, 4099-4124.

(52) Muthukrishnan, S.; Zhang, M.; Burkhardt, M.; Drechsler, M.; Mori, H.; Müller, A. H. E. *Macromolecules* **2005**, *38*, 7926-7934.

(53) Kumaki, J.; Hashimoto, T. *J. Am. Chem. Soc.* **2003**, *125*, 4907-4917.

(54) Severac, R.; Lacroix-Desmazes, P.; Boutevin, B. *Polym. Int.* **2002**, *51*, 1117-1122.

Chapter 4: Synthesis and characterization of glycopolymer brushes initiated from different macroinitiators

Abstract

We report the synthesis and characterization of a series of well-defined glycocylindrical brushes (molecular sugar sticks) with P(methyl 6-O-methacryloyl-α-D-glucoside) (P(6-O-MMAGIc)) side chains, using the "grafting from" approach via atom transfer radical polymerization (ATRP). The formation of well-defined glycocylindrical brushes with narrow molar mass distribution was confirmed by ^{1}H-NMR spectroscopy and size exclusion chromatography (SEC) with a multi-angle light scattering detector (SEC-MALLS). In order to obtain the glycocylindrical brushes with narrow molar mass distribution, the macroinitiators were synthesized via two different techniques, by ATRP, to ensure that well-defined polymers with a living character were produced. Four multifunctional macroinitiators with different chemical compositions and molar masses were prepared, including P(2-(2-bromoisobutyryloxy) ethyl methacrylate (P(BIEM)), P(2-(2-bromoisobutyryloxy) ethyl methacrylate-co-methyl methacrylate) (P(BIEM-co-MMA)), P(2-(2-bromoisobutyryloxy) ethyl methacrylate-b-methyl methacrylate) (P(BIEM-b-MMA)) and P(4-vinylbenzyl chloride-alt-maleic anhydride) (P(S_d-alt-MA). Their molar masses were characterized by SEC and their structures were confirmed by ^{1}H-NMR spectroscopy. The P(6-O-MMAGIc) side chains were cleaved from the backbones by base solvolysis with sodium methoxide. The cleaved side chains were analyzed by ^{1}H-NMR and SEC-MALLS (measurements) which, confirm the synthesis of well-defined glycocylindrical brushes. By comparing the absolute molar mass of the cleaved side chains to their theoretical molar mass (calculated from assuming a 100% initiation efficiency) the grafting efficiency was determined. The grafting efficiency of P(6-O-MMAGIc) from the macroinitiators P(BIEM), P(BIEM-co-MMA), P(BIEM-b-MMA) and P(S_d-alt-MA) were determined to be in the range $0.37 < f < 0.55$.

4.1 Introduction

Over the past two decades, tethered polymer systems have attracted increasing attention not only due to theoretical interest but also due to their potential applications.[1-5] Cylindrical brushes are one-dimensional macromolecules that contain a high density of side chains (SCs), that is, every monomer unit of the backbone carries a side chain.[6-8] The immobilized ends of the SCs prevent the chains from escaping from their neighbours, which leads to stretched conformations to avoid overlapping.[6,9,10] A significant overcrowding and entropically unfavorable extension of the backbone will prompt the backbone to stretch its conformation from a random coil to extended chain.[6] This gives rise to polymers with interesting properties, as observed in bulk,[11] in solution,[12,13] and at interfaces.[14-17] The properties of the molecular brushes depend on a variety of molecular parameters, including the degree of polymerization of the backbone and the side chains, grafting density, backbone topology, and chemical composition.[11,18] To better understand the structure-property relationships of these macromolecules, a series of well-defined polymers with various grafting densities, lengths of side chains and side chains architectures, as well as the structure of polymer backbone is required.[15] Both the synthesis and the characterization of polymer brushes are challenging.[16]

Typically, polymer brushes are synthesized by living polymerization techniques, such as living anionic polymerization[19] and controlled/living radical polymerization (CRP).[10,20] Using CRP methods cylindrical brushes can be synthesized by one of the three routes: "grafting onto",[15,21-23] "grafting through"[11,24,25] and "grafting from"[13-15]

Grafting onto involves the attachment of side chains onto a separately prepared backbone polymer that contains reactive functional groups along its chain via a coupling reaction. This approach is beneficial because it allows the individual synthesis and characterization of the backbone and SCs. However, the grafting density is limited since attachment becomes progressively more difficult with increasing conversion and/or SC length due to steric congestion.[9,21,26]

Grafting through involves the synthesis of macromonomers with polymerizable end groups. Grafting through ensures the attachment of SCs to every backbone unit however,

this method suffers from a low degree of polymerization (DP) of the backbone; it is dependent on the macromonomer length and type.[17,26,27]

Grafting from involves the preparation of a backbone polymer (macroinitiator) with a predetermined number of initiation sites that are subsequently used to initiate polymerization.

Well-defined polymer brushes with high grafting density and low PDI, of both backbone and side chains, can be prepared by this method. High molecular weight backbones can be used, and the grafting density is not adversely affected with increasing monomer conversion.[13] One consequence of using radical polymerization to grow the side chains from the backbone is that radical-radical coupling must be significantly suppressed otherwise, cross-linked polymers or polymers with multimodal molar mass distribution may result. To avoid this, various polymerization conditions, such as temperature, catalyst and initiator concentration, should be optimized.[14]

Recently, considerable attention has been paid to the design of biofunctional materials carrying carbohydrate (sugar) moieties on synthetic polymers.[28] Synthetic carbohydrate polymers (glycopolymers) with biocompatible and biodegradable properties have become increasingly important in their use as artificial materials for a number of biological, pharmaceutical and biomedical uses.[29,30]

Here we report on the synthesis and characterization of glycocylindrical brushes comprising P(methyl 6-O-methacryloyl-α-D-glucoside) (P(6-O-MMAGIc)) side chains using the grafting from approach via copper-mediated ATRP, as shown in Scheme 4.3. Two approaches were used to prepare the macroinitiators with different degrees of polymerization (DPs) and different ATRP initiating group densities along the polymer backbone. The synthetic paths leading to the different macroinitiators are outlined in Scheme 4.1 (section 4.2.3.1) and Scheme 4.2 (section 4.2.3.2). The first route involves the synthesis of P(HEMA), P(HEMA-co-MMA) and P(MMA-b-HEMA) via ATRP followed by subsequent esterification of the pendant hydroxyl groups of P(HEMA) with 2-bromoisobutyryl bromide to yield P(BIEM), P(BIEM-co-MMA) and P(MMA-b-BIEM) macroinitiators.

The second route involves the synthesis of HEMA-TMS, which was homo and copolymerized by ATRP to produce P(HEMA-TMS), P(HEMA-TMS-co-MMA) and P(HEMA-TMS-b-MMA). The TMS groups were subsequently transformed to 2-bromoisobutyrate groups to yield P(BIEM), P(BIEM-co-MMA) and P(BIEM-b-MMA) macroinitiators.

When considering brush synthesis by the grafting from technique, it is important to understand the fundamentals that affect grafting density since this is largely responsible for the resulting unique material properties. The grafting from technique allows accurate control of the backbone length, but control of the length of the side chains and the grafting density are less ideal. Preliminary results indicated that complete initiation was obtained for ATRP polymerization of n-butyl acrylate from a macroinitiator.[15] However, other studies show that not every initiating site along the backbone generates a side chain, due to the high local concentration of initiation sites present on the backbone, steric interactions may adversely affect the efficiency of the grafting process.[11,31]

4.2 Experimental

4.2.1 Chemicals

Triethylamine 99.5% (Sigma-Aldrich), 2-bromoisobutyryl bromide 98% (Sigma-Aldrich), sodium chloride 98% (Sigma-Aldrich), magnesium sulphate (anhydrous) 99% (Saarchem), diethyl ether 99.7% (Sigma-Aldrich), methanol 98% (Alfa Aesar), ethanol and hexane (Kimix CP), p-xylene 99% (Merck), 1,4-dioxane 99% (Saarchem uniLAB), pyridine 98% (Sigma-Aldrich), methyl ethyl ketone 99.7% (Sigma-Aldrich), maleic anhydride 99% (Acros Organics), 4-vinylbenzyl chloride (S_d) 90% (Sigma-Aldrich), copper (I) bromide 99% (Sigma-Aldrich), ethyl α-bromoisobutyrate 98% (Fluka), N,N-dimethylformamide 97% (Fluka), 4,4'-di-(5-nonyl)-2,2'-bipyridine 97% (Sigma-Aldrich), potassium fluoride 99% (Fluka), chlorotrimethylsilane (TMS-Cl) 98% (Fluka), tetrabutylammonium fluoride solution 75 wt% in H_2O (TBAF solution) (Sigma-Aldrich), p-toluenesulfonyl chloride 99% (Fluka), sodium methoxide 25% (w/w) solution in methanol (Sigma-Aldrich), Dowex MSC-1 (H) ion exchange resin (Sigma-Aldrich) and ethylene glycol dimethacrylate 98% (Sigma-Aldrich) were all used as received without

further purification. CIPDB, n-Pr-1 and 6-O-MMAGlc were synthesized as described in Chapter 3; distilled deionized water was obtained from a Millipore Milli-Q purification system. Methyl methacrylate 99% (Sigma-Aldrich) was purified by passing it through a column of basic aluminum oxide to remove inhibitor, 2-hydroxyethyl methacrylate 98% (Sigma-Aldrich) was purified according to literature.[32] An aqueous solution of HEMA in water (25% by volume) was washed with hexane four times to remove ethylene glycol dimethacrylate, the monomer was then salted out of the aqueous phase by addition of NaCl (300 g/L), dried over $MgSO_4$ and distilled under reduced pressure. 2,2'-Bipyridine (bpy) 98% (Sigma-Aldrich) was re-crystallized from ethanol to remove impurities. 2,2 Azobis(isobutyronitrile) (Riedel de Haën) was re-crystallized twice from ethanol and dried under vacuum before use.

4.2.2 Instrumental analysis

4.2.2.1 Nuclear magnetic resonance spectroscopy (NMR)

^{1}H-NMR and ^{13}C-NMR spectra were obtained using a Varian VXR 400 MHz instrument equipped with a Varian magnet (7.0 T), or a 600 MHz Varian Unity Inova spectrometer equipped with an Oxford magnet (14.09 T). Depending on the solubility of the synthesized compounds, deuterated chloroform ($CDCl_3$) and deuterated dimethyl sulfoxide (DMSO-d6) was used as solvent. All chemical shifts are reported in ppm downfield from tetramethylsilane (TMS), used as an internal standard (δ = 0 ppm).

4.2.2.2 Size exclusion chromatography (SEC)

Molar mass and molar mass distribution values were measured using size exclusion chromatography (SEC). The SEC instrument consisted of a Waters 117 plus auto-sampler, Waters 600, E system controller (run by Millennium^{32} V 3.05 software) and a Waters 610 fluid unit. A Waters 410 differential refractometer and Waters 2487 dual wavelength absorbance detector were used. A laser photometer miniDAWN (Wyatt Technology Corporation, Santa Barbara, CA) multi-angle laser light scattering with ASTRA software (Wyatt Technology Corporation) was used. The system was equipped with 50 x8 mm guard column and three 300x8 mm linear columns (PSS, $3x10^3$, 10^2, and

$3x10^3$ Å pore size; 10µm particle size). DMAc (HPLC grade, 0.03% w/v, LiCl, 0.05% BHT) was used as eluent at a flow rate of 1 mL/min, while the column oven was kept at 40 °C. 100 µL of polymer solutions of 5 mg/mL were injected. The system was calibrated with narrow PMMA standards ranging from 800 to 2 x 10^6 g/mol. All molar masses are reported as PMMA equivalents.

4.2.2.3 Atom force microscopy (AFM)

AFM measurements were performed with a Easy Scan II AFM (Nanosurf). The microscope was operated in tapping mode at a resonance frequency of 360 kHz and at ambient conditions. The samples were prepared by spin-casting from dilute water solutions of concentrations varying from 0.1 mg/mL to 0.2 mg/mL. Polymers were spin-coated at room temperature at 2000 rpm on freshly cleaved mica.

4.2.3 Preparation of ATRP macroinitiators

RAFT mediated polymerization and ATRP were employed for the synthesis of eight ATRP macroinitiators that had a different DPs and different distribution of initiating sites along their backbones. Two different synthetic routes were employed for the preparation of these ATRP macroinitiators.

All polymerizations were carried out in a pear-shaped 50 mL Schlenk flask heated in an oil bath. The polymerization mixture was degassed with a minimum of three freeze-pump-thaw cycles, followed by the introduction of high purity argon. The DP was calculated using equation 2.10, on the basis of monomer conversion. Typical polymerizations were performed as discussed below.

4.2.3.1 Preparation of ATRP macroinitiators via the first polymerization route

The first route includes the synthesis of P(HEMA), P(HEMA-co-MMA) and P(MMA-b-HEMA) via ATRP followed by subsequent esterification of the pendant hydroxyl groups of PHEMA with 2-bromoisobutyryl bromide yielding P(BIEM), P(BIEM-co-MMA) and P(MMA-b-BIEM) macroinitiators. The P(S_d-alt-MA) macroinitiator was synthesized via RAFT mediated polymerization. This synthetic route is outlined in Scheme 4.1.

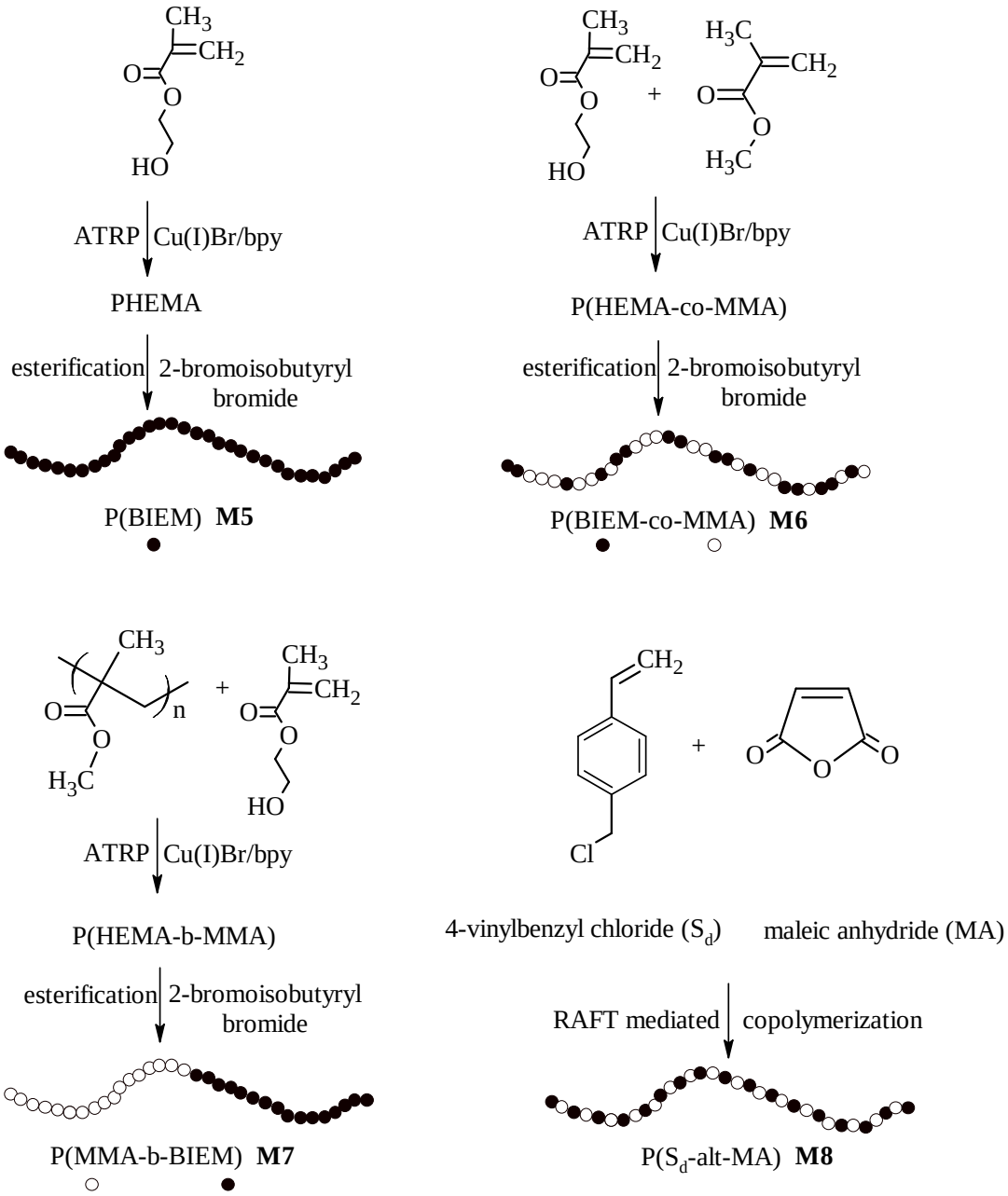

Scheme 4.1: Synthesis of ATRP macroinitiators by route 1.

a) Synthesis of P(BIEM) (M5) by ATRP

In a typical ATRP experiment,[32,33] Cu(I)Br (17.0 x 10^{-3} g, 1.1 x 10^{-5} mol), ethyl α-bromoisobutyrate initiator (23.0 x 10^{-3} g, 1.17 x 10^{-4} mol) and bpy ligand (32.0 x 10^{-3} g, 2.3 x 10^{-4} mol) were added to a 50 mL Schlenk flask. A solution of purified HEMA monomer (10 g, 0.076 mol) in MEK/1-propanol (10 g, 70/30:v/v) was added to the flask and the reaction mixture was degassed by three freeze-pump-thaw cycles, followed by the introduction of high purity argon. The flask was sealed with a rubber septum and placed in a preheated thermostatted oil bath at 50 °C.

The polymerization was stopped after 20 h by cooling to room temperature and opening the flask to air. The reaction solution was diluted with ethanol and passed though a column of neutral aluminum oxide three times to remove any traces of the catalyst, followed by precipitation in diethyl ether twice to remove unreacted monomer. The polymer was collected by filtration and dried in a vacuum oven at room temperature for 24 h. The yield was 7 g of isolated P(HEMA). The polymer was characterized by ^{1}H-NMR spectroscopy and SEC. According to SEC using PMMA calibration, the molar mass was M_n = 1.15 x 10^5 g/mol and the PDI = 1.47, with 70% monomer conversion. ^{1}H-NMR ($(CD_3)_2SO$): δ (ppm) = 4.82 (-**OH**), 3.89 (-**CH_2**-O-CO), 3.57 (-**CH_2**-OH), 2.01-1.64 (-**CH_2**-C), 1.0-0.68 (-**CH_3**).

In a 250 mL round-bottom flask filled with dry argon, a 5 g sample of P(HEMA) (-OH groups, 38.4 x 10^{-3} mol) was dissolved in 80 mL of anhydrous pyridine. Then 17.65 g (76.0 x 10^{-3} mol) of 2-bromoisobutyryl bromide was added drop-wise at 0 °C over 30 min. The mixture was stirred for 3 h at 0 °C followed by stirring at room temperature for 24 h. The insoluble salt was then removed by filtration and the solvent was removed under vacuum. The resulting polymer was purified by passing through a neutral aluminum oxide column using THF as solvent, followed by precipitation in methanol. The yield was 9.8 g of isolated P(BIEM), and the polymer was characterized by ^{1}H-NMR spectroscopy and SEC. According to SEC using PMMA calibration, the molar mass was M_n = 55.0 x 10^3 g/mol and the PDI = 1.38. ^{1}H-NMR ($(CD_3)_2SO$): δ (ppm) = 4.33 (-O-

CH_2-**CH_2**-O-CO-C(Br)(CH_3)$_2$), 4.13 (-O-**CH_2**-CH_2-O-CO-C(Br)(CH_3)$_2$), 1.92 [-C(Br)(**CH_3**)$_2$], 1.85-1.64 (-**CH_2**-C), 1.07-0.69 (-**CH_3**).

b) Synthesis of P(BIEM-co-MMA) (M6) by ATRP

In a typical ATRP experiment,[34,35] purified HEMA (5 g, 3.8 x 10^{-2} mol), MMA (3.8 g, 3.8 x 10^{-2} mol), ethyl α-bromoisobutyrate initiator (0.025 g, 1.3 x 10^{-4} mol), Cu(I)Br (0.018 g, 1.25 x 10^{-4} mol), bpy ligand (0.035 g, 2.5 x 10^{-4} mol) and 15 g of toluene were added to a 50 mL Schlenk flask equipped with a magnetic stirrer bar. The flask was sealed with a septum, degassed by three freeze-pump-thaw cycles, followed by the introduction of high purity argon, and then placed in an oil bath preheated to 80 °C. After 8 h the polymerization was stopped by cooling to room temperature and opening the flask to air. The solution was then diluted with toluene and passed though a column of neutral aluminum oxide three times to remove the catalyst, followed by precipitation in diethyl ether twice to remove unreacted monomer. The polymer was collected by filtration and dried in a vacuum oven at room temperature for 24 h to yield 7 g P(HEMA-co-MMA). The polymer was characterized by ^{1}H-NMR spectroscopy and SEC. According to SEC using PMMA calibration, the molar mass was M_n = 9.0 x 10^4 g/mol and the PDI = 1.42. Monomer conversion was 42% of MMA and 37% of HEMA. ^{1}H-NMR ((CD_3)$_2$SO): δ (ppm) = 4.79 (-**OH**), 3.91 (-**CH_2**-O-CO), 3.59 (-**CH_2**-OH), 3.54 (-O-**CH_3**), 2.01-1.64 (-**CH_2**-C), 1.01-0.61 (-**CH_3**).

In a 250 mL round-bottom flask filled with dry argon, a 2 g sample of P(HEMA-co-MMA) (-OH groups, 6.6 x 10^{-3} mol, obtained from ^{1}H-NMR spectroscopy) was dissolved in 25 mL anhydrous pyridine. Then 3 g (1.3 x 10^{-4} mol) 2-bromoisobutyryl bromide was added drop-wise at 0 °C over 10 min. The mixture was stirred for 3 h at 0 °C followed by stirring at room temperature for 24 h. The insoluble salt was then removed by filtration, and the solvent was removed under vacuum. The resulting polymer was purified by passing through a neutral aluminum oxide column using THF as solvent, followed by precipitation in a large amount of cold methanol. The yield was 2.8 g of isolated P(BIEM-co-MMA), and the polymer was characterized by ^{1}H-NMR spectroscopy and SEC. According to SEC using PMMA calibration, the molar mass was M_n = 5.1 x 10^4

g/mol and the PDI = 1.35. ^{1}H-NMR ($(CD_3)_2SO$): δ (ppm) = 4.34 (-O-CH_2-**CH_2**-O-CO-C(Br)$(CH_3)_2$), 4.15 (-O-**CH_2**-CH_2-O-CO-C(Br)$(CH_3)_2$), 3.53 (-O-**CH_3**), 1.94 [-C(Br)(**CH_3**)$_2$], 2.03-1.65 (-**CH_2**-C), 1.04-0.61 (-**CH_3**).

c) Synthesis of P(MMA-b-BIEM) (M7) diblock copolymer by ATRP

A typical ATRP reaction was carried out as follows.[32] Into a 50 mL Schlenk flask, purified HEMA (6 g, 4.6 x 10^{-2} mol), Cu(I)Br (0.014 g, 9.7 x 10^{-4} mol), bpy ligand (0.026 g, 1.9 x 10^{-4} mol) and MEK/1-propanol (4 g, 70/30:v/v) were added. PMMA with predominantly Br end groups (3.5 g, M_n 25.0 x 10^3 g/mol, PDI 1.12, prepared according to a procedure described in the literature[36]) was dissolved in MEK/1-propanol (8 g, 70/30:v/v). The solution of PMMA was then added to the mixture in the Schlenk flask. The mixture was degassed using three freeze-pump-thaw cycles, after which the flask was immersed in a thermostatted oil bath preheated at 60 °C. After 20 h reaction time, under magnetic stirring, the polymerization was stopped by cooling to room temperature and opening the flask to air. The solution was then diluted with MEK/1-propanol (70/30:v/v) and passed though a column of neutral aluminum oxide to remove the catalyst, followed by precipitation in diethyl ether twice to remove unreacted monomer. The polymer was collected by filtration and dried in a vacuum oven at room temperature for 24 h to yield 7.7 g P(MMA-b-HEMA). The polymer was then analyzed via SEC and ^{1}H-NMR spectroscopy. M_n = 9.5 x 10^4 g/mol, and PDI = 1.42 with, 70% monomer conversion. ^{1}H-NMR ($(CD_3)_2SO$): δ (ppm) = 4.8 (-**OH**), 3.89 (-**CH_2**-O-CO), 3.56 (-**CH_2**-OH), 3.55 (-O-**CH_3**), 2.1-1.6 (-**CH_2**-C), 1.03-0.58 (-**CH_3**).

In a 250 mL round-bottom flask filled with dry argon, a 4 g sample of P(MMA-b-HEMA) (-OH groups, 1.44 x 10^{-2} mol, obtained from ^{1}H-NMR spectroscopy) was dissolved in anhydrous pyridine (25 mL). Then 2-bromoisobutyryl bromide (6.6 g, 2.8 x 10^{-2} mol) was added drop-wise at 0 °C over 20 min. The mixture was stirred for 3 h at 0 °C, followed by stirring at room temperature for 24 h. The insoluble salt was then removed by filtration and the solvent was removed under vacuum. The resulting polymer was purified by passing through a neutral aluminum oxide column using THF as solvent, followed by precipitation in large amount of cold methanol. The yield was 6.6 g of

isolated P(MMA-b-BIEM). The polymer was characterized by ^{1}H-NMR spectroscopy and SEC. According to SEC using PMMA calibration, the molar mass was M_n = 5.2 x 10^4 g/mol and the PDI = 1.39. ^{1}H-NMR ($(CD_3)_2SO$): δ (ppm) = 4.33 (-O-CH_2-**CH_2**-O-CO-C(Br)$(CH_3)_2$), 4.14 (-O-**CH_2**-CH_2-O-CO-C(Br)$(CH_3)_2$), 3.57 (-O-**CH_3**), 1.92 [-C(Br)(**CH_3**)$_2$], 1.91-1.59 (-**CH_2**-C), 1.04-0.59 (-**CH_3**).

d) Synthesis of P(S_d-alt-MA) (M8) by RAFT mediated polymerization

A typical RAFT mediated polymerization was carried out as follows.[37,38] A stirrer bar was placed in a 50 mL Schlenk flask along with maleic anhydride (3.3 g, 3.3 x 10^{-2} mol), 4-vinylbenzyl chloride (5 g, 3.3 x 10^{-2} mol), RAFT agent (CIPDB, 0.002 g, 1.0 x 10^{-5} mol), AIBN (3.0 x 10^{-3}g, 2.0 x 10^{-6} mol), and MEK (12 g) were added. The solution was degassed by three freeze-pump-thaw cycles. The Schlenk flask was immersed in a thermostatted oil bath preheated at 60 °C. After 24 h of reaction time under magnetic stirring P(S_d-alt-MA) was isolated by precipitation in diethyl ether. The copolymer was collected by filtration and dried in a vacuum oven at room temperature for 24 h to yield 5 g P(S_d-alt-MA).[37-39] The copolymer was then analyzed via SEC and ^{1}H-NMR spectroscopy. M_n = 5.1 x 10^4 g/mol, PDI = 1.17. Monomer conversion was 31% of MA and 29% of S_d. ^{1}H-NMR ($CDCl_3$): δ (ppm) = 7.66-6.9 (**Ar**-H), 5.00-4.40 (-**CH_2**-Cl), 2.40-2.10 [-**CH**-**CH**-], 1.99-1.70 (-**CH_2**-).

4.2.3.2 Preparation of ATRP macroinitiators via the second route

The second route was applied to the synthesis of HEMA-TMS, which was homo- and copolymerized via ATRP to afford P(HEMA-TMS), P(HEMA-TMS-co-MMA) and P(HEMA-TMS-b-MMA). TMS groups were subsequently transformed to 2-bromoisobutyrate groups to yield P(BIEM), P(BIEM-co-MMA) and P(BIEM-b-MMA) macroinitiators. P(S_d-alt-MA) macroinitiator was synthesized via RAFT mediated polymerization as described in the previous section. This synthetic route is outlined in Scheme 4.2.

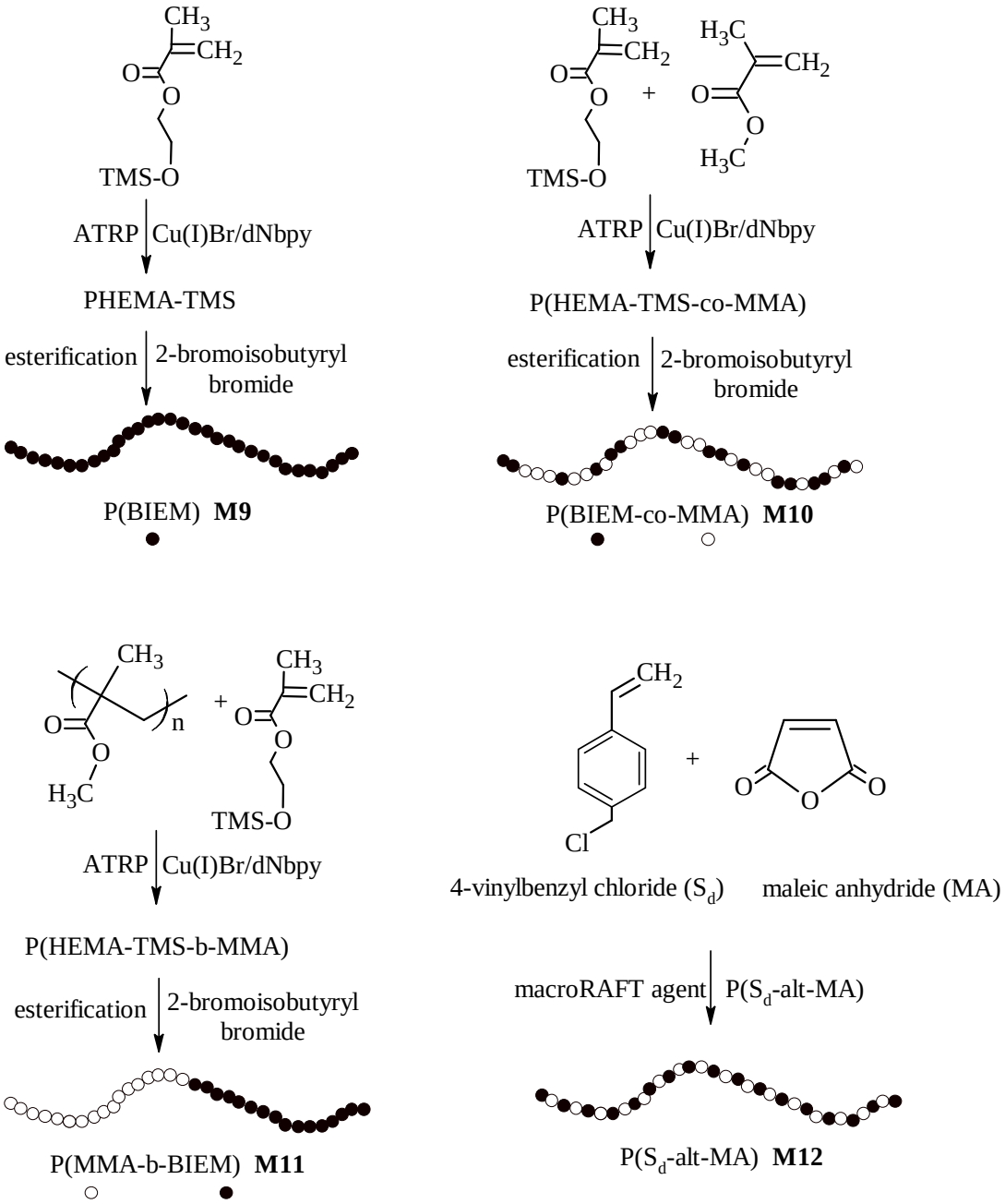

Scheme 4.2: Synthesis of ATRP macroinitiators by route 2.

a) Synthesis of 2-(trimethylsilyloxy)ethyl methacrylate (HEMA-TMS)

The synthesis of HEMA-TMS was carried out according to a method previously reported in the literature.[14,32] In a dry 500 mL round-bottom flask, under argon, a solution of purified HEMA (10 mL, 7.6 x 10^{-2} mol), triethylamine (10.6 mL, 7.6 x 10^{-2} mol) and ethyl ether (250 mL) was stirred at 0 °C. TMS-Cl (9.8 mL, 7.6 x 10^{-2} mol) was added drop-wise over 10 min. A white precipitate formed immediately. The mixture was stirred at 0 °C for 2 h and then filtered to remove the solids. The solid was washed with diethyl ether. The filtrate was washed with de-ionized water (3 x 100 mL), dried over $MgSO_4$, and the ether was removed by evaporation under reduced pressure. The purity was checked by ^{1}H-NMR spectroscopy and estimated to be 98.0%. Yield: 81%. ^{1}H-NMR ($CDCl_3$): δ (ppm) = 6.1 (s, 1H), 5.5 (s, 1H), 4.2 (t, 2H), 3.8 (t, 2H), 1.9 (s, 3H), 0.11 (s, 9H).

b) Synthesis of P(BIEM) (M9) by ATRP

In a typical ATRP experiment,[11,14,32] p-toluenesulfonyl chloride (6.0 x 10^{-3} g, 3.2 x 10^{-5} mol), HEMA-TMS (6 g, 0.029 mol), Cu(I)Br (4.5 x 10^{-3} g, 3.2 x 10^{-5} mol) and dNbPy (25.0 x 10^{-3} g, 6.4 x 10^{-5} mol) were combined and then added to a 50 mL Schlenk flask. The flask was degassed by three freeze-pump-thaw cycles, followed by argon backfill. The flask was then immersed in a thermostatted oil bath preheated at 80 °C. After 15 h of reaction time under magnetic stirring, the polymerization was stopped by cooling to room temperature and opening the flask to air. The polymer was then diluted with THF and passed through a column of neutral aluminum oxide to remove the catalyst, followed by precipitation in hexane twice to remove unreacted monomer. The polymer was collected by filtration and dried in a vacuum oven at room temperature for 24 h to yield 3.66 g P(HEMA-TMS). The polymer was then analyzed via SEC and ^{1}H-NMR spectroscopy. M_n = 1.07 x 10^5 g/mol, PDI = 1.18, with 61% monomer conversion. ^{1}H-NMR ($CDCl_3$): δ (ppm) = 4.1(-**CH_2**-O-CO), 3.77 (-**CH_2**-O-Si), 2.06-1.75 (-**CH_2**-C), 1.14-0.81 (-**CH_3**), 0.13 ((**CH_3**)$_3$-Si).

In a 250 mL round-bottom flask the product P(HEMA-TMS) (3 g, 1.5 x 10^{-2} mol of R–OTMS groups) was dissolved in dry THF (50 mL) under nitrogen. Potassium fluoride

(0.9 g, 15.5 x 10^{-3} mol), and a 75 wt% aqueous solution of TBAF (0.17 mL, 5.0 x 10^{-4} mol) were added, followed by the drop-wise addition of 2-bromoisobutyryl bromide (4.6 g, 2.0 x 10^{-3} mol), the reaction mixture was stirred at room temperature for 24 h. Triethylamine (1 mL) was added to ensure complete reaction. The solution was then stirred for an additional 3 h. The isolated polymer was precipitated from THF once into water/methanol (50/50) and three times into hexane and then dried under vacuum at room temperature for 24 h. The polymer was characterized by ^{1}H-NMR spectroscopy and SEC. According to SEC using PMMA calibration, the molar mass was M_n = 1.05 x 10^5 g/mol and the PDI = 1.16. ^{1}H-NMR ($CDCl_3$): δ (ppm) = 4.38 (-O-CH_2-**CH_2**-O-CO-C(Br)(CH_3)$_2$), 4.2 (-O-**CH_2**-CH_2-O-CO-C(Br)(CH_3)$_2$), 2.04 [-C(Br)(**CH_3**)$_2$], 1.78 (-**CH_2**-C), 1.03-0.85 (-**CH_3**).

c) Synthesis of P(BIEM-co-MMA) (M10) by ATRP

The ATRP copolymerization of HEMA-TMS and MMA was carried out in p-xylene.[16,40,41] A 50 mL Schlenk flask was charged with Cu(I)Br (5.0 x 10^{-3} g, 3.6 x 10^{-5} mol), dNbpy ligand (0.03 g, 7.3 x 10^{-5} mol), MMA (2.8 g, 2.7 x 10^{-2} mol), HEMA-TMS (5.6 g, 2.7 x 10^{-2} mol), ethyl α-bromoisobutyrate initiator (7.0 x 10^{-3} g, 3.6 x 10^{-2} mol) and p-xylene (9 g) and the flask was degassed by three freeze-pump-thaw cycles followed by argon backfill. The Schlenk flask was then placed in a thermostatted oil bath preheated at 85 °C. The reaction mixture was stirred for 21 h. The polymerization was then stopped by cooling to room temperature and opening the flask to air. The polymer was diluted with THF and passed though a column of neutral aluminum oxide to remove the catalyst, followed by precipitation in hexane twice to remove unreacted monomer. The polymer was collected by filtration and dried in a vacuum oven at room temperature for 24 h to yield 5.2 g P(HEMA-TMS-co-MMA). The polymer was then analyzed via size exclusion chromatography and ^{1}H-NMR spectroscopy. M_n = 1.41 x 10^5 g/mol, PDI = 1.21. Monomer conversion was 36% of HEMA-TMS and 24% of MMA. ^{1}H-NMR ($CDCl_3$): δ (ppm) = 4.01(-**CH_2**-O-CO), 3.76 (-**CH_2**-O-Si), 3.58 (-O-**CH_3**), 2.1-1.71 (-**CH_2**-C), 1.14-0.79 (-CH_3), 0.13 ((**CH_3**)$_3$-Si).

In a 250 mL round-bottom flask the product P(HEMA-TMS-co-MMA) (5 g, 10.4 x 10^{-3} mol of R–OTMS groups, from ^{1}H-NMR spectroscopy) was dissolved in dry THF (100 mL) under nitrogen. Potassium fluoride (0.61 g, 10.4 x 10^{-3} mol) and a 75 wt% aqueous solution of TBAF (0.03 mL, 1.0 x 10^{-4} mol) were added, followed by the slow addition of 2-bromoisobutyryl bromide (4 g, 17.3 x 10^{-3} mol). The reaction mixture was stirred at room temperature for 24 h. Triethylamine (3mL) was added to ensure complete reaction. The solution was then stirred for an additional 3 h. The isolated polymer was precipitated from THF once into water/methanol (50/50) and three times into hexane and then dried under vacuum at room temperature for 24 h. The polymer was characterized by ^{1}H-NMR spectroscopy and SEC. According to SEC using PMMA calibration, the molar mass was M_n = 1.34 x 10^5 g/mol and the PDI = 1.19. ^{1}H-NMR ($CDCl_3$): δ (ppm) = 4.37 (-O-CH_2-**CH_2**-O-CO-C(Br)(CH_3)$_2$), 4.2 (-O-**CH_2**-CH_2-O-CO-C(Br)(CH_3)$_2$), 3.58 (-O-**CH_3**), 2.01 [-C(Br)(**CH_3**)$_2$], 1.82 (-**CH_2**-C), 1.01-0.79 (-**CH_3**).

d) Synthesis of P(BIEM-b-MMA) (M11) diblock copolymer by ATRP

In a typical ATRP experiment,[32,33] MMA (1.5 g, 1.5 x 10^{-2} mol), Cu(I)Br (2.0 x 10^{-3} g, 1.4 x 10^{-5} mol), dNbpy ligand (11.0 x 10^{-3}g, 2.8 x 10^{-5} mol) and p-xylene (3 g) were added to a 50 mL Schlenk flask. A solution of P(HEMA-TMS) with predominantly Br end groups (1 g, M_n 55.0 x 10^3 g/mol, PDI 1.13, prepared as described above[11,14]) in p-xylene (2 g) was prepared. The solution of P(HEMA-TMS) was then added to the Schlenk flask and degassed using three freeze-pump-thaw cycles, after which the flask was immersed in a thermostatted oil bath preheated at 90 °C. After 15 h reaction time under magnetic stirring, the polymerization was stopped by cooling to room temperature and opening the flask to air. The solution was then diluted with THF and passed though a column of neutral aluminum oxide to remove the catalyst, followed by precipitation in hexane twice to remove unreacted monomer. The polymer was collected by filtration and dried in a vacuum oven at room temperature for 24 h to yield 2 g P(HEMA-TMS-b-MMA). The polymer was then analyzed via SEC and ^{1}H-NMR spectroscopy. M_n = 1.03 x 10^5 g/mol, PDI = 1.21 with 69% monomer conversion. ^{1}H-NMR ($CDCl_3$): δ (ppm) = 4 (-**CH_2**-O-CO), 3.76 (-**CH_2**-O-Si), 3.6 (-O-**CH_3**), 2.1-1.72 (-**CH_2**-C), 1.13-0.78 (-**CH_3**), 0.14 ((**CH_3**)$_3$-Si).

In a 250 mL round-bottom flask P(HEMA-TMS-b-MMA) (1.8 g, 3.8 x 10^{-3} mol of R–OTMS groups, from ^{1}H-NMR spectroscopy) was dissolved in dry THF (50 mL) under nitrogen. Potassium fluoride (0.23 g, 4.0 x 10^{-3} mol) and a 75 wt% aqueous solution of TBAF (0.02 mL, 6.0 x 10^{-5} mol) were added, followed by the slow addition of 2-bromoisobutyryl bromide (1.95 g, 8.5 x 10^{-3} mol). The reaction mixture was stirred at room temperature for 24 h. Triethylamine (2mL) was added to ensure complete reaction and the solution was stirred for an additional 3 h. The isolated polymer was precipitated from THF once into water/methanol 50/50 and three times into hexane, and then dried under vacuum at room temperature for 24 h. The polymer was characterized by ^{1}H-NMR spectroscopy and SEC. According to SEC using PMMA calibration, the molar mass was M_n = 1.08 x 10^5 g/mol and the PDI = 1.2. ^{1}H-NMR ($CDCl_3$): δ (ppm) = 4.39 (-O-CH_2-**CH_2**-O-CO-C(Br)(CH_3)$_2$), 4.22 (-O-**CH_2**-CH_2-O-CO-C(Br)(CH_3)$_2$), 3.59 (-O-**CH_3**), 1.98 [-C(Br)(**CH_3**)$_2$], 1.82 (-**CH_2**-C), 1.15-0.8 (-**CH_3**).

e) Synthesis of P(S_d-alt-MA) (M12) by RAFT mediated copolymerization

For a typical chain extension procedure,[42,43] a stirrer bar was placed in a 50 mL Schlenk flask and then the flask was charged with maleic anhydride (3.3 g, 3.3 x 10^{-2} mol), 4-vinylbenzyl chloride (5 g, 3.3 x 10^{-2} mol), AIBN (4.0 x 10^{-3} g, 0.02 x 10^{-3} mol) and MEK (10 g). P(S_d-alt-MA) (5.2 g, M_n = 50.0 x 10^3 g/mol, PDI 1.22, prepared according to procedure described in the previous section) was dissolved in MEK (10 g). The solution of P(S_d-alt-MA) was then added to the Schlenk flask and degassed using three freeze-pump-thaw cycles, after which the flask was immersed in a thermostatted oil bath preheated at 60 °C. After 20 h of reaction time, under magnetic stirring, P(S_d-alt-MA) was isolated by precipitation in diethyl ether. The polymer was collected by filtration and was dried in a vacuum oven at room temperature for 24 h to yield 8.9 g of P(S_d-alt-MA).The copolymer was then analyzed via SEC and ^{1}H-NMR spectroscopy. M_n = 1.18 x 10^5 g/mol and PDI = 1.24. Monomer conversion was 23% of MA and 22% of S_d. ^{1}H-NMR (($CDCl_3$): δ (ppm) = 7.54-6.83 (**Ar**-H), 4.91-4.45 (-**CH_2**-Cl), 2.40-2.10 [-**CH-CH**-], 1.99-1.70 (-CH_2-).

4.2.4 Synthesis of glycocylindrical brushes

A series of well-defined glycocylindrical brushes with glycopolymer side chains of approximately constant length and different grafting densities were prepared by using the grafting from approach. A general synthetic procedure for the glycocylindrical brushes is outlined in Scheme 4.3.

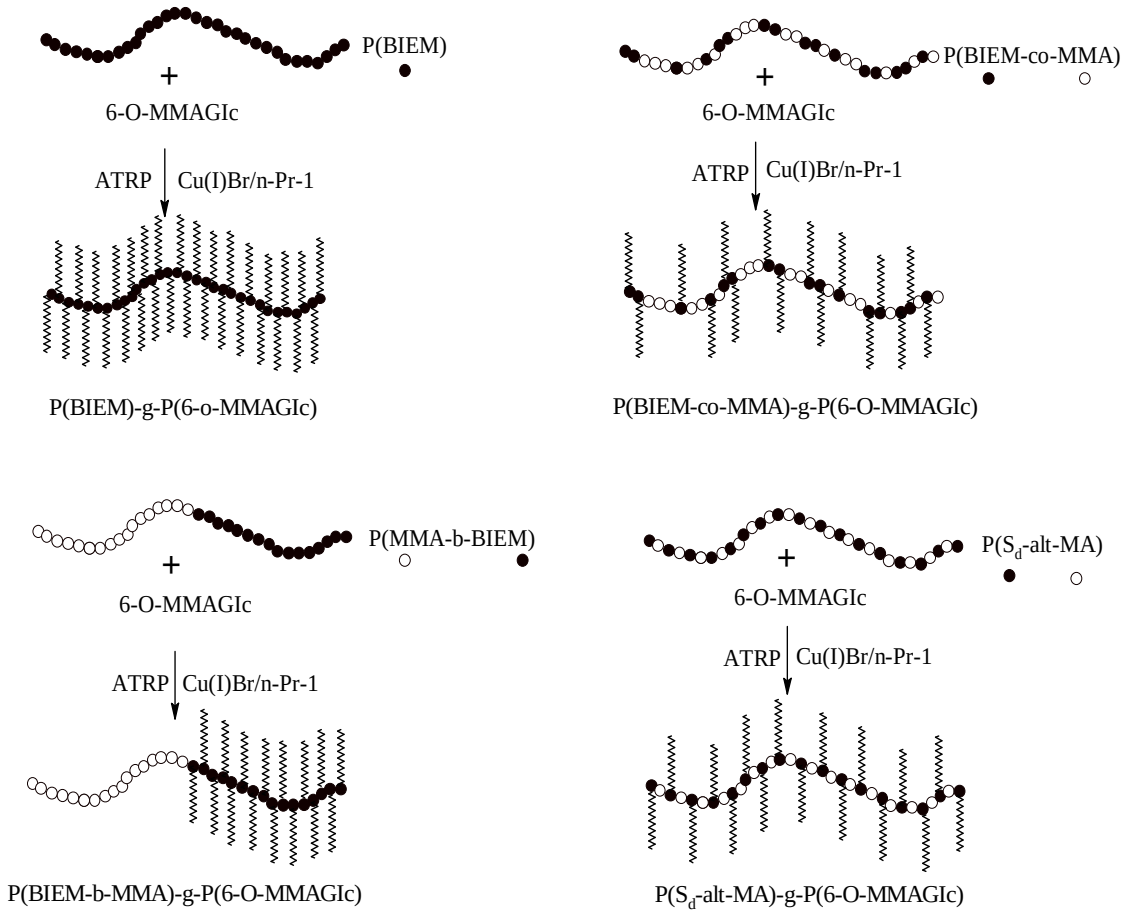

Scheme 4.3: Synthetic outline for glycopolymer brushes.

All polymerizations were carried out in a pear-shaped 50 mL Schlenk flask heated in an oil bath. The polymerization mixture was degassed with a minimum of three freeze-pump-thaw cycles followed by the introduction of high purity argon. Monomer conversion for graft polymerization was determined by polymer formation based on gravimetry. The degree of polymerization of the side chains was calculated using

equation 2.10, based on monomer conversion, assuming quantitative initiation from each Br or Cl atom. A typical polymerization was performed as follows:

4.2.4.1 Synthesis of P(BIEM)-g-P(6-O-MMAGIc)

To a 50 mL Schlenk flask containing a stirrer bar was added, PBIEM (M9, 4.2 x 10^{-2} g, 1.5 x 10^{-4} mol of initiating α-bromoester group), Cu(I)Br (0.01 g, 7.0 x 10^{-5} mol) and n-Pr-1 ligand (0.02g, 14 x 10^{-5} mol). To this DMF (4g) was added and the mixture was stirred for 15 minutes to completely dissolve the macroinitiator. A solution of 6-O-MMAGlc monomer (2 g, 7.0 x 10^{-3} mol) in DMF (2 g) was then added and the reaction mixture was degassed by three freeze-pump-thaw cycles, followed by the introduction of high purity argon. The flask was sealed with a rubber septum and placed in a preheated thermostatted oil bath at 60 °C. The polymerization was stopped after 1 h by cooling to room temperature and opening the flask to air. The polymerization solution was diluted with DMF and passed though a column of neutral aluminum oxide three times to remove any traces of the catalyst, followed by precipitation in diethyl ether twice to remove unreacted monomer. The yield was 0.73 g of isolated polymer and the monomer conversion was 36%. The polymer was characterized by ^{1}H-NMR spectroscopy and SEC. According to SEC using PMMA calibration, the molar mass was M_n = 7.20 x 10^5 g/mol and the PDI = 1.28.

4.2.4.2 Synthesis of P(BIEM-co-MMA)-g-P(6-O-MMAGIc)

The polymerization procedure used here was the same as described above. To a 50 mL Schlenk flask was added, P(BIEM-co-MMA) (M10, 0.1 g, 1.5 x 10^{-4} mol of initiating α-bromoester group, determined by ^{1}H-NMR spectroscopy), Cu(I)Br (0.01 g, 7.0 x 10^{-5} mol), n-Pr-1 ligand (0.02 g, 1.4 x 10^{-4} mol) and DMF (4 g). A solution of 6-O-MMAGlc monomer (2 g, 7.0 x 10^{-3} mol) in DMF (2 g) was then added to the reaction mixture. The polymerization was stopped after 1 h by cooling to room temperature and opening the flask to air. The yield was 0.7 g of isolated polymer and the monomer conversion was 35%. According to SEC (PMMA calibration): M_n = 480.0 x 10^3 g/mol and PDI = 1.34.

4.2.4.3 Synthesis of (P(BIEM)-b-P(MMA))-g-P(6-O-MMAGIc)

For a typical synthesis, a stirrer bar was placed in a 50 mL Schlenk flask along with P(BIEM)-b-P(MMA) (M11, 0.1 g, 1.5 x 10^{-4} mol of initiating α-bromoester group, obtained from ^{1}H-NMR spectroscopy), Cu(I)Br (0.01 g, 7.0 x 10^{-5} mol), n-Pr-1 ligand (0.02 g, 1.5 x 10^{-4} mol) and DMF solvent (4 g). The solution was stirred until a homogenous mixture was obtained. A solution of 6-O-MMAGlc monomer (2 g, 7.0 x 10^{-3} mol) in DMF (2 g) was then added to the reaction mixture. The reaction mixture was degassed by three freeze-pump-thaw cycles followed by the introduction of high purity argon. The flask was sealed with a rubber septum and placed in a preheated thermostatted oil bath at 60 °C. The polymerization was stopped after 80 min by cooling to room temperature and opening the flask to air. The polymerization solution was diluted with DMF and passed though a column of neutral aluminum oxide three times to remove the catalyst, followed by precipitation in diethyl ether twice to remove unreacted monomer. The yield was 0.85 g of isolated polymer and the conversion was 42% of 6-O-MMAGlc. According to SEC (PMMA calibration): M_n = 4.45 x 10^5 g/mol and PDI = 1.29.

4.2.4.4 Synthesis of P(S_d-alt-MA)-g-P(6-O-MMAGIc)

The polymerization procedure used was the same as described above. A 50 mL Schlenk flask was charged with P(S_d-alt-MA) (M12, 4.6 x 10^{-2} g, 1.5 x 10^{-4} mol of initiating α-bromoester group, obtained from ^{1}H-NMR spectroscopy), Cu(I)Br (0.01 g, 7.0 x 10^{-5} mol), n-Pr-1 ligand (0.02 g, 1.5 x 10^{-4} mol) and DMF (4 g). A solution of 6-O-MMAGlc monomer (2 g, 7.0 x 10^{-3} mol) in DMF (2 g) was then added to the reaction mixture. The polymerization was stopped after 90 min by cooling to room temperature and opening the flask to air. The yield was 0.7 g of isolated polymer; and the monomer conversion was 40%. According to SEC (PMMA calibration): M_n = 7.35 x 10^5 g/mol and PDI = 1.25.

4.2.4.5 Synthesis of cross-linked glycopolymer brushes P(BIEM)-g-P(6-O-MMAGIc-co-EGDMA)

The synthesis of four different glycopolymer brushes with cross-linked side chains was conducted under similar conditions.[44] A typical procedure for the ATRP of 6-O-

MMAGIc and EGDMA grafted from P(BIEM) is briefly described. The ratio of reagents used for the copolymerization was as follows:
$[6\text{-O-MMAGIc}]_0/[EGDMA]_0/[PBIEM]_0/[CuBr]_0/[\text{ n-Pr-1}]_0$: 91/9/2/1/2. A Schlenk flask was charged with 6-O-MMAGIc (2 g, 7.0×10^{-3} mol), EGDMA (0.15 g, 7.5×10^{-4} mol), n-Pr-1 ligand (0.029 g, 1.7×10^{-4} mol), CuBr (0.01 g, 8.0×10^{-5} mol), P(BIEM) (4.6×10^{-2} g, $0.1.7 \times 10^{-4}$ mol) and DMF (6 g). The flask was degassed by three freeze-pump-thaw cycles and backfilled with argon before it was immersed in an oil bath at 60 °C. The copolymerization reaction was stopped after 30 minutes by cooling to room temperature and opening the flask to air. The yield was 1.2 g of isolated polymer.

4.2.4.6 Solvolysis of the glycocylindrical brushes

The solvolysis of the brushes was achieved via base-catalyzed transesterification in THF.[8,31] The polymer brush (100 mg) was dissolved in DMF (25 g) in a capped vial. THF was added until the polymer precipitated, and then sodium methoxide (25% in methanol) was added. The capped vial was then placed in an oil bath and kept at 90 °C for 7 days. The solution was cooled and stirred for 2 h in the presence of a cationic ion-exchange resin (Dowex MSC-1 (H)). The solution was decanted and the solvent evaporated. The molecular weight of the resulting product was analyzed by conventional SEC, and SEC-MALLS measurements.

4.3 Results and discussion

The synthesis of a macroinitiator with a narrow MMD is essential to subsequently obtain uniform cylindrical brushes,[14,41] because the length distribution of the cylindrical brushes is largely dependent on the MMD of the backbone (macroinitiator). A macroinitiator with a broad MMD would result in the formation of brush polymers with broad MMD, irrespective of how well controlled the polymerization of the side chains is.[14,45] Therefore the preparation of well-defined macroinitiators was undertaken. The homopolymerizations of HEMA and HEMA-TMS and their copolymerizations with MMA as well as their transformations to ATRP macroinitiators were examined. The chemical composition of the polymers was determined by ^{1}H-NMR spectroscopy. Grafting of the 6-O-MMAGIc glycomonomer from the macroinitiators to form glycocylindrical brushes via ATRP was also examined. The mechanical and thermal properties and the morphologies, of the glycocylindrical brushes were studied by dynamic mechanical analysis (DMA), differential scanning calorimetry (DSC), thermogravimetric analysis (TGA) and wide angle X-ray scattering (WAXS), as will be discussed in the next chapter.

4.3.1 Strategy for the synthesis of ATRP macroinitiators

Two strategic pathways (routes 1 and 2) were used to prepare eight ATRP macroinitiators with different DPs and different distribution of initiating sites along the backbone (see Schemes 4.1 and 4.2). The synthetic details and characterization data are summarized in Table 4.1.

The first strategic pathway includes the homopolymerization of HEMA and copolymerization of HEMA with MMA via ATRP to prepare P(HEMA), P(HEMA-co-MMA) and P(MMA-b-HEMA), followed by the subsequent esterification of the pendant hydroxyl groups of HEMA with 2-bromoisobutyryl bromide to afford P(BIEM), P(BIEM-co-MMA) and P(MMA-b-BIEM) macroinitiators. These polymers consisted of methacrylate monomers, one of which (BIEM) comprises initiating moieties for the subsequent brush synthesis. The forth macroinitiator was P(S_d-alt-MA), which was synthesized via RAFT mediated polymerization, as discussed in the previous chapter.

The structure of the macroinitiators and the quantitative esterification of the pendant hydroxyl groups of HEMA to 2-bromoisobutyrate was confirmed by ^{1}H-NMR spectroscopy, as shown in Figure 4.1(A, B and C). The two peaks at 4.34 and 4.14 ppm represent the methylene protons between the two ester groups of the macroinitiators M5, M6 and M7. The peak at 4.82 ppm, which is assigned to the hydroxyl group of HEMA in the precursor polymer, has disappeared completely, indicating a successful esterification of HEMA to BIEM with 2-bromoisobutyryl bromide. Furthermore, a new peak appeared at 1.94 ppm, due to the presence of methyl groups of 2-bromoisobutyrate in the macroinitiator.[34,46,47]

The final copolymer composition was also determined by ^{1}H-NMR spectroscopy after functionalization to the corresponding macroinitiator. For macroinitiators M6 and M7 (Figure 4.1B and Figure 4.1C), the integration area of the three methyl ester protons of MMA at 3.54 ppm and the four protons from the methylene groups of BIEM in the macroinitiators at 4.34 and 4.14 ppm were compared in order to determine the final copolymer composition (Table 4.1). It is important to choose two monomers that have similar reactivity ratios to ensure that one monomer does not propagate faster than the other.[16,41] Two methacrylate derivatives, HEMA and MMA, were chosen in order to ensure random copolymerization.[16]

The ^{1}H-NMR spectrum of macroinitiator M8 is shown in Figure 4.1D. The resonance peak at 7.1-7.5 ppm is assigned to the protons of the benzene ring in 4-vinylbenzyl chloride, while the peak at 2.31 ppm is associated with the protons of the maleic anhydride backbone. The copolymer composition was determined from the ratio of the integration areas of 4-vinylbenzyl chloride and maleic anhydride (Table 4.1).[48-50]

Table 4.1: Final conversions and molar mass data for ATRP macroinitiators synthesized via ATRP and RAFT.

Macro-initiator	Conversion[a] (%)	$M_{n,th}$ (g/mol)[b]	$M_{n,SEC}$ (g/mol)[c]	Molar fraction of initiating moiety[d]	DP_n[e]	PDI (-)
M5	70	8.4×10^4	5.5×10^4	1	197	1.38
M6	80	6.9×10^4	5.1×10^4	0.43	288	1.35
M7	70	6.6×10^4	5.2×10^4	0.47	282	1.41
M8	60	8.0×10^4	5.1×10^4	0.49	408	1.17
M9	61	18.2×10^4	10.5×10^4	1	376	1.16
M10	62	22.7×10^4	13.4×10^4	0.42	514	1.19
M11	69	13.7×10^4	10.8×10^4	0.43	527	1.2
M12	45	13.0×10^4	11.8×10^4	0.52	933	1.24

a) Calculated via gravimetry

b) Calculations based on the DP of the side chains $DP_{n,conv} = \Delta[M]/[I]_0$

c) From SEC, calibrated with PMMA standards

d) Molar fraction of BIEM and S_d in the macroinitiators, calculated from ^{1}H-NMR

e) Number average degree of polymerization of the backbone (macroinitiator) calculated: $DP_n = M_n/[(1-x)M_{MMA} + x\ M_{BIEM}]$, where M_{MMA} = 100.11 g/mol and M_{BIEM} = 279.12 g/mol, and x is molar fraction of initiator BIEM units in the backbone. The DP_n of macroinitiators M8 and M12 were obtained in a similar way[40]

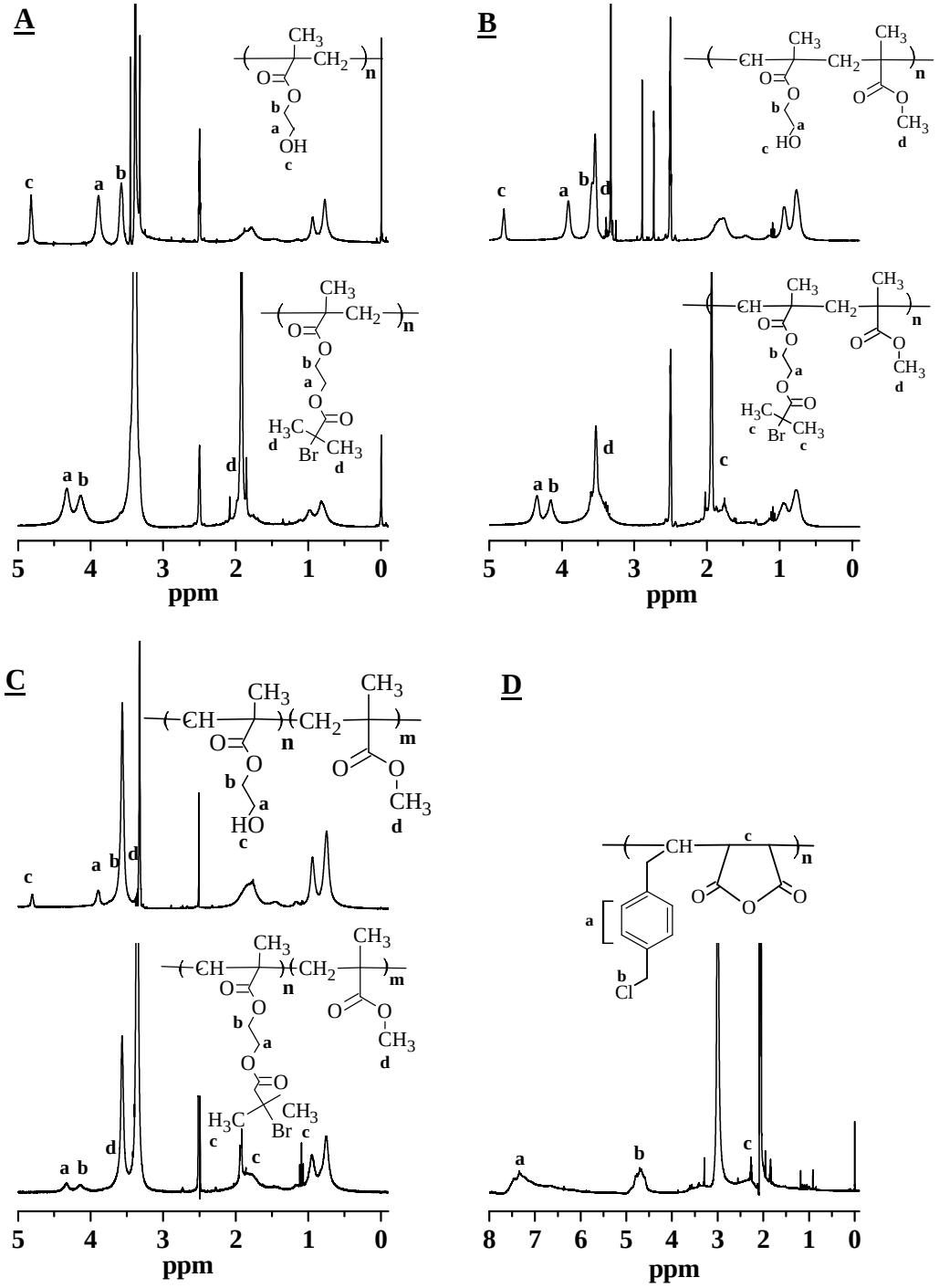

Figure 4.1: ^{1}H-NMR spectra of ATRP macroinitiators: (A) PHEMA and PBIEM (M5) (B) P(HEMA-co-MMA) and P(BIEM-co-MMA)(M6), (C) P(HEMA-b-MMA) and P(BIEM-b-MMA)(M7), and (D) P(S_d-alt-MA) (M8).

An alternative approach for the synthesis of well-defined PHEMA is to protect the hydroxyl groups of HEMA with a trimethylsilyl (-TMS) group to yield HEMA-TMS, as shown in Scheme 4.2. This second pathway includes the homopolymerization and copolymerization of HEMA-TMS with MMA via ATRP to produce P(HEMA-TMS), P(HEMA-TMS-co-MMA) and P(HEMA-TMS-b-MMA). The TMS groups were subsequently transformed to 2-bromoisobutyrate groups to afford P(BIEM), P(BIEM-co-MMA) and P(BIEM-b-MMA) macroinitiators. RAFT mediated polymerization was used for the synthesis of a P(S_d-alt-MA) macroinitiator. A polymer with a high DP was obtained in two steps. First, a low to intermediate molar mass P(S_d-alt-MA) was synthesized, and in the second step this polymer was chain extended with S_s and MA to obtain a high molar mass P(S_d-alt-MA).

The precursor polymers and their corresponding macroinitiators P(BIEM), P(BIEM-co-MMA), P(BIEM-b-MMA) and P(S_d-alt-MA) were characterized by ^{1}H-NMR spectroscopy, as shown in Figure 4.2.

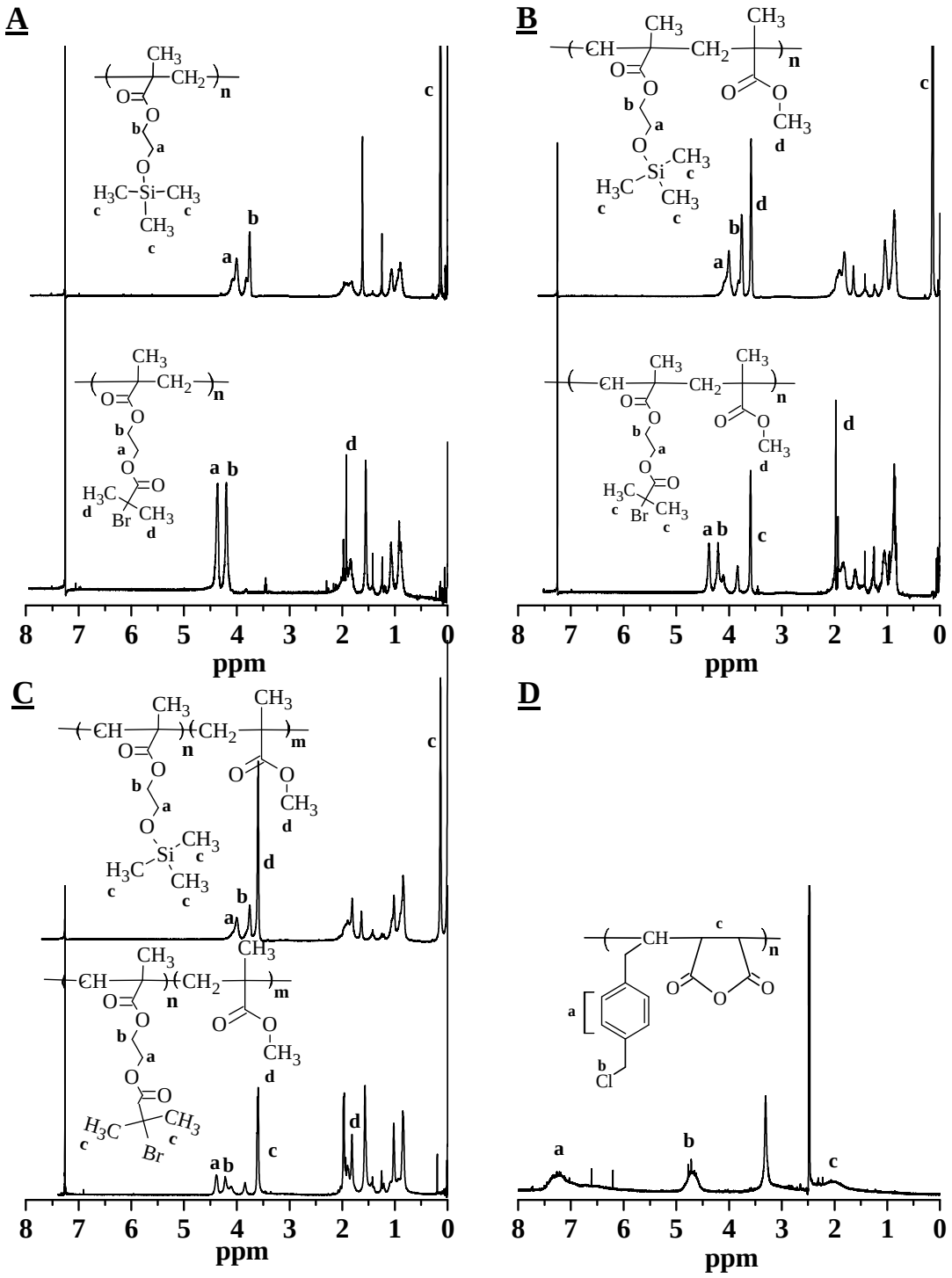

Figure 4.2: ^{1}H-NMR spectra of ATRP macroinitiators: (A) P(HEMA-TMS) and P(BIEM) (M9), (B) P(HEMA-TMS-co-MMA) and P(BIEM-co-MMA)(M10), (C) P(HEMA-TMS-b-MMA), and P(BIEM-b-MMA)(M11) (D) P(S_d-alt-MA) (M12).

The ^{1}H-NMR spectra of the macroinitiators M9 and M10 in Figure 4.2 show no peak at 0.14 ppm, related to the TMS groups of P(HEMA-TMS) indicating the complete esterification of PHEMA-TMS with 2-bromoisobutyryl bromide to yield PBIEM, and P(BIEM-co-MMA) macroinitiators. However, 91% esterification was obtained in the case of macroinitiator M11 to afford P(BIEM-b-MMA). The final chemical composition of macroinitiators M10 and M11 were also determined by ^{1}H-NMR spectroscopy (Figures 4.2B and 4.2C). The integration area of the three methyl ester protons of MMA at 3.53 ppm and the four protons from the methylene groups of BIEM in the macroinitiators at 4.35 and 4.18 ppm were compared in order to determine the final copolymer composition (see Table 4.1).

4.3.2: SEC results of the ATRP macroinitiators and their corresponding glycocylindrical brushes

SEC analyses clearly show that the ATRP macroinitiators prepared via the second strategic pathway (M9-M12) have higher molar mass and narrower MMD than the ATRP macroinitiators that were obtained via the first strategic pathway (M5-M8) (see Table 4.1).

It was observed that the PDI of the precursor polymers P(HEMA), P(HEMA-co-MMA) and P(MMA-b-HEMA) gradually increased when higher molar masses were targeted, suggesting that progressively loss of control over the polymerization occured.[33] Nevertheless, predetermined molar masses and reasonably narrow molar mass distributions were obtained for targeted DP_n up to 300. To access higher DP_n without significant loss of living character, the active hydroxyl groups of the HEMA monomer had to be protected with a TMS group to yield HEMA-TMS. As shown in Scheme 4.2, HEMA-TMS was used for the synthesis of the precursor polymers P(HEMA-TMS), P(HEMA-TMS-co-MMA) and P(HEMA-TMS-b-MMA). The advantage of protecting the active hydroxyl groups of HEMA, as reported by Matyjaszewski and Müller is to suppress the side reactions that might occur because of the hydroxyl groups.[14,32,46]

It is also noteworthy to mention that the molar masses of the precursor polymers, P(HEMA), P(HEMA-co-MMA) and P(MMA-b-HEMA) obtained from SEC analysis

using refractive index detection relative to PMMA standards, are not accurate. This discrepancy was due to the fact that the hydrodynamic volume of these polymers is not the same as the hydrodynamic volume of PMMA standards at similar molar masses. The theoretical molar mass obtained from the equation $DP_{n,conv} = \Delta[M]/[I]_0$ is nearly half the value of the experimental molar mass obtained from conventional SEC using PMMA standards (see experimental section). Beers et al. reported significant differences between their SEC data and their targeted molar masses of P(HEMA), where their SEC protocol overestimated the true molar mass by a factor of two.[32] Armes et al. reported that SEC analysis appears to overestimate the true molar mass of P(HEMA) by a factor of five to ten.[51] However, the experimental and theoretical molar mass values were fairly similar in the case of the precursor polymers P(HEMA-TMS), P(HEMA-TMS-co-MMA) and P(HEMA-TMS-b-MMA).

A variety of well-defined glycocylindrical brushes with similar side chain length, schematically shown in Scheme 4.3, were prepared by grafting 6-O-MMAGIc glycomonomer from the ATRP macroinitiators. The synthetic conditions used and SEC results of glycocylindrical brushes are presented in Table 4.2. It should be noted that the macroinitiators with higher molar mass dissolve much slower in the reaction mixture than the macroinitiators with lower molar mass. Thus the time of stirring before the polymerization starts should be long enough to ensure complete dissolution of the macroinitiator. Otherwise the PDI of the final product (glycocylindrical brushes) will be broader.[8,46] Low conversion of 6-O-MMAGIc glycomonomer is maintained in all cases in order to obtain well-defined glycocylindrical brushes. It was observed that even at such low conversions, the reaction mixture becomes very viscous due to the very high molar mass of the resulting brushes.

Table 4.2. Synthesis and characterization of glycocylindrical brushes via ATRP[a]

Brush	Macroinitiator	$[M_0]:[I]_0$	Time (min)	Conv (%)[b]	M_{nSEC} (g/mol)[c]	$M_{n,abs}$ (g/mol)[d]	$DP_{n,sc}$[e]	PDI
1	M5	47:1	60	49	3.58×10^5	5.32×10^5	10	1.48
2	M6	47:1	90	30	1.01×10^5	1.96×10^5	6	1.49
3	M7	47:1	80	41	1.92×10^5	3.20×10^5	8	1.52
4	M8	47:1	90	45	3.71×10^5	5.65×10^5	10	1.21
5	M9	47:1	60	36	7.20×10^5	10.9×10^5	10	1.28
6	M10	47:1	60	32	4.80×10^5	5.57×10^5	7	1.34
7	M11	47:1	80	42	4.45×10^5	5.50×10^5	7	1.29
8	M12	47:1	90	40	7.35×10^5	11.2×10^5	8	1.25
10	M9	100:1	50	31	8.8×10^5	1.8×10^6	17	1.29
11	M10	100:1	55	35	6.2×10^5	9.3×10^5	14	1.35
12	M11	100:1	65	40	6.3×10^5	9.8×10^5	14	1.32
13	M12	100:1	80	43	8.8×10^5	2.6×10^6	20	1.26

a) Solution polymerization in DMF (75 wt% to 6-O-MMAGIc) at 60 °C and at constant $[I]_0:[CuBr]_0:[L]_0 = 1:0.5:1$

b) Calculated via gravimetry

c) Determined from SEC, calibrated with PMMA standards

d) Determined by SEC-MALLS in DMAc

e) Calculated from $M_{n,abs}$ assuming a 100% initiation efficiency according to $DP_{sc} = (M_{n,brush} - M_{n,macroinitiator})/(x \times DP_{n,\ macroinitiator} \times M_{n,6\text{-O-MMAGIc}})$, where $M_{n,6\text{-O-MMAGIc}}$ = 262 g/mol and *x* is molar fraction of initiator BIEM unites in the backbone

The evaluation of experimental molar mass and molar mass distribution of the macroinitiators (M9, M10, M11 and M12) and their corresponding glycocylindrical brushes (5, 6, 7 and 8, Table 4.2) was carried out using SEC analysis. Evidence for the controlled polymerization of 6-O-MMAGIc from the macroinitiators was obtained by SEC analysis as shown in Figure 4.3. Each chromatogram exhibited a narrow monomodal molar mass distribution. During the synthesis of the brushes, the SEC traces completely

shifted to higher molar mass, indicating the formation of high molar mass brushes. No significant tailing or shoulder could be observed, suggesting the absence of brush-brush coupling reactions indicating a controlled polymerization reaction.[14,16] Using a high molar ratio of monomer to initiator and stopping the polymerization at a low conversion are sufficient to suppress undesirable side reaction and to obtain the desired well-defined glycocylindrical brushes.[15]

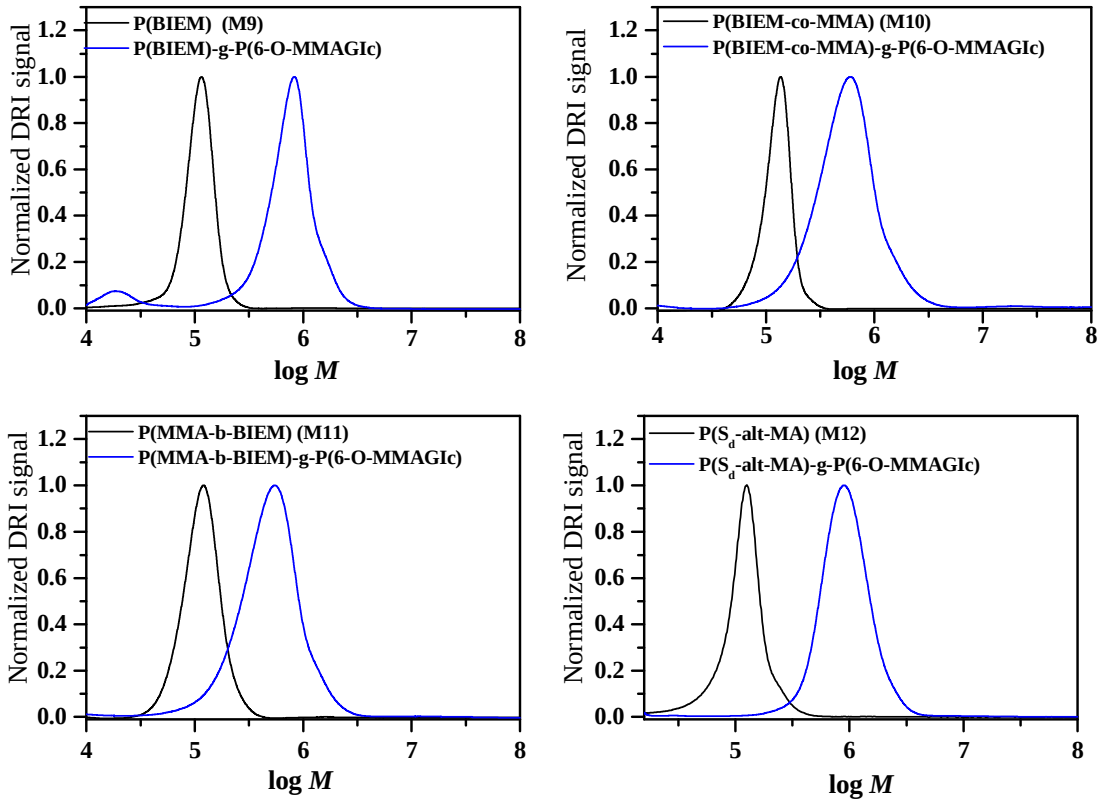

Figure 4.3: SEC chromatograms measured in DMAc of macroinitiators and their corresponding glycopolymer brushes.

The molar masses obtained from SEC analysis using refractive index detection relative to PMMA standards are just apparent ones.[7,52] It is known that the hydrodynamic volume of branched polymers decreases and therefore branched polymers elute later during SEC analysis as compared to their linear analogues.[52-54] In order to obtain a more accurate estimate of the molar mass and PDI of the glycopolymer brushes, SEC analysis with a multi-angle laser light scattering detector (MALLS) was performed in DMAc. The dn/dc value used (0.092 ± 0.004 mL/g) was based on the composition of the side chains P(6-O-

MMAGlc) since they comprised the bulk of the material (> 95%).[14,55] It is clear from the values listed in Table 4.2 that the absolute molar masses are significantly higher than the molar masses obtained from conventional SEC using PMMA standards.

The PDI values of the synthesized glycocylindrical brushes (1, 2 and 3) are higher than the PDI values of the macroinitiators (Table 4.2). Since the molar mass distribution of the brush is merely determined by the molar mass distribution of the macroinitiator, some side reactions might have occurred.[15] A possible explanation for these side reactions could be that some of the remaining low molar mass halide (ethyl α-bromoisobutyrate) used for the synthesis of M5, M6 and M7 macroinitiators can act as an ATRP initiator which was not completely removed after the transesterfication. Polymerization of 6-O-MMAGIc glycomonomer could be initiated by this remaining initiator to produce P(6-O-MMAGIc) homopolymer. The spontaneous cleavage of some side chains due to strong intramolecular repulsion between the densely grafted side chains could be another reason.[15]

^{1}H-NMR spectroscopy was used to characterize the glycocylindrical brushes in order to demonstrate the incorporation of the side chains from the macroinitiators and hence to provide evidence for the formation of glycocylindrical brushes. ^{1}H-NMR spectra in Figure 4.4 clearly show peaks ascribed to the macroinitiators and P(6-O-MMAGlc) side chains. A broad peak attributed to all carbohydrate ring protons of the sugar moieties (4.5-5.3 ppm) appeared. There are two typical peaks at 4.34 and 4.14 ppm, which represent the methylene protons between the two ester groups of the macroinitiator. Other characteristic peaks for the macroinitiator were seen at 0.5-1.3 ppm. This indicates the successful formation of glycocylindrical brushes with P(6-O-MMAGlc) side chains.

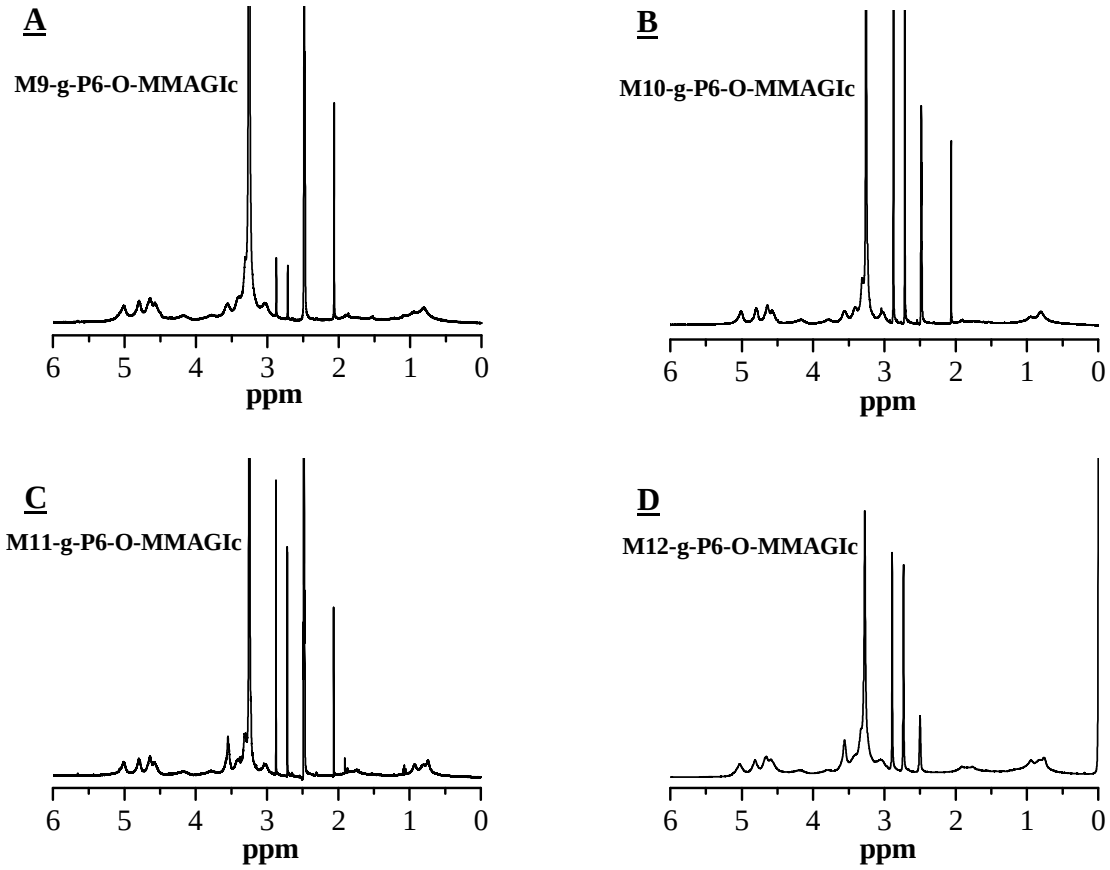

Figure 4.4: ^{1}H-NMR spectra of glycopolymer brushes: (A) P(BIEM)-g-P(6-O-MMAGIc), (B) P(BIEM-co-MMA)-g-P(6-O-MMAGIc), (C) P(BIEM-b-MMA)-g-P(6-O-MMAGIc), and (D) P(S_d-alt-MA)-g-P(6-O-MMAGIc).

4.3.3 Synthesis of cross-linked glycopolymer brushes

The introduction of a small amount of divinyl cross-linker into the controlled radical copolymerization of vinyl monomers is a convenient method by which to prepare cross-linked homogeneous polymer networks.[44,56,57]

In this study, the grafting from approach via ATRP was used to copolymerize 6-O-MMAGIc with ethylene glycol dimethacrylate (EGDMA) cross-linker to prepare glycopolymer brushes with cross-linked side chains. Since the side chains are cross-linked and covalently attached to the backbone, no entanglement is expected. This provides more stability against deformation and prevents the network from collapsing.[11]

In order to obtain homogeneous cross-linked side chains, EGDMA was selected as a

cross-linker. The reason is that it contains two methacrylate groups, which are expected to have similar reactivity as the methacrylate glycomonomer during the copolymerization. Because of the reactivity of a methacrylate group, both the incorporation rate of EGDMA into the polymer side chain and the consumption rate of pendant methacrylate group were similar.[44] As a result viscosity builds up quickly and insoluble polymer precipitated out of solution in the early stages of the reaction (low conversion). Mechanical and thermal studies of the cross-linked brushes were carried out, and will be discussed in the next chapter.

4.3.4 Analysis of the grafted side chains

The degree of polymerization of the side chains ($DP_{n,sc}$) was calculated based on the assumption that every initiating site along the backbone generates a side chain, i.e. 100% initiation efficiency. Therefore, $DP_{n,sc}$ is underestimated if the grafting density is low.[31] In order to determine the exact length of the side chain, and thus the initiation efficiency, the grafted side chains were cleaved from the backbone via base-catalyzed transesterification in methanol. However the side chain of the P(S_d-alt-MA)-g-P(6-O-MMAGIc) can not be cleaved, since there is not an ester group present in this particular polymer brush.

^{1}H-NMR spectra of the resulting side chains (Figure 4.5) revealed that solvolysis with sodium methoxide resulted in side chains consisting of a random copolymer of 13% MMA and 87% 6-O-MMAGIc units. The copolymer composition was determined by comparing the peaks (a,b) at 3.37-3.56 ppm attributed to the methyl ester protons (-OCH_3) of MMA and 6-O-MMAGIc units and peak (c) at 5.12 ppm attributed to the single proton in the carbohydrate ring of the sugar moieties (6-O-MMAGIc).[8,58] Similar results were obtained for brushes 6 and 7. Table 4.3 summarizes the detailed characterization of the side chains cleaved by solvolysis and the corresponding initiation efficiencies (*f*).

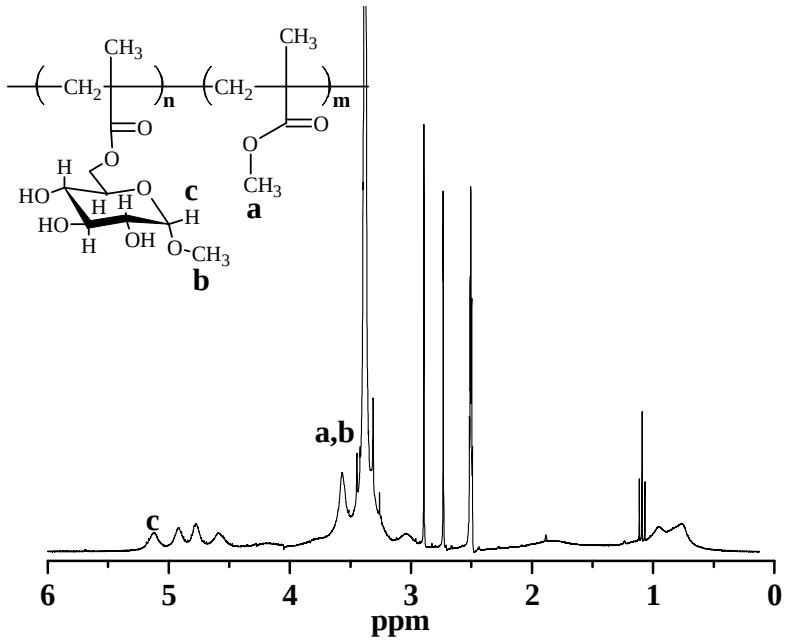

Figure 4.5: ^{1}H-NMR spectrum ($(CD_3)_2SO$) of cleaved side chains of P(BIEM)-g-P(6-O-MMAGIc) glycopolymer.

The SEC traces of brush 5 and the cleaved side chains are shown in Figure 4.6 below. The monomodal character of the cleaved side chains shows the absence of inter- and intramolecular coupling reactions. The absolute molar mass of the cleaved side chains was determined by SEC-MALLS measurements. It should be noted that the dn/dc value used (0.092 mL/g) was based on the assumption that the side chains (P(6-O-MMAGlc)) comprised the bulk of the material. Therefore the molar mass values obtained are inclusive of some errors. The PDI of the cleaved arms was < 1.3, and the initiating efficiency of the brushes was found to be in the range 37-55%, as shown in Table 4.3. Müller et al.[59] have demonstrated that the initiating efficiency was in the range 23% < *f* < 38% for the polymerization of 3-O-methacryloyl-1,2:5,6-di-O-isopropylidene-D-glucofuranose (MAIGlc) using P(BIEM) macroinitiator. Matyjaszewski et al.[31] have also demonstrated that the initiating efficiency is limited to approximately 50% for the polymerization of MMA using P(BIEM) macroinitiator. In this study, the increased bulkiness of the 6-O-MMAGIc glycomonomer could contribute to the low initiating efficiency of the brushes. The large steric congestion of the grafted side chains might

restrict the access to the initiating moiety, which involved in the initiation of 6-O-MMAGIc glycomonomer into the brushes.[7]

Table 4.3. Results from the side chains cleaved from the glycocylindrical brushes in order to investigate the initiation site efficiency (f) as a function of conversion

Side chains from brush	M_{nSEC}[a] (g/mol)	$M_{n,abs}$[b] (g/mol)	$DP_{n,exp}$[c]	$DP_{n,calc}$[d]	*F* (%)[e]	PDI
5	7.2 x 10^3	4.7 x 10^3	18	10	55	1.22
6	6.1 x 10^3	4.1 x 10^3	16	7	44	1.25
7	7.5 x 10^3	5.0 x 10^3	19	7	37	1.26

a) Determined from SEC, calibrated with PMMA standards

b) Determined by SEC-MALLS in DMAc

c) $DP_{n,exp} = M_{n,abs} / M_{n,6\text{-}O\text{-}MMAGIc}$ where $M_{n,6\text{-}O\text{-}MMAGIc}$ = 262 g/mol

d) Calculated from $M_{n,abs,brush}$ assuming a 100% initiation efficiency (see Table 4.2)

e) $f = DP_{n,calc} / DP_{n,exp}$

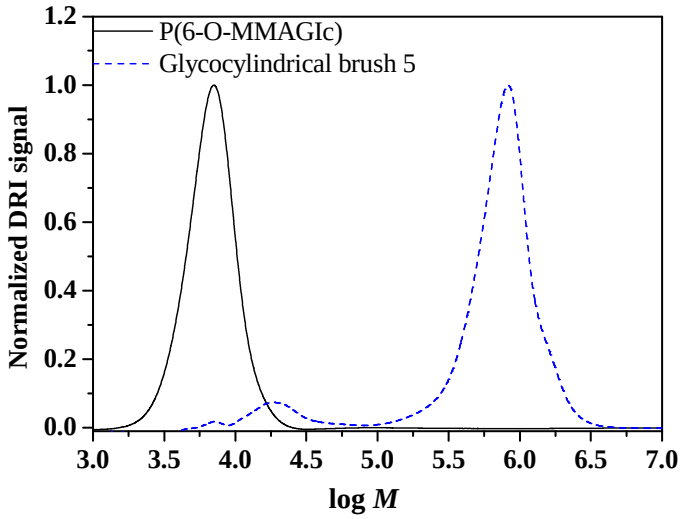

Figure 4.6: Molar mass distribution of glycocylindrical brush 5 and the corresponding cleaved side chains P(6-O-MMAGIc).

4.3.5 Visualization of glycopolymer brushes by atomic force microscopy

Characterization of the glycopolymer brushes by AFM was attempted in order to visualize the polymer morphology.[8,27,60,61] Many micrographs of the different glycopolymer brushes were taken, two of which are shown in Figure 4.7. Unfortunately, single brush molecules on the freshly cleaved mica could not be observed; only clusters of several polymer molecules were visible as opposed to individual brushes in earlier study. The reasons why single brush molecules were not observed have been discussed in the chapter 3.

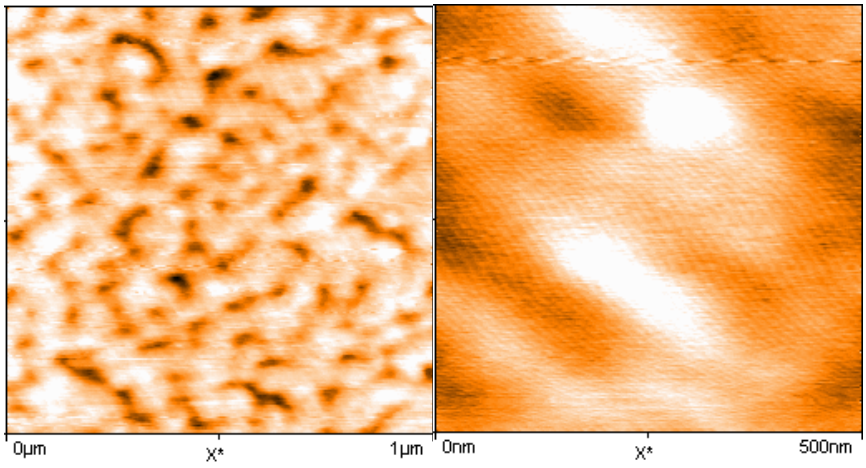

Figure 4.7: Tapping-mode AFM images of a P(BIEM)-g-P(6-O-MMAGIc) glycopolymer brush polymer spin coated from, a dilute water solution on mica. Shown are hight images

4.4: Conclusions

Successful preparation of the well-defined glycocylindrical brushes (sugar sticks) P(BIEM)-g-P(6-O-MMAGIc), P(BIEM-co-MMA)-g-P(6-O-MMAGIc), P(BIEM-b-MMA)-g-P(6-O-MMAGIc) and P(S_d-alt-MA)-g-P(6-O-MMAGIc) with different grafting densities, by using the grafting from method via ATRP has been demonstrated. This work demonstrated that the CuBr/n-Pr-1 catalyst system was successfully used for the polymerization of unprotected 6-O-MMAGIc in the "grafting from" process, leading to well-defined glycocylindrical brushes. ATRP was also used to prepare the ATRP macroinitiators P(BIEM), P(BIEM-co-MMA) and P(MMA-b-BIEM), which differ in DP and distribution of initiating sites along the backbone.

Two different synthetic routes were employed for the synthesis of the macroinitiators. The first involved, the synthesis of P(HEMA), P(HEMA-co-MMA) and P(MMA-b-HEMA) via ATRP, followed by subsequent esterification of the pendant hydroxyl groups of P(HEMA) with 2-bromoisobutyryl bromide, to yield the ATRP macroinitiators. This method yields polymers with higher PDI when higher molar masses were targeted, which indicates poorer control over the polymerization. However, to achieve higher molar mass without significant loss of living character, the active hydroxyl groups of HEMA were protected with a TMS group to yield HEMA-TMS.

The second route involved the homopolymerization of HEMA-TMS and copolymerization of HEMA-TMS with MMA by ATRP to produce P(HEMA-TMS), P(HEMA-TMS-co-MMA) and P(HEMA-TMS-b-MMA). The resulting precursor polymers were transformed to the corresponding ATRP macroinitiators, P(BIEM), P(BIEM-co-MMA) and P(BIEM-b-MMA). P(S_d-alt-MA) macroinitiators were synthesized via RAFT mediated polymerization.

The monomodal character and low PDI of the SEC chromatograms of the cleaved side chains showed the absence of inter- and intramolecular coupling reactions. Analysis of the cleaved side chains indicated that the grafting efficiency was approximately $0.37 < f < 0.55$. The grafting densities were low due to the large steric congestion of the grafted side chain, restricting the incorporation of more side chains into the brushes, which causes

incomplete initiation of the backbone. Such glycocylindrical brushes can be used for various biological and medicinal applications.

Furthermore, glycopolymer brushes with cross-linked side chains were successfully obtained via copolymerizing 6-O-MMAGIc glycomonomer with EGDMA cross-linker.

4.5 References

(1) Ito, Y.; Ochiai, Y.; Park, Y. S.; Imanishi, Y. *J. Am. Chem. Soc* **1997**, *119*, 1619-1623.

(2) Ionov, L.; Minko, S.; Stamm, M.; Gohy, J.-F.; Jerome, R.; Scholl, A. *J. Am. Chem. Soc.* **2003**, *125*, 8302-8306.

(3) Johnson, P. A.; Gaspar, M. A.; Levicky, R. *J. Am. Chem. Soc.* **2004**, *126*, 9910-9911.

(4) Unsworth, L. D.; Sheardown, H.; Brash, J. L. *Langmuir* **2005**, *21*, 1036-1041.

(5) Ohsedo, Y.; Takashina, R.; Gong, J. P.; Osada, Y. *Langmuir* **2004**, *20*, 6549-6555.

(6) Sumerlin, B. S.; Neugebauer, D.; Matyjaszewski, K. *Macromolecules* **2005**, *38*, 702-708.

(7) Gao, H.; Matyjaszewski, K. *J. Am. Chem. Soc.* **2007**, *129*, 6633-6639.

(8) Muthukrishnan, S.; Zhang, M.; Burkhardt, M.; Drechsler, M.; Mori, H.; Müller, A. H. E. *Macromolecules* **2005**, *38*, 7926-7934.

(9) Zhang, M.; Müller, A. H. E. *J. Polym. Sci. Part A: Polym. Chem.* **2005**, *43*, 3461-3481.

(10) Matyjaszewski, K.; Davis, T. P. *Handbook of Radical Polymerization*; John Wiley and Sons: Canada, 2002.

(11) Neugebauer, D.; Zhang, Y.; Pakula, T.; Sheiko, S. S.; Matyjaszewski, K. *Macromolecules* **2003**, *36*, 6746-6755.

(12) Fischer, K.; Schmidt, M. *Macromol. Rapid Comm.* **2001**, *22*, 787-791.

(13) Cheng, G.; Boker, A.; Zhang, M.; Krausch, G.; Müller, A. H. E. *Macromolecules* **2001**, *34*, 6883-6888.

(14) Beers, K. L.; Gaynor, S. G.; Matyjaszewski, K.; Sheiko, S. S.; Möller, M. *Macromolecules* **1998**, *31*, 9413-9415.

(15) Borner, H. G.; Beers, K.; Matyjaszewski, K.; Sheiko, S. S.; Moller, M. *Macromolecules* **2001**, *34*, 4375-4383.

(16) Borner, H. G.; Duran, D.; Matyjaszewski, K.; da Silva, M.; Sheiko, S. S. *Macromolecules* **2002**, *35*, 3387-3394.

(17) Qin, S.; Matyjaszewski, K.; Xu, H.; Sheiko, S. S. *Macromolecules* **2003**, *36*, 605-612.

(18) Neugebauer, D.; Zhang, Y.; Pakula, T.; Matyjaszewski, K. *Polymer* **2003**, *44*, 6863-6871.

(19) Yagci, Y.; Atilla Tasdelen, M. *Prog. Polym. Sci.* **2006**, *31*, 1133-1170.

(20) Braunecker, W.; Matyjaszewski, K. *Prog. Polym. Sci.* **2007**, *32*, 93-146.

(21) Fredrickson, G. H. *Macromolecules* **1993**, *26*, 2825-2831.

(22) Subbotin, A.; Saariaho, M.; Ikkala, O.; ten Brinke, G. *Macromolecules* **2000**, *33*, 3447-3452.

(23) Muchtar, Z.; Schappacher, M.; Deffieux, A. *Macromolecules* **2001**, *34*, 7595-7600.

(24) Yamada, K.; Miyazaki, M.; Ohno, K.; Fukuda, T.; Minoda, M. *Macromolecules* **1998**, *32*, 290-293.

(25) Roos, S. G.; Müller, A. H. E.; Matyjaszewski, K. *Macromolecules* **1999**, *32*, 8331-8335.

(26) Advincula, R. C.; Brittain, W. J.; Caster, K. C.; Ruhe, J. *Polymer Brushes : Synthesis, Characterization, Applications*; Wiley-VCH: Weinheim, 2004.

(27) Mori, H.; Müller, A. H. E. *Prog. Polym. Sci.* **2003**, *28*, 1403-1439.

(28) Narain, R.; Armes, S. P. *Biomacromolecules* **2003**, *4*, 1746-1758.

(29) You, L. C.; Lu, F. Z.; Li, Z. C.; Zhang, W.; Li, F. M. *Macromolecules* **2003**, *36*, 1-4.

(30) Albertin, L.; Stenzel, M. H.; Barner-Kowollik, C.; Foster, L. J. R.; Davis, T. P. *Macromolecules* **2005**, *38*, 9075-9084.

(31) Neugebauer, D.; Sumerlin, B. S.; Matyjaszewski, K.; Goodhart, B.; Sheiko, S. S. *Polymer* **2004**, *45*, 8173-8179.

(32) Beers, K. L.; Boo, S.; Gaynor, S. G.; Matyjaszewski, K. *Macromolecules* **1999**, *32*, 5772-5776.

(33) Weaver, J. V. M.; Bannister, I.; Robinson, K. L.; Bories-Azeau, X.; Armes, S. P.; Smallridge, M.; McKenna, P. *Macromolecules* **2004**, *37*, 2395-2403.

(34) Gong, s.-m.; Li, q.-s.; Yan, s.; Fu, z.-f.; Jiao, s.-k.; Yang, w.-t. *Chin. J. Polym. Sci.* **2003**, *21*, 427-431.

(35) Guice, K. B.; Loo, Y.-L. *Macromolecules* **2006**, *39*, 2474-2480.

(36) Haddleton, D. M.; Jasieczek, C. B.; Hannon, M. J.; Shooter, A. J. *Macromolecules* **1997**, *30*, 2190-2193.

(37) Germack, D. S.; Harrisson, S.; Brown, G. O.; Wooley, K. L. *J. Polym. Sci. Part A: Polym. Chem.* **2006**, *44*, 5218-5228.

(38) Moad, G.; Rizzardo, E.; Thang, S. H. *Aust. J. Chem.* **2005**, *58*, 379-410.

(39) Zhang, Y.; Huang, J.; Chen, Y. *Macromolecules* **2005**, *38*, 5069-5077.

(40) Lord, S. J.; Sheiko, S. S.; LaRue, I.; Lee, H.-I.; Matyjaszewski, K. *Macromolecules* **2004**, *37*, 4235-4240.

(41) Lee, H.; Matyjaszewski, K.; Yu, S.; Sheiko, S. S. *Macromolecules* **2005**, *38*, 8264-8271.

(42) Zhu, M.-Q.; Wei, L.-H.; Li, M.; Jiang, L.; Du, F.-S.; Li, Z.-C.; Li, F.-M. *Chem. Commun.* **2001**, 365-366.

(43) Harrisson, S.; Wooley, K. L. *Chem. Commun.* **2005**, 3259-3261.

(44) Gao, H.; Miasnikova, A.; Matyjaszewski, K. *Macromolecules* **2008**, *41*, 7843-7849.

(45) Venkatesh, R.; Klumperman, B. *Macromol. Chem. Phys.* **2004**, *205*, 2161-2168.

(46) Zhang, M.; Breiner, T.; Mori, H.; Müller, A. H. E. *Polymer* **2003**, *44*, 1449-1458.

(47) Ojha, U.; Feng, D.; Chandekar, A.; Whitten, J. E.; Faust, R. *Langmuir* **2009**, *25*, 6319-6327.

(48) Wang, T.-L.; Lee, H.-M.; Kuo, P.-L. *J. App. Polym. Sci.* **2000**, *78*, 592-602.

(49) Saad, G. R.; Morsi, R. E.; Mohammady , S. Z.; Elsabee, M. Z. *J. Polym. Res.* **2008**, *15*, 115-123.

(50) Montaudo, M. S. *Macromolecules* **2001**, *34*, 2792-2797.

(51) Robinson, K. L.; Khan, M. A.; de Paz Banez, M. V.; Wang, X. S.; Armes, S. P. *Macromolecules* **2001**, *34*, 3155-3158.

(52) Dupayage, L.; Save, M.; Dellacherie, E.; Nouvel, C.; Six, J.-L. *J. Polym. Sci. Part A: Polym. Chem.* **2008**, *46*, 7606-7620.

(53) Vosloo, J. J.; van Zyl, A. J. P.; Nicholson, T. M.; Sanderson, R. D.; Gilbert, R. G. *Polymer* **2007**, *48*, 205-219.

(54) Gerle, M.; Fischer, K.; Roos, S.; Müller, A. H. E.; Schmidt, M.; Sheiko, S. S.; Prokhorova, S.; Moller, M. *Macromolecules* **1999**, *32*, 2629-2637.

(55) Besenius, P.; Slavin, S.; Vilela, F.; Sherrington, D. C. *React. Funct. Polym.* **2008**, *68*, 1524-1533.

(56) Liu, G.; Hu, N.; Xu, X.; Yao, H. *Macromolecules* **1994**, *27*, 3892-3895.

(57) Heger, R.; Goedel, W. A. *Supramol. Sci.* **1997**, *4*, 301-307.

(58) Muthukrishnan, S.; Plamper, F.; Mori, H.; Müller, A. H. E. *Macromolecules* **2005**, *38*, 10631-10642.

(59) Muthukrishnan, S.; Zhang, M.; Burkhardt, M.; Drechsler, M.; Mori, H.; Müller, A. H. E. *Macromolecules* **2005**, *38*, 7926-7934.

(60) Djalali, R.; Li, S.-Y.; Schmidt, M. *Macromolecules* **2002**, *35*, 4282-4288.

(61) Sheiko, S. S.; Moller, M. *Chem. Rev.* **2001**, *101*, 4099-4124.

Chapter 5: Structure and properties of high density glycopolymer brushes

Abstract

The thermal and mechanical properties of a series of novel glycopolymer brushes with various degrees of polymerization of the backbone and various grafting densities were established. Modulated differential scanning calorimetry was found to be an effective tool for the characterization of the thermal behaviour of these glycopolymer brushes. There was little difference among the glass transition temperatures of the different glycopolymer brushes. The elastic features of each glycopolymer predominate (G'>G"), while at higher frequencies the G" curve overtook the G' curve, indicating the predominance of the viscous response.

5.1 Introduction

Polymers are becoming significantly more complex in order to meet the increasing demand for lower cost materials and improved physical and mechanical properties.[1-3] It is subsequently becoming increasingly difficult to characterize the structure and properties of polymers, which are often architecturally intricate. For example, the complexity of the structure of polymer brushes makes prediction and control of their physical and mechanical properties complicated.[4-7] The specific architecture and characteristic shape of molecular brushes that define their intramolecular density distribution give rise to a variety of interesting physical phenomena. The high density and proportion of relatively short side chains present in molecular brushes also has an important effect on their resulting bulk properties. Due to the radial distribution and extended nature of the backbone, chain packing can be significantly hindered, leading to morphologies that are different to those expected for simple linear polymers with the same identity as the side chains.[8]

Branching in conventional free radical polymerization is random in both the degree of polymerization of the side chain and the branching frequency. Therefore, studying structure-property relationships in densely branched systems is not an easy task.[9,10] The development of controlled free radical polymerization techniques has enabled the synthesis of polymers with controlled and predictable architectures.[1,11,12] Due to the ability of preparing brushes with a wide range of molecular characteristics (see Chapter 2), and with well-defined compositions, architecture and functionality, these materials demonstrate the potential utility of macromolecular engineering for preparing new advanced materials.[8] It is therefore, important to understand the fundamental structure-property relationships inherent to molecular brushes.[10,13-16]

Polymer brushes have gained increasing scientific and practical interest during the past decades due to their unique properties. Much effort has been devoted to characterizing their properties and considerable improvements have been made.[2,17-19] However, much more work is needed in order to develop new products and understand the flow behaviour (rheology) of the polymer brushes. The evaluation of the rheological properties of

polymer brushes can also provide valuable information related to the behaviour of a polymer under processing conditions prior to the formation of the final product.[20]

Unfortunately, some polymer solutions are non-Newtonian fluids, where the shear viscosity is a function of shear rate or shear stress. Therefore, the viscosity measured at a single shear rate is not an adequate representation of the rheology of the system and, as a result, a comprehensive characterization of the rheology of the polymer is required.[10,21]

Rheology describes the deformation of a material under the influence of stress.[21] Two classical ideal states describe the two extremes of rheology. At one end lies a Hookean solid, which deforms proportionally to the stress applied and stores the energy to affect a complete recovery of the original state when the applied stress is removed. At the other end is a Newtonian liquid that flows proportionally to the stress applied, and shows no recovery when the stress is removed. The energy required for the deformation is dissipated within the fluid in the form of heat and can not be recovered simply by removing the stress. Polymers exhibit neither ideal solid nor ideal liquid behaviour and their rheological behaviour lies somewhere between the two ideal states. Polymers exhibit both viscous and elastic behaviour and are therefore referred to as viscoelastic materials.[22,23] The ability to interpret changes in observed physical properties in terms of changes in chemical structure requires knowledge of the way in which polymer chains are organized at the molecular level. For example, the structure of an amorphous polymer differs significantly from a crystalline polymer.[24]

Amorphous materials possess some unique properties important in industrial applications; for example, the glass transition, which can be used to determine the stability of polymer product during storage.[25-27] The determination of the glass transition temperature (T_g) of glycopolymers that are used in pharmaceutical products is critical to considerations of proper handling, manufacture and storage conditions of these materials.[25-27] The T_g represents the temperature below which the molecular mobility of a glassy amorphous solid is dramatically reduced and above which the amorphous material takes on a rubbery character with increases in the number and magnitude of molecular motions. Given that increased molecular mobility can lead to increased chemical reactivity and the tendency for a stable amorphous material to crystallize over time, amorphous solids should be handled and stored well below the glass transition

temperature, which makes accurate determinations of the T_g imperative in pharmaceutical formulation development.[26,28] The most common method used to determine the glass transition temperature is differential scanning calorimetry (DSC), which detects the change in heat flow associated with thermal events and obtains information on physical and or chemical transformations as a function of temperature.[29] Although DSC is an invaluable analytical tool, the technique does suffer from limitations with respect to its ability to delineate complex transitions into individual contributing components.[10,25,26,30]

Many thermograms contain complex transitions with overlapping events, which may potentially be resolved by decreasing the heating rate and sample size at the expense of sensitivity.[25] Modulated DSC (MDSC) is now being used to increase the sensitivity and resolution of complex thermal events. MDSC differs from conventional DSC in the sample is subjected to a more complex heating program, incorporating a sinusoidal temperature modulation accompanied by an underlying linear heating ramp.[31] Whereas DSC is only capable of measuring the total heat flow, MDSC provides the total heat flow, the non-reversible (kinetic component) and the reversible (heat capacity component) heat flows.[25,26]

The focus of this section of the study was to gather information on the thermal and viscoelastic behaviour exhibited by a series of well-defined glycopolymers brushes, namely (P(BIEM)-g-P(6-O-MMAGIc)), (P(BIEM-co-MMA)-g-P(6-O-MMAGIc)), (P(BIEM-b-MMA)-g-P(6-O-MMAGIc)) and (P(S_d-alt-MA)-g-P(6-O-MMAGIc)). Variation in architecture, length of the side chains and structure of the polymer backbone are needed to better understand the structure-property relationships. The gathered information is crucial to improve properties and, accordingly, to consider applications of the glycopolymers. Analyses were carried out, on films using thermogravimetry for the understanding of their thermal stability and dynamic mechanical analysis to investigate their viscoelasticity.

5.2 Instrumental analysis

5.2.1 Thermogravimetric analysis (TGA)

TGA measurements were carried out on a TGA-50 SHIMADZU thermogravimetric instrument with a TA-50WSI thermal analyzer under a nitrogen atmosphere at flow rate of 50 mL/min. Samples of less than 20 mg were used for all analyses and they were analyzed from ambient temperature to 800 °C, using a heating rate of 10 °C/min.

5.2.2 Differential scanning calorimetry (DSC)

The T_g was determined by DSC. Samples were run on a TA Instruments Q 100 DSC system, calibrated with indium metal according to standard procedures. Heating and cooling rates were maintained at a standard 10 °C/min. The samples were first subjected to a heating ramp up to 200 °C, after which the temperature was kept isothermal at 200 °C for 1 min to remove thermal history. The cooling cycle followed the isothermal stage, followed by a subsequent second heating scan, from which the T_g was determined.

5.2.3 Wide angle X-ray diffraction (WAXD)

Wide angle X-ray diffraction (WAXD) was used to characterize the structure of the bulk material. WAXD was performed at iThemba LABS (South Africa) on 2D position sensitive detectors (Bruker) AXS D8 advanced diffractometer at room temperature, with filtered CuKα radiation (λ = 0.154 nm). Samples were scanned at 2θ angles (diffraction angle) ranging from 6° to 50°, with a sampling width of 0.02°. Each test sample had a thickness of 0.82 mm and diameter of 14.8 mm.

5.2.4 Dynamic mechanical analysis (DMA) and rheology

DMA and rheology measurements of the glycopolymer brush films were carried out using a Physica MCR 501 apparatus (Anton Paar, Germany).

Rheology measurements were carried out using an angular frequency range of 0.1-100 rad/sec, parallel-plate geometry (diameter 25 mm), with a gap distance of 1 mm. Strain sweep experiments were conducted to determine the linear region of the viscoelastic

(LVE) response. This was done for all the samples. An appropriate strain of 1% was selected, in order to carry out measurements within the LVE range.

5.3 Results and discussion

5.3.1 Bulk structure and thermal analysis of glycopolymer brushes

The thermal stability of the glycopolymer brushes, whose chemical structure is presented in Scheme 4.3, was analyzed by TGA in a nitrogen atmosphere and the results are shown in Figure 5.1. The thermal decomposition behaviour of these glycopolymer brushes has four major degradation steps. Up to approximately 200°C, all polymers experience little weight loss, in the order of 5% on average, which may represent loss of any water, solvent or small organic molecules. The first degradation step takes place over a wide temperatures range (60-110 °C) and is due to the elimination of absorbed and adsorbed water, since these materials are highly hygroscopic.[25,32] This behaviour is very similar to that shown in the thermal degradation of other natural or synthetic polysaccharides.[33-36] Subsequently, two degradation steps, at 235 °C and 295 °C, appear almost simultaneously. These are attributed to the decomposition of carbohydrate pendant groups. From approximately 300-500 °C weight loss is noted. It corresponds to high temperature volatilization of residues and the remaining macromolecular chain.[32]

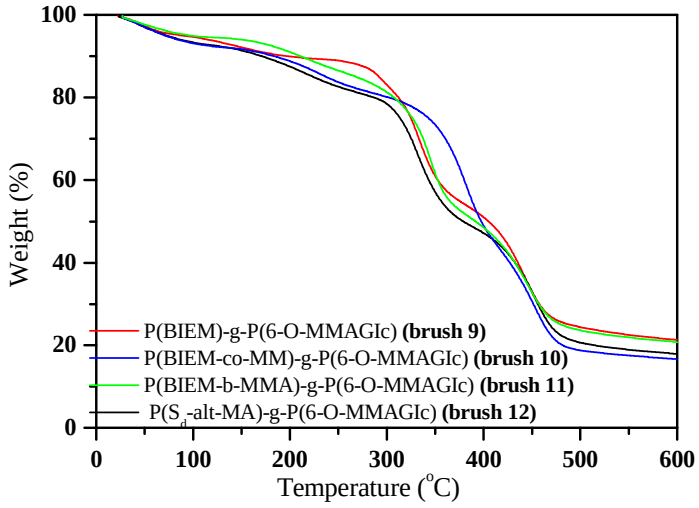

Figure 5.1: Thermal degradation curves of glycopolymer brushes under a N_2 atmosphere.

The glycopolymer brushes were also characterized by DSC. DSC analysis revealed the effect of the architecture of the backbone as well as the grafting density of the side chains on the T_g. Typical examples of DSC thermograms of glycopolymer brushes with different grafting densities are shown in Figure 5.2. For all samples, a single T_g was observed in the scanned temperature range of -50 to 200 °C, which indicates that in all cases the copolymers are miscible in bulk and that no phase separation is present. No melting phenomena were detected, even after repeated heating and cooling cycles, suggesting that these glycopolymer brushes are amorphous.[37]

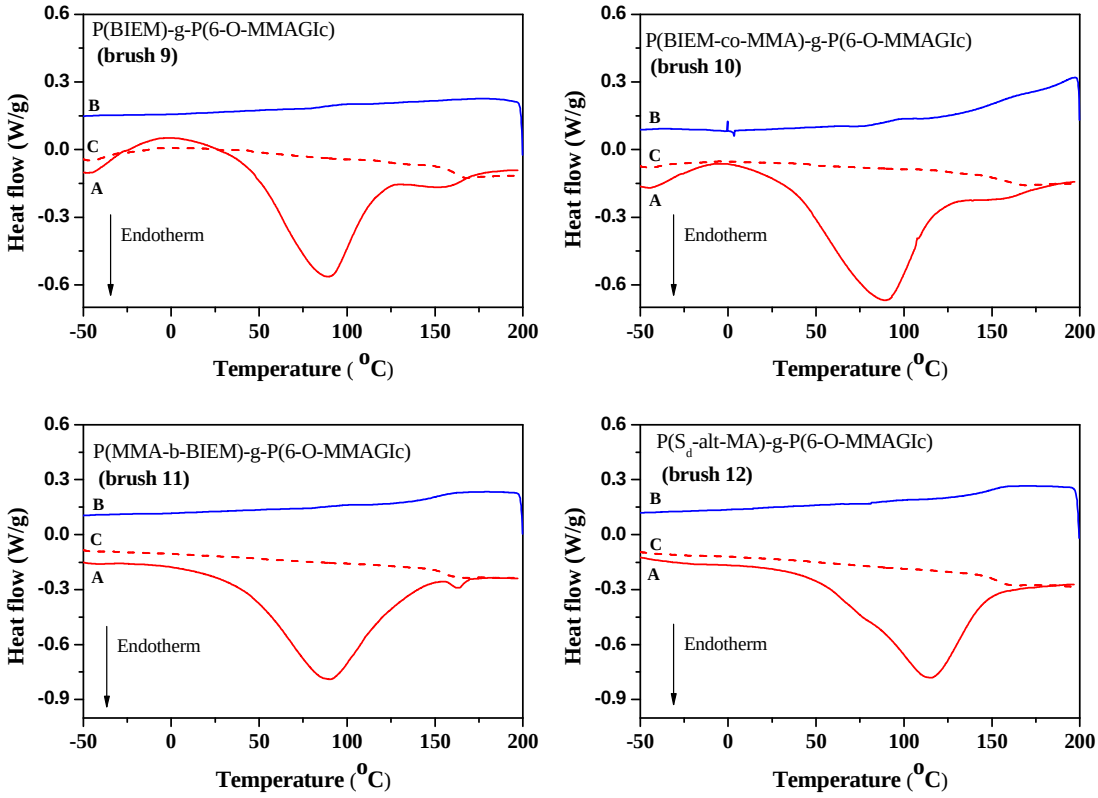

Figure 5.2: DSC thermograms of the glycopolymer brushes: scanning rate (A) 10 °C/min (heating), (B) 10 °C/min (cooling), (C) 10 °C/min (reheating).

The structure of the glycopolymer brushes was also examined by X-ray diffraction at room temperature. The wide angle X-ray diffractograms presented in Figure 5.3 display only an amorphous halo at wide angles, confirming the results obtained from DSC.

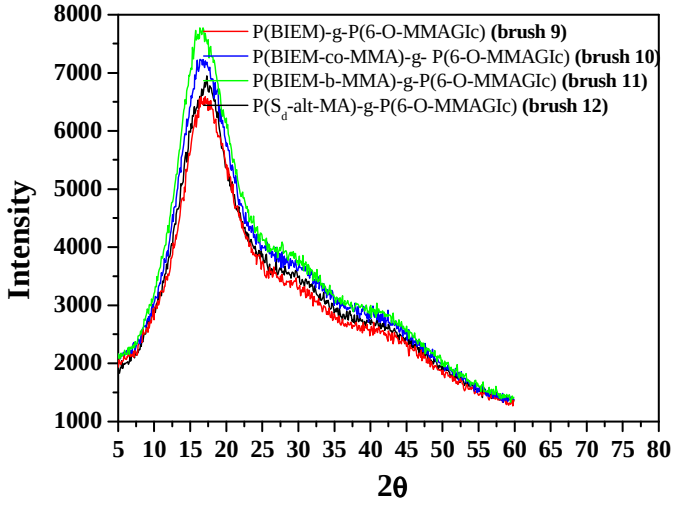

Figure 5.3: X-ray diffractograms of the glycopolymer brushes at room temperature.

The difference in T_g between the glycopolymer brushes with different amounts of branching was barely significant. The molar mass and molar mass distribution of the backbone of the glycopolymer brushes also had no significant impact on the T_g. The T_g for P(BIEM)-g-P(6-O-MMAGIc) is 160 °C., which displays the highest T_g value. The T_g value is consistent with the presence of bulky and polar side chains that hinder rotation about the backbone, and hydrogen bonding might also play a role.[37]

The T_g values of the glycopolymer brushes were lower than the T_g value of the P(6-O-MMAGIc) homopolymer (T_g = 180 °C). This could be due to the increased free volume resulting from linking of the side chains along the formed backbone.[37] The branch ends will be highly mobile and their motion will cause an increase in free volume. This postulate includes the possibility that the branches can disrupt the packing of the polymer chains and, in doing so, effectively act as internal plasticizer.[9] Moisture in amorphous material can act as a plasticizer and therefore may decrease the T_g value.[25] This phenomenon is seen in Figure 5.2, in which the enthalpic relaxation is observed in the heat flow signals. The loss of moisture upon heating typically results in a broad endothermic peak ranging from 50 to 125 °C and which may confound the measurement

of the T_g by DSC, since a preconditioning heating step is required before the T_g can be determined.

The use of conventional DSC to measure the T_g of these glycopolymer brushes requires that the sample be subjected to a heat-cool-reheat cycle. Given the plasticizing effect of water and the fact that the T_g is reduced in the presence of water, determination of T_g by conventional DSC may misrepresent the T_g, giving artificially high values in the absence of water. Therefore, MDSC may give a more meaningful value of T_g. The ability of MDSC to discriminate between non-reversible processes from those that are at equilibrium (reversible) is a useful aid in the characterization of thermal events. Examples of non-reversible processes include, but are not limited to, crystallization phenomena and decomposition of polymers. Thermograms showing reversible and non-reversible processes are shown in Figure 5.4. The sensitivity of MDSC allows the detection of a broad non-reversible endothermic peak at 50-125 °C, which corresponds to the loss of moisture. Furthermore, the reversible heat flow shows a clear shift in the base line at its T_g, which represents a change in the polymer from a brittle state to a less brittle state because of increased segmental mobility. It is important to mention that glycopolymers degrade before melting, therefore the reversible endothermic melt peaks are not observed.[32] However, decomposition of the glycopolymer brushes is observed as an exothermic peak in the non-reversing signal when the polymer was heated above 200 °C.

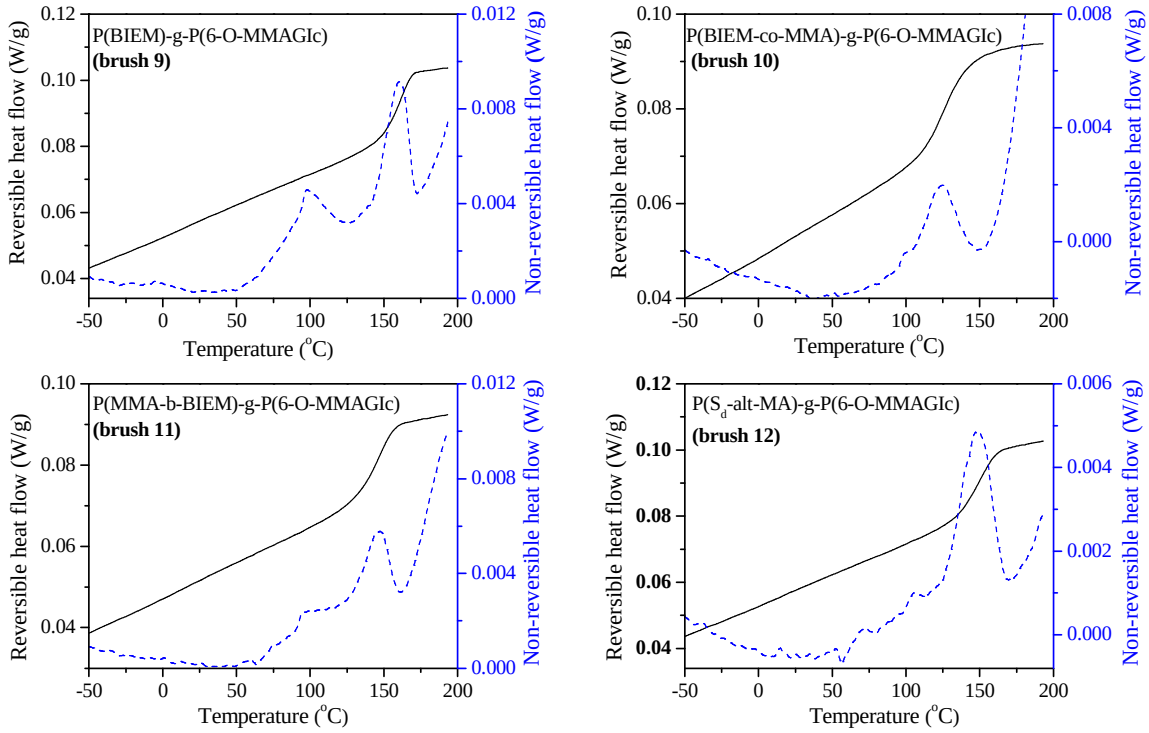

Figure 5.4: Modulated DSC thermograms of glycopolymer brushes illustrating the loss of moisture as a broad non-reversible endotherm and the glass transition in the reversible signal.

5.3.2 Mechanical properties

A potential application for these glycopolymers is their use as biomedical membranes, energy storage or implant materials.[38] As mentioned earlier (Chapter 2), some mechanical requirements have to be accomplished for these applications. The determination of the viscoelastic behaviour over a wide range of frequencies, ranging from 0.1 to 100 rad/s, provides knowledge on the relaxation processes that can take place in a polymer, and that govern its overall mechanical response.[32] DMA of the glycopolymer brushes was performed in the form of frequency dependencies of the storage modulus and loss modulus within a broad frequency range to characterize their viscoelastic behaviour. The three main parameters of DMA measurements are (I) the storage modulus (G'), which is a measure of elastic response to the deformation; (II) the loss modulus (G"), which is a measure of the viscous response; and (III) loss factor tanδ, i.e. the ratio of G"/G', which

is used to determine molecular mobility.[20] The storage modulus in bulk at room temperature was found to be high for all glycopolymer brushes due to the great number of hydrogen bonding interactions that confer sufficient rigidity to the final material despite its amorphous nature.[32]

Figure 5.5 shows the frequency dependence of the storage modulus G' and the loss modulus G" of the glycopolymer brushes at a temperature slightly higher than the T_g (170 °C). Both moduli rapidly decrease with decreasing frequency, and at low frequencies the elastic features of each polymer predominate (G'>G"), while at higher frequencies the G" curve overtakes the G' curve, indicating the predominance of the viscous response.

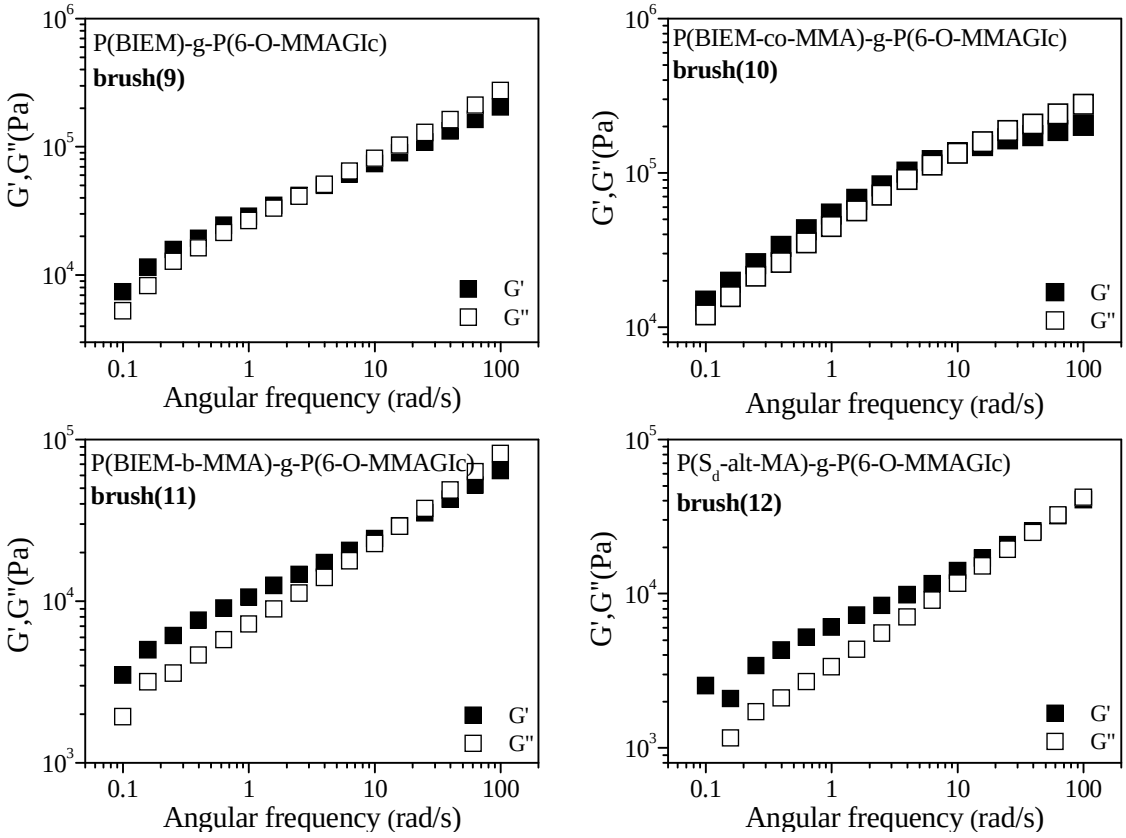

Figure 5.5: Frequency dependence of the storage modulus G' and loss modulus G" for non-cross-linked glycopolymer brushes obtained by the grafting from method

The magnitude of the difference in moduli (G' and G") for brush 9 and brush 10 that have higher grafting density is probably well within the possible error associated with the measurements, but can still be explained in terms of the constraints imposed by branch

points, when compared to the brushes with lower grafting density. It is important to realize that in brush systems like these (with a high branching density, up to 55%), the branch motions completely dominate the material properties.[10] Another important parameter related to the DMA of glycopolymer brushes is the crossover frequency (i.e. the frequency at which the value of storage and loss moduli are equal). This angular frequency point gives an indication on the relaxation time of the polymer chains.[16,20,39] When a polymer reaches the frequency range at which a chain movement occurs, the energy dissipated increases up to a maximum. Therefore, information on a dynamics of the polymer in bulk can be obtained from the study of the storage modulus G' and loss modulus G".[32] Moreover, analysis of the storage modulus (G') ascribed to the part of energy absorbed into the polymer provides a direct estimation about the stiffness along the frequency.[32] The high frequency relaxation is the segmental motion corresponding to the T_g of the system. In Figure 5.5 the characteristic relaxation process due to either the segmental relaxation or the side chains relaxation can be distinguished. This was also observed for nBA brush homopolymers. [39]

Figure 5.6 shows the frequency dependence of the storage modulus G' and loss modulus G" of the cross-linked glycopolymer brushes at 170 °C. A dominant storage modulus G' is observed over the entire frequency range for the cross-linked glycopolymer brushes. It is clear that the presence of crosslinker has increased the solid-like rheological behaviour (elastic features) of the glycopolymer brushes. The most likely reason for this behaviour is that the mobility of the short side chains was restricted by cross-linking, resulting in polymer brushes with more solid (gel) properties, even at high angular frequency.[16]

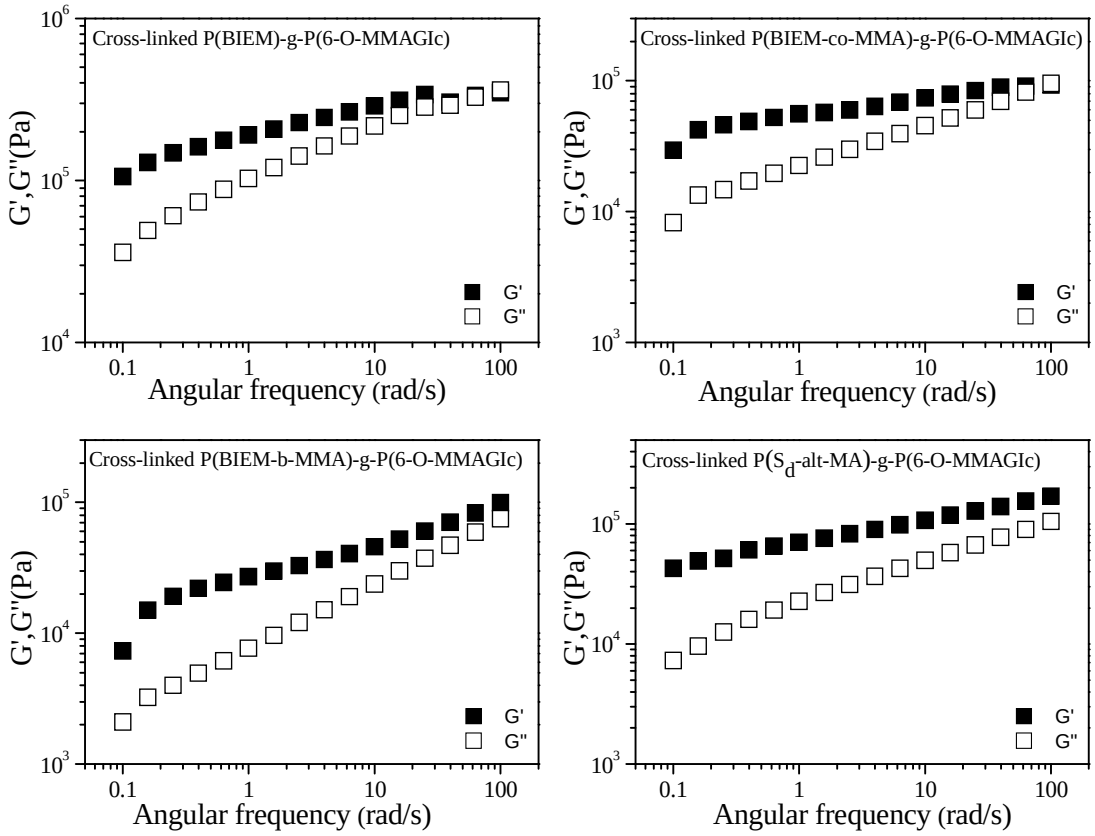

Figure 5.6: Frequency dependence of the storage modulus G' and the loss modulus G" for cross-linked glycopolymer brushes obtained by the grafting from method.

5.3.3 Solution rheological behaviour

Melt rheological properties of polymer brushes are important in the consideration of their possible processing. However, only solution rheological properties for glycopolymers can be investigated because glycopolymers degrade before they melt.[32,40] Frequency sweeps over a wide frequency range enable a useful comparison of the rheological properties of the different glycopolymer brushes. The relationship between the polymer structure and solution rheological properties was established for the glycopolymer brushes P(BIEM)-g-P(6-O-MMAGIc), P(BIEM-co-MMA)-g-P(6-O-MMAGIc), P(BIEM-b-MMA)-g-P(6-O-MMAGIc) and P(S_d-alt-MA)-g-P(6-O-MMAGIc).

Figure 5.7 shows the effects of grafting density and angular frequency on the complex viscosity of solutions of the glycopolymer brushes in DMF, at a concentration of 4.0 mg/mL. At low angular frequency and at ambient temperature the solutions of the

glycopolymer brushes exhibit non-Newtonian shear-thinning behaviour, in which the viscosity linearly decreases with increasing frequency up to about 10 rad/s. For higher angular frequencies the complex viscosity tends to increase and exhibit non-Newtonian shear-thickening behaviour. This was less pronounced for brush 1 and brush 9. Increased flow resistance at high frequency could be caused by flow instabilities and turbulences.[23] While the angular frequency increases over time, the macromolecules interact and recoil more and more, and as a consequence the viscosity of the solution increases again.[13,21,23,41]

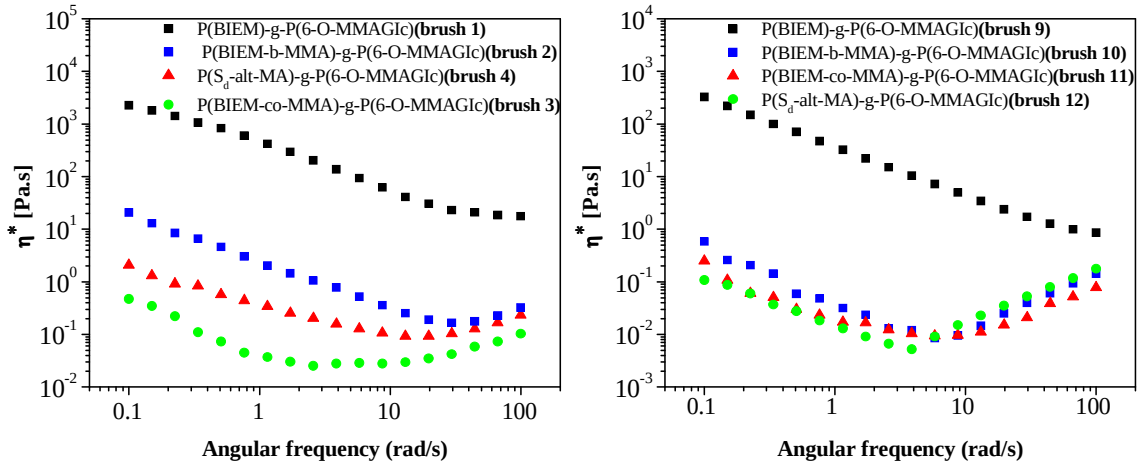

Figure 5.7: Complex viscosity as a function of angular frequency for glycopolymer brushes in DMF at constant temperature and constant concentration (4.0 mg/mL).

It is noticed that the value of the complex viscosity increases with an increase in the grafting density. The solution of P(BIEM)-g-P(6-O-MMAGIc) with the highest grafting density has the highest complex viscosity, whereas the solution of P(S_d-alt-MA)-g-P(6-O-MMAGIc)) has the lowest complex viscosity. In general, shear-thickening effects are rarely observed in common polymer solutions or melts, but they are well known to occur in complex fluids, including concentrated suspensions[41] and associated polymers.[42,43] Shear-thickening behaviour is related to shear-induced changes of the fluid microstructure, such as shear-induced cross-linking, shear-induced non-Gaussian chain stretching, and shear-induced polymer association or aggregation, including temporary network formation during shear.[44]

5.4 Conclusion

Different series of novel glycopolymer brushes enabled a systematic investigation of the effect of various structure parameters on the thermal and viscoelastic properties of these polymers. Analysis of the structure and properties of glycopolymer brushes show that the specific macromolecular architecture, consisting of a different distribution of glycopolymer side chains along the backbone, can lead to amorphous, homogeneous bulk materials. DSC and MDSC measurements showed insignificant differences among the glass transition temperatures of the different glycopolymer brushes. The thermal degradation of these glycopolymer brushes is almost identical and it is independent on the number of glycopolymers side chains incorporated in the glycopolymer brushes. All glycopolymer brushes showed viscoelastic responses that are characteristic for brushes. The elastic features of each polymer predominate (G'>G") at low angular frequency, while at higher frequency the G" curve overtakes the G' curve, indicating the predominance of the viscous response. However, the cross-linked glycopolymer brushes showed a dominant storage modulus G' over the entire frequency range. The solutions of glycopolymer brushes in DMF showed non-Newtonian shear-thinning behaviour, in which the viscosities linearly decreased with increasing frequency up to about 10 rad/s. For higher angular frequencies the complex viscosity tend to increase and exhibit non-Newtonian shear-thickening behaviour.

5.5 References

(1) Matyjaszewski, K.; Davis, T. P. *Handbook of Radical Polymerization*; John Wiley and Sons: Canada, 2002.

(2) Ionov, L.; Minko, S.; Stamm, M.; Gohy, J.-F.; Jerome, R.; Scholl, A. *J. Am. Chem. Soc.* **2003**, *125*, 8302-8306.

(3) Advincula, R. C.; Brittain, W. J.; Caster, K. C.; Ruhe, J. *Polymer Brushes : Synthesis, Characterization, Applications*; Wiley-VCH: Weinheim, 2004.

(4) Zhang, M.; Müller, A. H. E. *J. Polym. Sci. Part A: Polym. Chem.* **2005**, *43*, 3461-3481.

(5) Barbey, R.; Lavanant, L.; Paripovic, D.; SchuIwer, N.; Sugnaux, C.; Tugulu, S.; Klok, H.-A. *Chem. Rev.* **2009**, *109*, 5437-5527.

(6) Mori, H.; Müller, A. H. E. *Prog. Polym. Sci.* **2003**, *28*, 1403-1439.

(7) Besenius, P.; Slavin, S.; Vilela, F.; Sherrington, D. C. *React. Funct. Polym.* **2008**, *68*, 1524-1533.

(8) Rathgeber, S.; Pakula, T.; Wilk, A.; Matyjaszewski, K.; Beers, K. L. *J. Chem. Phys.* **2005**, *122*, 1-13.

(9) Xia, Y.; Olsen, B. D.; Kornfield, J. A.; Grubbs, R. H. *J. Am. Chem. Soc.* **2009**, *131*, 18525-18532.

(10) Vosloo, J. J.; van Zyl, A. J. P.; Nicholson, T. M.; Sanderson, R. D.; Gilbert, R. G. *Polymer* **2007**, *48*, 205-219.

(11) Moad, G.; Solomon, D. *The Chemistry of Radical Polymerization*, 2nd ed.; Elsevier: Heidelberg, 2006.

(12) Rizzardo, E.; Chiefari, J.; Chong, B. Y. K.; Ercole, F.; Krstina, J.; Jeffery, J.; Le, T. P. T.; Mayadunne, R. T. A.; Meijs, G. F.; Moad, C. L.; Moad, G.; Thang, S. H. *Macromol. Symp.* **1999**, *143*, 291-307.

(13) Nikoubashman, A.; Likos, C. N. *Macromolecules* **2010**, *43*, 1610-1620.

(14) Yang, Y.; Xie, X.; Yang, Z.; Wang, X.; Cui, W.; Yang, J.; Mai, Y.-W. *Macromolecules* **2007**, *40*, 5858-5867.

(15) Tsubaki, K.; Ishizu, K. *Polymer* **2001**, *42*, 8387-8393.

(16) Neugebauer, D.; Zhang, Y.; Pakula, T.; Sheiko, S. S.; Matyjaszewski, K. *Macromolecules* **2003**, *36*, 6746-6755.

(17) Ito, Y.; Ochiai, Y.; Park, Y. S.; Imanishi, Y. *J. Am. Chem. Soc.* **1997**, *119*, 1619-1623.

(18) Unsworth, L. D.; Sheardown, H.; Brash, J. L. *Langmuir* **2005**, *21*, 1036-1041.

(19) Ohsedo, Y.; Takashina, R.; Gong, J. P.; Osada, Y. *Langmuir* **2004**, *20*, 6549-6555.

(20) Samakande, A.; Sanderson, R. D.; Hartmann, P. C. *Polymer* **2009**, *50*, 42-49.

(21) Gary Leal, L.; Oberhauser, J. P. *Korea-Australia Rheology Journal* **2000**, *12*, 1-25.

(22) Larson, R. G. *The Structure and Rheology of Complex Fluids*; Oxford University Press, New York, 1999.

(23) Mezger, T. *The rheology Handbook for Users of Rotational and Oscillatory Rheometers*; Vincentz Network: Hannover, 2002.

(24) Jiang, Z.; Tang, Y.; Rieger, J.; Enderle, H.-F.; Lilge, D.; Roth, S. V.; Gehrke, R.; Wu, Z.; Li, Z.; Men, Y. *Polymer* **2009**, *50*, 4101-4111.

(25) Rabel, S. R.; Jona, J. A.; Maurin, M. B. *J. Pharm. Biomed. Anal.* **1999**, *21*, 339-345.

(26) Rahman, M. S.; Al-Marhubi, I. M.; Al-Mahrouqi, A. *Chem. Phys. Lett.* **2007**, *440*, 372-377.

(27) Levine, H.; Slade, L. *Carbohydr. Polym.* **1986**, *6*, 213-244.

(28) Hancock, B. C.; Zografi, G. *J. Pharm. Sci.* **1997**, *86*, 1-12.

(29) Kasapis, S.; Al-Marhoobi, I. M.; Mitchell, J. R. *Carbohydr. Res.* **2003**, *338*, 787-794.

(30) Williams, M. L.; Landel, R. F.; Ferry, J. D. *J. Am. Chem. Soc.* **1955**, *77*, 3701-3707.

(31) Bell, L. N.; Touma, D. E. *J. Food Sci.* **1996**, *61*, 807-810.

(32) Cerrada, M. L.; Sanchez-Chaves, M.; Ruiz, C.; Fernandez-Garcia, M. *Eur. Polym. J.* **2008**, *44*, 2194-2201.

(33) Stewart, F. F.; Harrup, M. K.; Lash, R. P.; Tsang, M. N. *Polym. Int.* **2000**, *49*, 57-62.

(34) Cao, L.-Q.; Xu, S.-M.; Feng, S.; Wang, J.-D. *J. App. Polym. Sci.* **2005**, *96*, 2392-2398.

(35) Kweon, D.-K.; Cha, D.-S.; Park, H.-J.; Lim, S.-T. *J. App. Polym. Sci.* **2000**, *78*, 986-993.

(36) Don, T.-M.; Chen, H.-R. *Carbohydr. Polym.* **2005**, *61*, 334-347.

(37) Albertin, L.; Stenzel, M. H.; Barner-Kowollik, C.; Foster, L. J. R.; Davis, T. P. *Macromolecules* **2005**, *38*, 9075-9084.

(38) Albertin, L.; Claudia., K.; Martina., S.; R., F. L. J.; P, D. T. *Biomacromolecules* **2004**, *5*, 255-260.

(39) Neugebauer, D.; Zhang, Y.; Pakula, T.; Matyjaszewski, K. *Polymer* **2003**, *44*, 6863-6871.

(40) Dwek, R. A. *Chem. Rev.* **1996**, *96*, 683-720.

(41) Otsubo, Y. *Langmuir* **1999**, *15*, 1960-1965.

(42) Tam, K. C.; Jenkins, R. D.; Winnik, M. A.; Bassett, D. R. *Macromolecules* **1998**, *31*, 4149-4159.

(43) Smith, G. L.; McCormick, C. L. *Macromolecules* **2001**, *34*, 5579-5586.

(44) Witten, T. A.; Cohen, M. H. *Macromolecules* **1985**, *18*, 1915-1918.

Chapter 6: General conclusions

6.1 Conclusions

1. The synthesis of methyl 6-O-methacryloyl-α-D-glucoside (6-O-MMAGIc) and 2-(2-bromoisobutyryloxy) ethyl methacrylate (BIEM), has been achieved as confirmed by NMR, and ESI-MS spectroscopy.
2. The RAFT process through the use of 2-cyanoprop-2-yl dithiobenzoate RAFT agent was used successfully to prepare well-defined ATRP macroinitiators, P(2-(2-bromoisobutyryloxy) ethyl methacrylate (P(BIEM)), P(2-(2-bromoisobutyryloxy) ethyl methacrylate-co-methyl methacrylate) (P(BIEM-co-MMA)), P(2-(2-bromoisobutyryloxy) ethyl methacrylate-b-methyl methacrylate) (P(BIEM-b-MMA)) and P(4-vinylbenzyl chloride-alt-maleic anhydride) (P(S_d-alt-MA).
3. Two different synthetic routes were successfully used for the synthesis of the ATRP macroinitiators. The first involved, the synthesis of P(HEMA), P(HEMA-co-MMA) and P(MMA-b-HEMA) via ATRP, followed by subsequent esterification of the pendant hydroxyl groups of P(HEMA) with 2-bromoisobutyryl bromide. The second route involved the homopolymerization of HEMA-TMS and copolymerization of HEMA-TMS with MMA by ATRP to produce P(HEMA-TMS), P(HEMA-TMS-co-MMA) and P(HEMA-TMS-b-MMA). The resulting precursor polymers were transformed to the corresponding ATRP macroinitiators.
4. Successful preparation of the well-defined glycocylindrical brushes (sugar sticks) P(BIEM)-g-P(6-O-MMAGIc), P(BIEM-co-MMA)-g-P(6-O-MMAGIc), P(BIEM-b-MMA)-g-P(6-O-MMAGIc) and P(S_d-alt-MA)-g-P(6-O-MMAGIc) with different grafting densities were prepared by using the grafting from method via ATRP. This work demonstrated that the CuBr/n-Pr-1 catalyst system could be successfully used for the polymerization of unprotected 6-O-MMAGIc in the “grafting from” process, leading to well-defined glycopolymer brushes.
5. The monomodal character and low PDI of the SEC chromatograms of the cleaved side chains showed the absence of inter- and intramolecular coupling

reactions. Analysis of the cleaved side chains indicated that the grafting efficiency was approximately $0.37 < f < 0.55$, these results are in good agreement with results published in the literature.

6. The thermal degradation of the glycopolymer brushes was almost identical, and it was independent on the number of glycopolymers side chains incorporated into the brushes. All glycopolymer brushes showed viscoelastic responses. The elastic features of each polymer predominated (G'>G") at low angular frequency, while at higher frequency the G" curve overtook the G' curve, indicating the predominance of the viscous response.